Sónia Isabel Pereira Branco

Licenciatura em Ciências da Engenharia Química e Bioquímica

Aqueous Biphasic System based on Cholinium Ionic Liquids: Extraction of Biologically Active Phenolic Acids

Dissertação para obtenção do Grau de Mestre em
Engenharia Química e Bioquímica

Orientador: Doutora Isabel Maria Delgado Jana Marrucho Ferreira, Investigadora Coordenadora, Laboratório de Termodinâmica Molecular, ITQB-UNL

Presidente: Doutora Susana Filipe Barreiros
Arguente: Doutor Alexandre Babo de Almeida Paiva
Vogal: Doutora Isabel Maria Delgado Jana Marrucho Ferreira

FACULDADE DE CIÊNCIAS E TECNOLOGIA
UNIVERSIDADE NOVA DE LISBOA

Setembro 2014

UNIVERSIDADE NOVA DE LISBOA

Faculdade de Ciências e Tecnologia

Departamento de Química

Aqueous Biphasic System based on Cholinium Ionic Liquids: Extraction of Biologically Active Phenolic Acids

Sónia Isabel Pereira Branco

Dissertação apresentada na Faculdade de Ciências e Tecnologia da Universidade Nova de Lisboa para obtenção do grau Mestre em Engenharia Química e Bioquímica

Orientadores: Doutora Isabel Maria Delgado Jana Marrucho Ferreira

2014

Aqueous Biphasic Systems based on Cholinium Ionic Liquids: Extraction of Biologically Active Phenolic Acids

COPYRIGHT

Sónia Isabel Pereira Branco

Faculdade de Ciências e Tecnologia

Universidade Nova de Lisboa

Agradecimentos

Durante a realização desta tese, contei com o apoio de várias pessoas sem as quais não teria concluído esta etapa. A realização desta tese e as pessoas que me acompanharam nos últimos meses permitiu-me crescer tanto a nível pessoal como intelectual.

Quero começar por agradecer à minha orientadora, a investigadora Doutora Isabel Marrucho, por me ter facultado esta oportunidade em realizar a minha dissertação de mestrado num local prestigiado como o ITQB. Foi uma experiência única onde pude aprender novos conceitos que espero que me sejam úteis para o meu futuro como Engenheira.

Quero também retribuir à Catarina Florindo a aprendizagem que ela me concedeu desde o primeiro dia no ITQB e pela paciência que teve para me incentivar a trabalhar sempre e especialmente com garra quando o trabalho e o ânimo estavam em baixo.

Não poderia deixar de agradecer às minhas colegas de curso que ao longo destes cinco anos me apoiaram, me ensinaram e me fizeram ser uma pessoa mais confiante e com maior autoestima. Foram laços de amizade que se criaram e que permanecerão para sempre.

Um especial obrigado à minha colega da tese, Andreia Gouveia, que me aturou nos últimos sete meses e foi o meu ombro de apoio em dias cinzentos. Quero agradecê-la pelos intermináveis desabafos e pela partilha de bons momentos. Pela amizade, companhia de mesa de secretária e pelo apoio nos momentos de maior angústia.

Ao meu namorado Diogo Duarte, que substituiu a presença dos meus pais, cuidou de mim, levou-me sempre a acreditar que seria capaz de chegar ao fim e esteve sempre presente nos momentos bons e menos bons. Graças a ele, consegui superar todos os obstáculos e lutei constantemente para conseguir chegar o mais longe possível. Ensinou-me a nunca *desistir* dos meus sonhos.

E finalmente à minha família, em especial aos meus pais, um enorme obrigado por terem acreditado em mim e por me terem ensinado a ser a pessoa que sou hoje. Apesar da distância, da tristeza e de muito choro pelo meio, quero retribuir e compensar todo o carinho, apoio e dedicação que me foi oferecido ao longo destes anos. Pais, dedico-vos esta tese.

O meu sincero obrigado a todos!

Palavras-chave

Sistemas aquosos bifásicos, líquidos iónicos, ácidos fenólicos, extração, compostos naturais bioativos.

Resumo

Os ácidos fenólicos são metabolitos secundários provenientes de plantas aromáticas e amplamente espalhados por todo o reino vegetal. Uma vez que as suas propriedades biológicas e farmacológicas têm vindo a desempenhar um papel importante na fitoterapia, estão a ser estudadas e desenvolvidas técnicas para a separação e purificação destes compostos naturais.

Esta tese tem como objetivo explorar novos processos de separação sustentáveis com base em líquidos iónicos (LIs) para a extração de ácidos fenólicos biologicamente ativos. Para tal, foram selecionados três ácidos fenólicos com estruturas químicas semelhantes: ácido cinâmico, ácido p-cumárico e ácido cafeico. Nos últimos anos, tem sido demonstrado que os sistemas aquosos bifásicos (SABs) baseados em líquidos iónicos são alternativas válidas para extração, recuperação e purificação de biomoléculas, quando comparado com SABs convencionais ou com extrações feitas com solventes orgânicos. As colinas representam um avanço em direção a uma química mais sustentável, proporcionando meios para a implementação de técnicas mais eficientes para a separação e purificação de biomoléculas.

Neste trabalho, os sistemas aquosos bifásicos foram implementados utilizando colinas e usando um sal inorgânico de alta densidade de carga (K_3PO_4) ou um polímero de baixo peso molecular – polietileno glicol (PEG) – para promover a separação de fases de soluções aquosas que contenham os três ácidos fenólicos. Estes sistemas permitem a avaliação do efeito da estrutura química de anião sobre a eficiência da extração. Foi apenas utilizado um líquido iónico baseado num catião imidazólio, de forma a avaliar o efeito da sua estrutura química. Foi também estudada a extração seletiva de um único ácido. Em geral, observou-se que os ácidos fenólicos exibem comportamentos muito complexos em soluções aquosas, desde dimerização a polimerização mas também associação com outras moléculas. Estes fenómenos são bastante frequentes, dependendo das condições de pH, e consequentemente dificultam a correta quantificação destes ácidos em solução.

Keywords

Aqueous biphasic systems, ionic liquids, phenolic acids, extraction, biologically active natural compounds.

Abstract

Phenolic acids are aromatic secondary plant metabolites, widely spread throughout the plant kingdom. Due to their biological and pharmacological properties, they have been playing an important role in phytotherapy and consequently techniques for their separation and purification are in need.

This thesis aims at exploring new sustainable separation processes based on ionic liquids (ILs) in the extraction of biologically active phenolic acids**.** For that purpose, three phenolic acids with similar chemical structures were selected: *cinnamic acid*, *p-coumaric acid* and *caffeic acid*. In the last years, it has been shown that ionic liquids-based aqueous biphasic systems (ABSs) are valid alternatives for the extraction, recovery and purification of biomolecules when compared to conventional ABS or extractions carried out with organic solvents. In particular, cholinium-based ILs represent a clear step towards a greener chemistry, while providing means for the implementation of efficient techniques for the separation and purification of biomolecules.

In this work, ABSs were implemented using cholinium carboxylate ILs using either high charge density inorganic salt (K_3PO_4) or polyethylene glycol (PEG) to promote the phase separation of aqueous solutions containing three different phenolic acids. These systems allow for the evaluation of effect of chemical structure of the anion on the extraction efficiency. Only one imidazolium-based IL was used in order to establish the effect of the cation chemical structure. The selective extraction of one single acid was also researched. Overall, it was observed that phenolic acids display very complex behaviours in aqueous solutions, from dimerization to polymerization and also hetero-association are quite frequent phenomena, depending on the pH conditions. These phenomena greatly hinder the correct quantification of these acids in solution.

Contents

List of Abbreviations ..... *XV*

Lisf of Simbology ..... *XVII*

List of Figures ..... *XIX*

List of Tables ..... *XXIII*

1. Introduction *25*

1.1 Motivation 27

1.2 ABS – Aqueous Biphasic System 28

1.3 Ionic Liquids-based Aqueous Biphasic Systems 30

1.3.1 Salting effects in Ionic Liquid aqueous solutions 33

1.3.2 Applications of ionic liquid-based ABS: extraction of biomolecules and added-value compounds 35

1.4 Phenolic Acids 37

1.5 Objectives 41

2. Methodologies *43*

2.1 Chemicals and equipment 45

2.2 Methods 47

2.2.1 Physicochemical properties of IL-based ABS 47

2.2.2 Partitioning coefficients and extraction efficiencies 48

3. Quantification of Phenolic Acids *51*

3.1 Cinnamic, p-Coumaric and Caffeic Acids 53

3.2 Calibration Curves 57

4. Ionic Liquid + Phenolic Acid (aq.) + K_3PO_4 systems *67*

4.1 Implementation of K_3PO_4-based aqueous biphasic systems for the extraction of phenolic acids 69

4.3 Physicochemical properties of IL-based ABS 70

4.4 Partitioning coefficients and extraction efficiencies 72

4.5 Influence of Ionic liquid ions in phenolic acids partitioning 74

4.6 Effect of concentration of the phenolic acids in their partitioning 76

5. Ionic Liquid + Phenolic Acid (aq.) + Polyethylene Glycol systems *81*

5.1 Implementation of PEG-based ABS 83

5.2 Physicochemical properties of IL-based ABS 84

5.3 Partitioning coefficients and extraction efficiencies 87

5.4 Influence of Ionic liquid ions in phenolic acids partitioning 91

6. Selective Extraction *93*

7. General Conclusions *99*

8. References *103*

References 105

Appendix A *109*

Spectra of Phenolic Acids 111

Appendix B *115*

Calibration Curves 117

Appendix C *120*

Physicochemical Properties of Ionic Liquids 122

Experimental Data of the Partition Coefficients 123

Synthesis of Ionic Liquids 125

Appendix D *126*

Mass Transfer 128

Mass Transfer in IL + Phenolic Acids (aq.) + K_3PO_4 systems 128

Mass Transfer in IL + Phenolic Acids (aq.) + Polyethylene Glycol systems 130

Appendix E *131*

NMRs spectrums of Ionic Liquids 133

List of Abbreviations

ABS	Aqueous Biphasic System
IL	Ionic Liquid
IS	Inorganic Salt
CIN	Cinnamic Acid
COU	p-Coumaric Acid
CAF	Caffeic Acid
UV-Vis	Ultra-Violet Visible
NMR	Nuclear Magnetic Resonance
K_3PO_4	Potassium Phosphate Tribasic
PEG 600	Polyethylene Glycol 600
H_2O	Pure water (system Milli-Q)
$[C_4mim]Cl$	1-butyl-3-methylimidazolium Chloride
[Ch]Cl	Cholinium Chloride
[Ch][Ac]	Cholinium Acetate
[Ch][Suc]	Cholinium Succinate
[Ch][Glu]	Cholinium Glutarate
[Ch][Lev]	Cholinium Levulinate
Abs	Absorbance
K_{ACID}	Partition Coefficient of Acid
$LogK_{ACID}$	Logarithm of Partition Coefficient of Acid
TLL	Tie Line Length
EE	Percentage Extraction Efficiency
$[ACID]_{IL}$	Concentration of Acid in the IL-rich phase
$[ACID]_{K3PO4}$	Concentration of Acid in the K_3PO_4-rich phase
$[ACID]_{PEG}$	Concentration of Acid in the PEG 600-rich phase
$m_{ACID-IL}$	Mass of Acid in the IL-rich phase
$m_{ACID-K3PO4}$	Mass of Acid in the K_3PO_4-rich phase
$m_{ACID-PEG}$	Mass of Acid in the PEG 600-rich phase
pKa	Acid Dissociation Constant
ppm	Parts-per million
nm	Nanometer

Lisf of Simbology

λ	Wavelength
ρ	Density
μ	Dynamic Viscosity
S	Solubility
A	Absorbance
ε	Molar Absorptivity
b	Path Length
M_w	Molecular Weight
R^2	Coefficient of determination
K	Partition coefficient

List of Figures

Figure 1.1 – Some commonly used cations and anions in ionic liquids. 30
Figure 1.2 – Chemical structures, respective name and acronyms of all ILs investigated. 32
Figure 1.3 – Chemical structures of the phenolic acids investigated. 38
Figure 1.4 – Extraction techniques and instrumental quantification analysis for phenolic acids. 39
Figure 2.1 – Water activities at room temperature of cholinium-based ABSs: (●) [Ch]Cl; (×) [Ch][Ac]; (■) [Ch][Suc]; (◊) [Ch][Glu]. 46
Figure 2.2 – (a) Experimental set up used for the determination of the partition coefficients and extraction efficiencies of phenolic acids and (b) macroscopic appearance of an ABS composed of an ionic liquid (used in this work) and an inorganic salt (K_3PO_4). 49
Figure 2.3 – Generalized flow sheet of the liquid–liquid extraction of phenolic acids. 49
Figure 3.1 – Chemical species and speciation of cinnamic acid. 53
Figure 3.2 – Chemical species and speciation of p-coumaric acid. 54
Figure 3.3 – Chemical species and speciation of caffeic acid. 54
Figure 3.4 – Spectras of cinnamic, p-coumaric and caffeic acids in water at room temperature. 55
Figure 3.5 – SHIMADZU UV-1800 Spectrophotometer (UV/vis) used in this work. 57
Figure 3.6 – UV-vis spectra of cinnamic acid in water (full line) and in aqueous solution of 40% of K_3PO_4 (dashed line). 58
Figure 3.7 – UV-Vis spectra of p-coumaric acid in water (full line) and in an aqueous solution of 40% of K_3PO_4 (dashed line). 58
Figure 3.8 – UV-Vis spectra of caffeic acid in water (full line) and in an aqueous solution of 40% of K_3PO_4 (dashed line). 59
Figure 3.9 – Possible mechanism of p-coumaric complexation with K_3PO_4. 60
Figure 3.10 – Possible mechanism of caffeic acid complexation with K_3PO_4. 61
Figure 3.11 – Scheme of the partitioning of caffeic acid in alkaline medium. 62
Figure 3.12 – Experimental UV spectra of p-coumaric acid at different compositions of K_3PO_4 (%wt.) and respective pH values with [COU] = 0.0133 $g \cdot L^{-1}$, at room temperature. 63
Figure 3.13 – Experimental UV spectra of caffeic acid at different compositions of K_3PO_4 (%wt.) and respective pH values with [CIN] = 0.0195 $g \cdot dm^{-1}$, at room temperature. 63
Figure 4.1 – Phase diagrams of the ternary systems composed of K_3PO_4 + ionic liquid + H_2O at 298 K (percentage weight fraction): (•)[Ch]Cl; (+) [Ch][Ac]; (■) [Ch][Suc]; (◊) [Ch][Glu]; (▲) [Ch][Lev]; (●) [C_4mim]Cl, literature data [3, 8, 40]. 69
Figure 4.2 – Density (ρ) and viscosity (η) of the coexisting phases in ABS composed of IL + K_3PO_4 + H_2O at 298.15 K. 70
Figure 4.3 – Partition coefficients (K_{ACID}) and extraction efficiencies percentages (%EE_{ACID}) of cinnamic acid (■), p-coumaric acid (■) and caffeic acid (■) for the systems composed of IL + K_3PO_4 at room temperature. 73
Figure 4.4 – Influence of the IL on the partition coefficient of the cinnamic acid (0.147 $g \cdot dm^{-3}$) using IL-based ABS and K_3PO_4, at room temperature. 74

Figure 4.5 – Influence of the IL on the partition coefficient for p-coumaric acid (0.800 g·dm^{-3}) using IL-based ABS and K_3PO_4, at room temperature. 75
Figure 4.6 – Influence of the IL on the partition coefficient for caffeic acid (0.672 g·dm^{-3}) using IL-based ABS and K_3PO_4, at room temperature. 75
Figure 4.7 – Influence of the concentration of cinnamic acid on the partition coefficient, K_{CIN}, using ABS based on IL: ■ – [Ch]Cl; ■ – [Ch][Ac]; ■ – [C_4mim]Cl. Th results were obtained with a concentration between 4.79×10^{-4} and 1.54×10^{-3} mol·dm^{-3} at room temperature..... 78
Figure 4.8 – Influence of the concentration of p-coumaric acid on the partition coefficient, K_{COU}, using ABS based on IL: ■ – [Ch]Cl; ■ – [Ch][Ac]; ■ – [C_4mim]Cl. This results were obtained with a concentration between 4.00×10^{-3} and 6.05×10^{-3} mol·dm^{-3} at room temperature..... 78
Figure 4.9 – Influence of the concentration of caffeic acid on the partition coefficient, K_{CAF}, using ABS based on IL: ■ – [Ch]Cl; ■ – [Ch][Ac]; ■ – [C_4mim]Cl. This results were obtained with a concentration between 2.89×10^{-3} and 4.93×10^{-3} mol·dm^{-3} at room temperature..... 79
Figure 5.1 – Phase diagrams of the ternary systems composed of PEG 600 + ionic liquid + H_2O at 298 K (percentage weight fraction): (•)[Ch]Cl; (+) [Ch][Ac]; (■) [Ch][Suc]; (◊) [Ch][Glu]. [13, 32] 83
Figure 5.2 – Experimental density (ρ) as a function of temperature for the PEG-rich phase (full symbols) and IL-rich phase (open symbols) for systems composed by ILs: (■) [Ch]Cl; (●) [Ch][Ac]; (●) [Ch][Suc]; (■) [Ch][Glu]. 84
Figure 5.3 – Experimental viscosity (η) as a function of temperature for the PEG-rich phase (full symbols) and IL-rich phase (open symbols) for systems composed by ILs: (■) [Ch]Cl; (●) [Ch][Ac]; (●) [Ch][Suc]; (■) [Ch][Glu]. 85
Figure 5.4 – Viscosity (η) of the coexisting phases in ABS composed of IL + PEG 600 + H_2O at 298.15 K. 85
Figure 5.5 - Partition coefficients (K_{ACID}) and extraction efficiencies percentages (%EE_{BIO}) of cinnamic acid (■), p-coumaric acid (■) and caffeic acid (■) for PEG 600-based ABS at room temperature. 89
Figure 5.6 – Logarithm representation of the phenolic acids partition coefficients (logK_{ACID}) for PEG 600-based ABS at room temperature. The pH values of the top (IL) and bottom (PEG 600) phases are also presented. 90
Figure 5.7 – Influence of the IL on the partition coefficient for cinnamic acid (0.147 g·dm^{-3}) using IL-based ABS and PEG 600 at room temperature. 91
Figure 5.8 – Influence of the IL on the partition coefficient for p-coumaric acid (0.800 g·dm^{-3}) using IL-based ABS and PEG 600 at room temperature. 92
Figure 5.9 – Influence of the IL on the partition coefficient for caffeic acid (0.672 g·dm^{-3}) using IL-based ABS and PEG 600 at room temperature. 92
Figure 6.1 – Logarithmic function of cinnamic and caffeic acids partition coefficients (logK_{acid}) in the ABS composed of PEG 600 + [Ch]Cl and [Ch][Ac] at room temperature. 97
Figure 6.2 – Logarithmic function of p-coumaric and caffeic acids partition coefficients (logK_{acid}) in the ABS composed of PEG 600 + [Ch][Ac] at room temperature. 98

Figure 9.1 – Spectra of cinnamic acid absorbance at a wavelength of 270.1 nm in different diluted aqueous solutions. 111
Figure 9.2 – Spectra of p-coumaric acid absorbance at a wavelength of 286 nm in different aqueous solutions. 111
Figure 9.3 – Spectra of caffeic acid absorbance at a wavelength of 290 nm in different diluted aqueous solutions. 112
Figure 9.4 – Spectra of p-coumaric acid absorbance at a wavelength of 331 nm in different diluted aqueous solutions of K_3PO_4. 112
Figure 9.5 – Spectra of caffeic acid absorbance at a wavelength of 267.5 nm in different diluted aqueous solutions of K_3PO_4. 113
Figure 9.6 – Spectra of p-coumaric acid (286 nm) in IL-rich phase of system composed of PEG 600 + Cholinium-based IL. 113
Figure 9.7 – Spectra of p-coumaric acid (286 nm) in PEG 600-rich phase of system composed of PEG 600 + Cholinium-based IL. 114
Figure 10.1 – Calibration curve for cinnamic acid (270.1 nm) in aqueous solution at room temperature. 117
Figure 10.2 – Calibration curve for p-coumaric acid (286 nm) in aqueous solution at room temperature. 117
Figure 10.3 – Calibration curve for caffeic acid (290 nm) in aqueous solution at room temperature. 117
Figure 10.4 – Calibration curve for caffeic acid (312 nm) in aqueous solution at room temperature. 118
Figure 10.5 – Calibration curve for p-coumaric acid (331 nm) in aqueous solution of K_3PO_4 at room temperature. 118
Figure 10.6 – Calibration curve for caffeic acid (267.5 nm) in aqueous solution of K_3PO_4 at room temperature. 118
Figure 10.7 – Calibration curve for p-coumaric acid in PEG 600 (●) and IL-rich (▲) phases at room temperature. 119
Figure 13.1 – ^{1}H-NMR spectrum of [Ch][Suc] in D_2O. 133
Figure 13.2 – ^{1}C-NMR spectrum of [Ch][Suc] in D_2O. 133
Figure 13.3 – ^{1}H-NMR spectrum of [Ch][Glu] in D_2O. 134
Figure 13.4 – ^{1}C-NMR spectrum of [Ch][Glu] in D_2O. 134

List of Tables

Table 1.1 – Structures of some prominent naturally occurring phenolic acids. 37
Table 2.1 – Typical water content data obtained for all the ILs studied in this work. 45
Table 3.1 – Solubility in water (S_W) and dissociation constants of phenolic acids at 298.2 K [31-33]. 53
Table 3.2 – Wavelengths of functional group constituents of phenolic acids. 56
Table 3.3 – Wavelengths corresponding to the maximum absorption and respective pH in water and in an aqueous solutions of K_3PO_4. 59
Table 3.4 – Effect of the compositions of K_3PO_4 in the absorbance p-Coumaric acid and pH values, at room temperature. 64
Table 3.5 – Effect of the compositions of K_3PO_4 in the absorbance p-Coumaric acid and pH values, at room temperature. 64
Table 3.6 - Calibration curves for each phenolic acid in aqueous solutions with or without K_3PO_4. 65
Table 4.1 – Composition of the initial mixtures used to prepare the ampoules. 69
Table 4.2 – Comparison of the pH, density and viscosity at 298.15 K for the two phase in equilibrium in the K_3PO_4 - based ABS used in the present work 70
Table 4.3 – Partition coefficient and extraction efficiencies of phenolic acids obtained in this work at room temperature. 72
Table 4.4 – Concentration of the phenolic acids in two new aqueous solutions, at room temperature. 76
Table 4.5 – Initial concentration and partition coefficient of phenolic acids obtained in this work at room temperature. 77
Table 4.6 – Initial concentration and extraction efficiencies of phenolic acids ($\%EE_{ACID}$) obtained in this work at room temperature. 77
Table 5.1 - Compositions of ionic liquid and PEG at the initial mixture used to prepare the ampoules. 83
Table 5.2 – Experimental pH, density and viscosity for the cholinium-rich phase and PEG-600-rich phase for systems composed by IL + PEG + H_2O at 298.15 K. 84
Table 5.3 – Solubility of p-coumaric acid in both aqueous phases. 88
Table 5.4 – Weight fraction composition of the initial mixture, TLL and partition coefficient of phenolic acids obtained at room temperature. 88
Table 5.5 – Standard deviations and errors obtained for the partition coefficients values at room temperature. 88
Table 6.1 – Selectivity parameters for caffeic/cinnamic ($S_{CAF/CIN}$) and caffeic/coumaric ($S_{CAF/COU}$) considering all PEG 600-ILs-based ABS tested at room temperature. 96
Table 6.2 – Partition coefficients of caffeic (K_{CAF}) and cinnamic (K_{CIN}), and selectivity parameters for the caffeic + cinnamic ($S_{CAF/CIN}$) pair in the ABS composed of PEG 600 + [Ch][Ac] at 298.15 K. 96

Table 6.3 – Partition coefficients of caffeic (K_{CAF}) and p-coumaric (K_{COU}), and selectivity parameters for the caffeic + p-coumaric ($S_{CAF/COU}$) pair in the ABS composed of PEG 600 + [Ch][Ac] at room temperature. 98
Table 10.1 – Viscosity (η) and density (ρ) of the coexisting phases in ABS composed of cholinium-based ionic liquid + PEG 600 + H_2O at various temperatures. 122
Table 10.2 – Partition coefficients (K), respective standard deviations (σ) and mixture compositions at room temperature. 123
Table 10.3 – Partition coefficients (K), respective standard deviations (σ) and mixture compositions at room temperature. 124
Table 11.1 – Validation of cinnamic acid quantification through mass balance. 128
Table 11.2 – Validation of p-coumaric acid quantification through mass balance. 129
Table 11.3 – Validation of caffeic acid quantification through mass balance. 129
Table 11.4 – Validation of the quantification of cinnamic acid through mass transfer. 130
Table 11.5 – Validation of the quantification of caffeic acid through mass transfer. 130
Table 11.6 – Validation of the quantification of p-coumaric acid through mass transfer. 130

1. Introduction

1. Introduction

1.1 Motivation

Separation and purification technologies play a central role in the chemical industry not only due to their impact in the quality of the final product, but also to the high level of energy and enormous amounts of solvent mixtures to separate. Typically, organic volatile solvents (VOCs) are mostly used in separation processes due not only to their properties such as immiscibility in water, but also to its low cost. As environmental concerns about VOCs increase and new more restrictive regulations are imposed, there is a growing interest in finding novel environmental friendly replacement solvents for the liquid–liquid separation processes. As alternatives to VOCs ionic liquids have been emerging as a new class of solvents. Ionic liquids belong to the organic salt class and present an attractive combination of properties. Among these properties, the most important is, perhaps, their flexibility to be designed and thus the possibility of tuning the chemical structure and thus the properties given any specific application. The advantages of the implementation of extraction techniques using these solvents was soon realized by the scientific community and research on this topic has been proficuous. In particular, the development of aqueous biphasic systems, systems where water is the major component in both phases, has been reported as an attractive technique for the separation and purification of biomolecules.

The recent interest in compounds derived from natural sources, opposing compounds synthesized through chemical routes, has been motivating a lot of research not only on the benefits of natural compounds and extracts but also on the development of extraction techniques suitable for natural matrices. In particular, phenolic acids present in fruits and vegetables, display an important protective role against oxidative damage diseases (coronary heart disease, stroke and cancers).

All these aspects motivated the research presented in this thesis. Consequently, new extraction techniques, in this case aqueous biphasic systems, were chosen to be investigated in the extraction of phenolic acids. Environmentally benign ionic liquids were chosen to implement this technique and several experimental variables will be manipulated in order to understand the mechanism of extraction and achieve the best separation performance.

1.2 ABS – Aqueous Biphasic System

In industry, liquid–liquid extraction processes are important techniques used for the extraction and purification of biomolecules due to their high versatility, ranging from an higher yield, improved purity degree, proper selectivity, technological simplicity and lower cost, to a good combination between the recovery and purification steps.[1] The extraction of biomolecules is typically carried out using volatile organic solvents because of their immiscibility with aqueous media. The most commonly used organic solvents present some disadvantages, such as high volatility and toxicity. Aiming at avoiding the use of organic volatile solvents as the extractive phase, one of the potential methods relays on the implementation of aqueous biphasic systems (ABSs). This technique is relatively simple and inexpensive, of easy operation allowing its scale-up, and further ensures the purification and concentration stages to be integrated in a single step procedure.

Since ABSs are mainly composed of water they were immediately recognized as biocompatible processes. In the last decade (since the 1980's), it has been extended to the separation of cells, membranes, viruses, proteins, nucleic acids, enzymes and other added-value biomolecules. Separation of biomolecules using ABSs as an alternative to traditional liquid–liquid extraction techniques, dates to 1958 and was introduced by Albertson.[2]

An aqueous biphasic system consist of two aqueous-rich phases containing typically *polymer–polymer*, *polymer–salt* or *salt–salt* combinations that phase separate above a given concentration: one of the aqueous phases will be enriched in one of the solutes while in the other phase there is prevalence for the second polymer or salt.[3, 4] Traditionally, ABSs are formed by combining aqueous solutions of two hydrophilic polymers, such as polyethylene glycol (PEG) and dextran, or alternatively, a polymer and an inorganic salt, such as the PEG-sodium phosphate system.[5] Recently, other species, namely proteins or surfactants, have also been studied to induce the formation of ABSs when mixed with polymers or salts. However, of all the solutes capable of forming ABS, the recent application of ionic liquids (ILs) appears as one of the most attractive. In 2003, Rogers and co-workers[6] showed that ABSs could be formed by mixing a hydrophilic IL and a high charge density inorganic salt.

Polymer-based systems usually exhibit two hydrophobic phases and the difference in polarities depends essentially on the amount of water in each phase. On the other hand, *polymer–salt* ABS have a hydrophobic phase constituted by the polymer and a hydrophilic (and more ionic) phase, typically formed by high charge-density salts. The restricted difference in polarities between the two phases prevents a vast use of *polymer-based* ABS for extraction purposes. By virtue of their tenability, ionic liquids can "ideally" cover the whole hydrophilicity–hydrophobicity range. Even when dealing with conventional ABS, the addition of small amounts of ILs as adjuvants allows the adjustment of intrinsic properties of the coexisting phases and tuning of extraction efficiencies for a given biomolecule. *Polymer–salt* ABS provide more advantages over systems formed by

polymer–polymer combinations, such as a low interfacial tension, fast and high phase separation rates and low cost, which makes them practical for downstream processing.[7]

1.3 Ionic Liquids-based Aqueous Biphasic Systems

The study of a new group of environmentally friendly solvents, ionic liquids, has grew intensely during the last decade and the implementation of ionic liquid-based ABSs for the effective extraction and purification of the most diverse biomolecules, where results up to complete extraction and concentration factors up to 100 times, were achieved.[7-9]

Ionic liquids are commonly defined as organic salts composed entirely of ions, in contrast to common electrolytes, with melting temperatures lower than 373 K (100 °C). They were originally suggested as alternative solvents for the replacement of volatile organic compounds (VOC) currently used in industrial processes. In addition, the tenability of the IL physicochemical properties, resulting from a proper combination of their ions, allows the preparation of specific solvents for separation and purification processes.[10] This means that all properties can be tuned by varying the structure of the component ions to obtain desired characteristics, e.g. polarity, density, viscosity, hydrophobicity, hydrogen-bonding capability, thermal stability or toxicity. This aspect is indeed a major benefit of ionic-liquid-based ABS, given the difficulty of overcoming the limited polarity range of *polymer-based* ABS as defined previously.

The interest in the applications of these fluids has led to the development of an extensive range of IL ions, and to the exploitation of applications, including the use as electrolytes, lubricants, biphasic chemical processes, or biomass processing.[11]

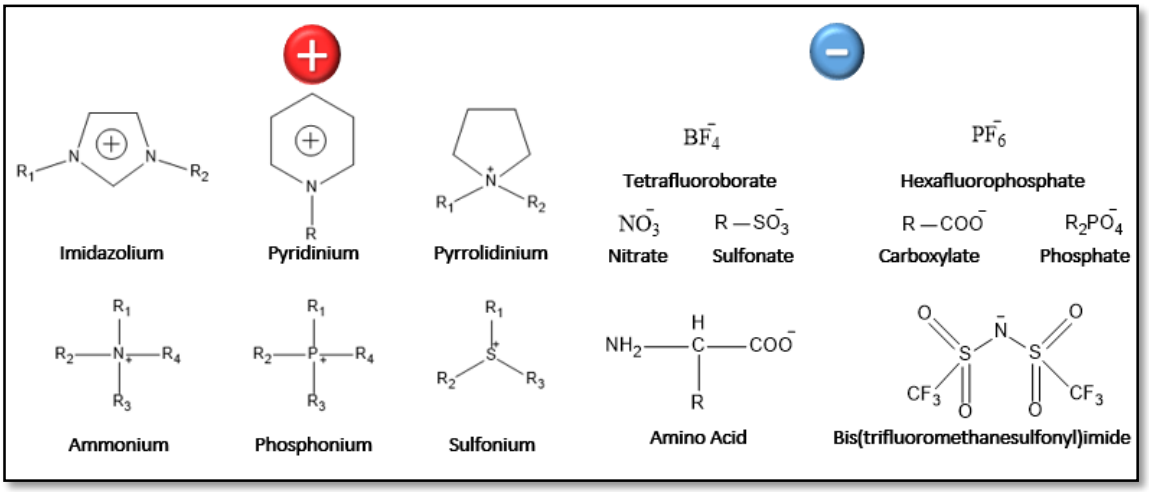

Figure 1.1 – Some commonly used cations and anions in ionic liquids.

A recent review on IL-based ABS addressed their phase diagrams and highlighted their excellent performance in the extraction of a variety of biomolecules.[4] In particular, IL-based ABS shown better extractive over conventional polymer-based systems, since the limited hydrophobic-hydrophilic range exhibited by the coexisting phases formed by two polymers or one polymer and an inorganic salt is overcome when employing ILs. On top of that, the addition of small amounts of ILs as adjuvants in polymer-salt ABSs allows the adjustment of the intrinsic properties of the coexisting phases and tuning of the extraction efficiencies for a given biomolecule.[12]

Why are ionic liquids being used for "*greener chemistry*"? A handful of properties characterizes these solvents, such as:

- No vapour pressure: low volatility and low flammability;
- Thermal and chemical stability;
- Liquid over large range of temperature;
- Electric conductivity;
- Tuneable solvating properties: density, viscosity, hydrophobicity, toxicity;
- Easy to buy and simple to prepare.

Ionic liquid's chemical diversity offers unique opportunities to develop solvents for specific purposes by modifying the structures of both cation and/or anion. In bio-extraction and bio-purification processes, their most important property in terms of clean chemistry is the negligible vapour pressure of these fluids and their low toxicity by design, since these processes are all carried out at low temperatures. Moreover, despite from the fact that the early ILs generations were expensive and somewhat toxic, ILs can also be designed from affordable materials, providing ILs that are easy to handle, less toxic and cheaper than the more commonly studied ILs.

Considering the potential application of ABS for the extraction of added-value compounds and their mandatory biocompatibility and biodegradability issues, a new class of ABS composed of cholinium-based cations ($[Ch]^+$) ILs and K_3PO_4 (as the inorganic salt) was recently proposed as a valuable alternative.[8] The cholinium-based ILs/salts are constituted by the 2-hydroxyethyl-N,N,N-trimethylammonium cation combined with anions as diverse as chloride, bicarbonate, acetate, succinate, malate, among others. While the cation has a deciding role in the toxicity of the IL, both cation and anion play an essential role in the ionic liquid's physicochemical properties, and it is known that the anion also to contribute to the overall toxicity, but its effect is usually neglected. The ABS formation is controlled by the interplay of the relative strengths of the solute (ions from the ionic liquid), the salting agent (ions from the inorganic salt) and the solvent (water), with a significant contribution from hydration phenomena and thus specific hydrogen-bonding between the IL and inorganic salt.

Chemical structures of the cholinium-based ABS employed in this work are shown in Figure 1.2.

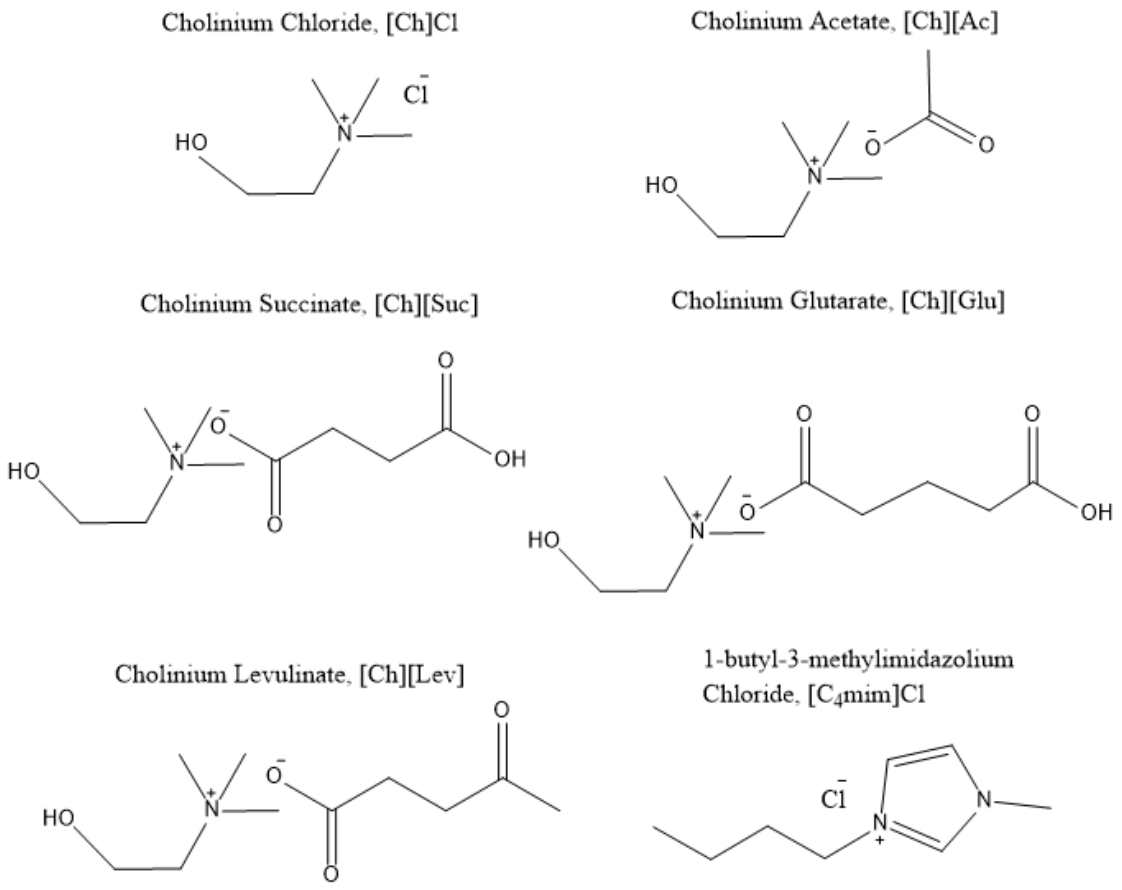

Figure 1.2 – Chemical structures, respective name and acronyms of all ILs investigated.

The possibility of forming polymer-IL-based ABS was also reported [10, 13, 14], although it seems to be by far more complex. For example, for polyethylene glycol (PEG), the molecular phenomenon which governs the formation of an immiscible is intricate with similar contributions from IL-water, PEG-water and PEG-IL. Nevertheless, the use of polyethylene glycol is frequent because it presents high biodegradability, low toxicity, low volatility, low melting temperature, large water miscibility and low cost.

The efficient application of ABS for separation, extraction, or purification, requires the knowledge of the specific mechanism behind the product partitioning between the two aqueous phases of an ABS.

1.3.1 Salting effects in Ionic Liquid aqueous solutions

When a high charge density salt such as tripotassium phosphate (K_3PO_4) is dissolved in an aqueous solution, the isolated ions are surrounded by a layer of water molecules, a phenomenon known as ionic hydration.[15] Those water molecules are immobilized and their role as solvents to other molecules or ions is reduced. When an inorganic salt such as potassium phosphate tribasic is added to a solution of a hydrophilic ionic liquid, they compete with each other for the solvent molecules. The competition is "won" by the inorganic ions (with a stronger affinity for the solvent), conversely, those of the ionic liquid "lose". There is a migration of solvent molecules away from the ions of the ionic liquid to those of the inorganic salt, which, in turn, decreases the hydration and hence the solubility of the ions of the ionic liquid. As a consequence, a phase-rich in ionic liquid separates from the rest of the solution. This means that the salting-out effect must be directly correlated to the hydration strength of the different ions of the inorganic salt.

During the partition of biomolecules there are several competing interactions between the IL, the inorganic salt, the biomolecules and the water. Hydrogen–bonding, π – π interactions, dispersive interactions, as well as electrostatic interactions between different compounds (complexations interactions), are some examples of these interactions to be taken into account in the partitioning coefficients.

To better understand the mechanism of the formation of aqueous biphasic systems, it is important to know the salting effects occurring during the phase separation of an ABS. A salting effect can be defined as the process by which the solubility of a solute in a given solution is changed when a salting agent is added to that solution.

If the solubility of the solute is decreased when the salting agent is added, which can lead to the solute precipitation (separation from the solution), the process is called a *salting-out* effect. Conversely, a *salting-in* effect occurs when the solubility of the solute increases upon addition of the salting agent. Traditionally, salting effects have been studied in aqueous solutions in which the solutes are non-electrolytes or low-solubility electrolytes and the salting agents are strong electrolytes, namely soluble inorganic salts with high solubility in water.

Since ionic liquids are composed exclusively of anions and cations (although some non-charged aggregates can also be found), they can be used either as salting agents, in the presence of a non-electrolyte solute, or as solutes in the presence of an inorganic electrolyte. Meanwhile, IL are liquid at room temperature and consequently they do not precipitate when "salted-out" from the aqueous solution by a strong salting agent; on the contrary, they form a second liquid phase in equilibrium with the initial aqueous solutions: they promote the formation of aqueous biphasic systems. Thus, when using an inorganic salt, such as K_3PO_4, as salting-out inducing agents, the ionic liquid behaves as a solute.

When dealing with polyethylene glycol – a polymer – the addition of a strong electrolyte will decrease substantially the solubility of PEG in water (salting-out effect). When replacing the traditional salting agents by ionic liquids, a new type of salting effect behaviour emerges.

Depending on the nature of the ionic liquid one witnesses a whole range of salting-in (higher PEG solubility) or salting-out effects (lower PEG solubility). However, ionic liquids can promote salting-in effects and be used as switches to trigger miscibility in PEG aqueous solutions, in a way similar to that of inorganic salts that are commonly used to trigger the opposite outcome. Therefore, polyethylene glycol can be used as solute in salting processes involving ionic liquids.[16]

1.3.2 Applications of ionic liquid-based ABS: extraction of biomolecules and added-value compounds

The key elements of ILs are organic cations, which determine their chemical stability. They are produced by alkylation of, for example, amines, imidazoles, pyridines or phosphines. Among them, ammonium and imidazolium salts are especially stable. By varying the inorganic anions, the physical properties of the IL can be optimized specifically. Therefore, ILs are sometimes called "designer solvents", as they can be custom designed to fit different requirements.

This opens up a wide range of possible applications in which ionic liquids can be used, for example:

- As reaction media in chemical processes;
- As process chemicals for separation processes;
- As liquid–liquid extraction or distillation;
- As cleaning agents;
- As process chemicals in metal treatment and cleaning;
- As electrolytes in batteries or capacitors.

Although many of these applications are still in the stage of basic research, a few ILs have already been exploited in the chemical industry.[17]

Some ILs are suitable for conventional liquid–liquid water-based extractions because of their immiscibility with water, which allows the formation of two immiscible phases, as well as the partition of a vast solutes in aqueous solutions of ILs. However, the implementation of extraction processes based on hydrophobic ionic liquids on a large scale will be limited due to monetary and environmental costs, since these types of ionic liquids usually contain expensive and non-stable anions. Given this limitation, the potential to apply hydrophilic ionic liquids in separation schemes is much greater due to the availability of ''greener'' anions and less expensive materials. One way to achieving a separation process using hydrophilic ILs is through the combined use of a salting out agent, such a salt, a polymer, an aminoacid, a sugar. The design of safe and environmentally benign separation processes plays an increasingly important role in the development of extraction technology.[18]

Two main applications were found in the literature for ionic-liquid-based ABS and will be presented in this thesis: the recovery of ionic liquids from aqueous media; and the extraction of a wide range of biomolecules, from alcohols, through pharmaceuticals and proteins, and up to phenolic acids.[4]

Although ionic liquid-based ABS are mostly used in the extraction of biomolecules, their intrinsic nature also provides an effective direction for the recovery of hydrophilic ionic liquids from aqueous solutions. As the environmental impact of ILs is still an open issues, their removal from water is especially important when dealing with their application on a large scale and in related wastewater streams. In fact, for the industrial application of these ionic liquids, their recovery and recycling are a very important step. The use of aluminium-based salts to form ABS, for removing

and recovering ionic liquids from aqueous media, has been recently approached.[19] Indeed, aluminium-based salts are actually widely used as coagulants in drinking water treatment processes.

The use of inorganic salts as salting-out agents, which usually contain highly charged anions (mostly phosphate, hydroxide, and carbonate), can cause environmental risks due to the high concentrations of salt required. Consequently, the introduction of these types of ions complicates the recycling of the ionic liquids. However, as an alternative, carbohydrates can be introduced and thus develop sustainable IL-based ABS, since they are non-charged, biodegradable, non-toxic and a renewable feedstock.

The ability to control the aqueous miscibility of hydrophilic ionic liquids by implementing salting-out phenomenon to induce phase separation is of particular importance for the recovery of this type of ionic liquids from aqueous solutions, hence overcoming wastewater contamination issues and promoting the industrial application of the novel solvents.

Extractions of added-value compounds have been studied in a vast range of literature and are divided by four main classes of solutes: alkaloids, pharmaceuticals, amino acids and proteins.[20]

Freire and co-workers[21] showed that the complete extraction of *alkaloids*, such as caffeines and nicotine, is possible and achieved in a single-step procedure by a proper tailoring of the ionic liquid employed in the ABS formulation. The results showed that complete extraction of each alakaloid is attained at a partition coefficient greater than 120. *Amino acids* are a class of useful bio-products which are Ionic-liquid-based ABS have been successfully applied to the extraction of amino acids.[7, 22]

1.4 Phenolic Acids

Phenolic acids are aromatic secondary plant metabolites, with more than 8 000 structures known, widely spread throughout the plant kingdom. There is an interest in phenolic acids because of their biological roles as secondary metabolites and their function in food quality and they are partially responsible for the organoleptic properties of plant foods. Recent interest in phenolic acids stems from their potential protective role, through ingestion of fruits and vegetables, against oxidative damage diseases (coronary heart disease, stroke and cancers).[23] They are widespread constituents of plant foods (fruits, vegetables, cereals, olive, legumes, chocolate, etc.) and beverages (tea, coffee, beer, wine…).[24]

Phenolic acids can also be raw materials for the synthesis of different molecules with industrial interest, such as nutraceuticals, cosmetics, antioxidants, and flavours; they also can be used in the preparation of resins, plasticizers, dyes and pharmaceutical products.[25]

The term phenolic acid, in general, designates phenols that possess one carboxylic acid functionality. These naturally occurring phenolic acids contain two distinctive carbon frameworks: the *hydroxycinnamic* and *hydroxybenzoic* structures, depicted in Table 1.1. Although the basic skeleton remains the same, the numbers and position of the hydroxyl groups on the aromatic ring make the difference and establish variety.[26]

Table 1.1 – Structures of some prominent naturally occurring phenolic acids.

Hydroxybenzoic Acids					**Hydroxycinnamic Acids**				
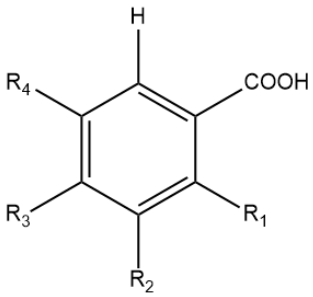					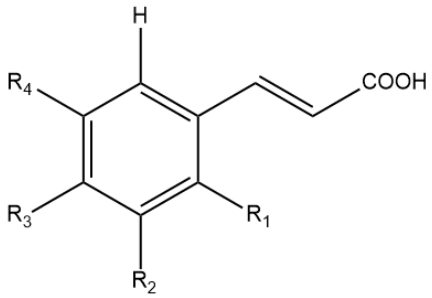				
Name	**R_1**	**R_2**	**R_3**	**R_4**	**Name**	**R_1**	**R_2**	**R_3**	**R_4**
Benzoic acid	H	H	H	H	**Cinnamic acid**	H	H	H	H
p-Hydroxybenzoic acid	H	H	OH	H	**o-Coumaric acid**	OH	H	H	H
Vanillic acid	H	OCH_3	OH	H	**m-Coumaric acid**	H	OH	H	H
Gallic acid	H	OH	OH	OH	**p-Coumaric acid**	H	H	OH	H
Protocatechuic acid	H	OH	OH	H	**Ferulic acid**	H	OCH_3	OH	H
Salicylic acid	OH	H	H	H	**Caffeic acid**	H	OH	OH	H

Hydroxycinnamic acids and their derivatives are almost exclusively derived from p-coumaric acid, caffeic acid, and ferulic acid whereas sinapic acid is, in general, less encountered. Caffeic acid and its esterified derivatives are the most abundant hydroxycinnamic acids in a variety of fruits and vegetables. Ferulic acid and its derivatives are the most abundant hydroxycinnamic acids found in cereal grain. On the other hand, tea can be an important source of gallic acid which is a hydroxybenzoic acid. Despite all this diversity in plants, only a minor fraction exists in the free acid form. This variety is one of the factors contributing to the complexity of the analysis of phenolic acids.

The phenolic acids studied in this work are three particular phytochemical compounds, they are: cinnamic acid, p-coumaric acid and caffeic acid. These phenolic acids were chosen because of their important role in the diet of humans.

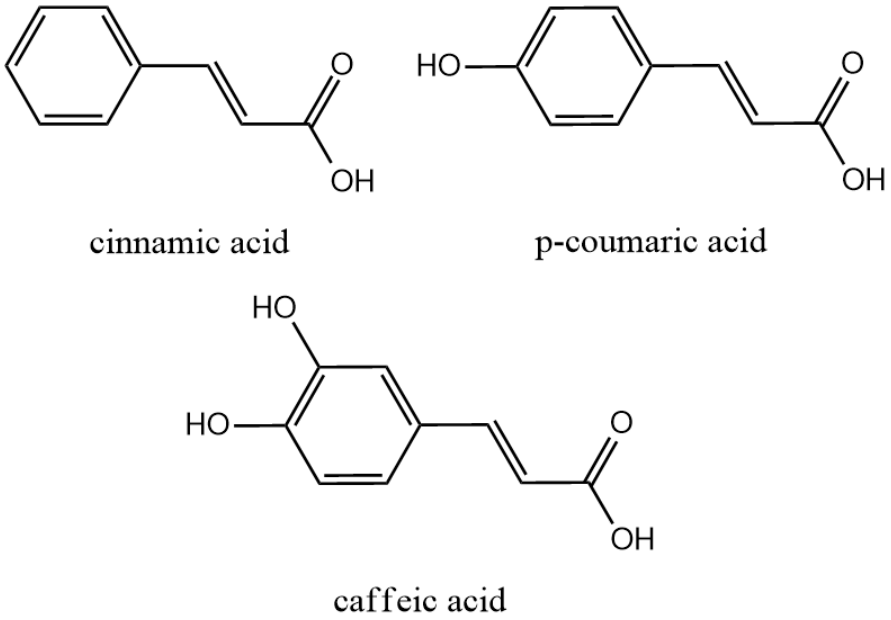

Figure 1.3 – Chemical structures of the phenolic acids investigated.

Cinnamic acid (*3-phenyl-2-propenoic acid*) has a particular place in plant metabolism. The progenitor of the name is the spice cinnamon, known and used by humans for at least 4000 years. Generally present in trace quantities, this compound may be the major constituents of certain natural oils and resins, namely oils of basil and cinnamon.[27, 28] Cinnamic acid is also used in flavours and certain pharmaceuticals.

p-Coumaric acid (*3-(4-hydroxyphenyl)-2-propenoic acid*) is another phenolic acid of great interest due to its chemoprotectant and anti-oxidant properties. This hydroxycinnamic acid related to cinnamic acid is a phenolic phytochemical found in plants.[29]

Caffeic acid (*3-(3,4-dihydroxyphenil*)-2-propenoic acid) is a well-known phenolic phytochemical present in many foods and is one the most common phenolic acids frequently occurred in fruits, vegetables, cereals, legumes and in beverage of plant such as wine, tea and coffee.[30] Recent

studies suggested that caffeic acid exerts anticarcinogenic effects.[31] It is found in all plants because it is a key intermediate in the biosynthesis of lignin, one of the principal components of plant biomass and its residues.[32] Their chemical structures are shown in Figure 1.3.

The extraction of bioactive compounds from plant materials is the first step in the utilization of phytochemicals in the preparation of dietary supplements or nutraceuticals, food ingredients, pharmaceutical, and cosmetic products. Phenolics can be extracted from fresh, frozen or dried plant samples. The selection of the detection method is influenced by their chemical nature, the extraction method employed, sample particle size, as well as the presence of interfering substances.

Schematic of strategies for the determination of phenolic acids in biological fluids, beverages, plants, and food is shown in Figure 1.4.[23, 24, 26]

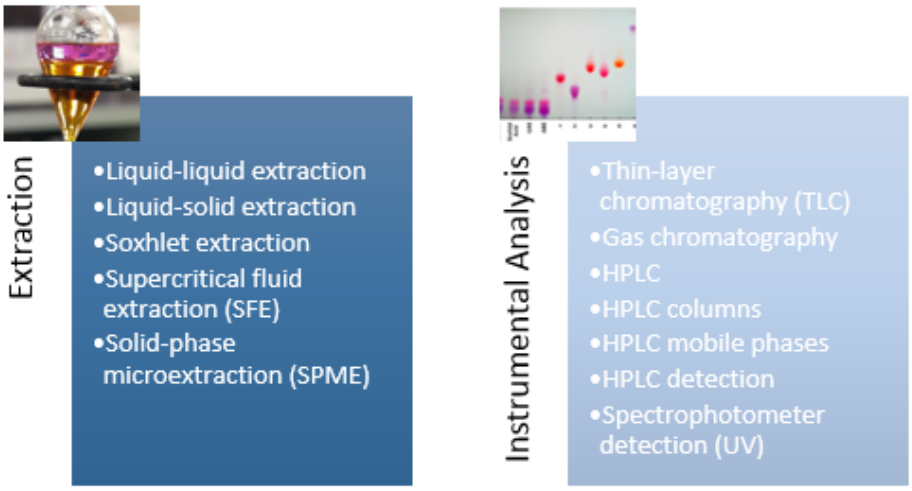

Figure 1.4 – Extraction techniques and instrumental quantification analysis for phenolic acids.

Liquid-liquid and solid-liquid extraction are the most commonly used procedures to extract phenolics from natural plant matrixes. This is due to their ease of use, efficiency, and wide-ranging applicability. Solvent extractions most commonly used are alcohols (methanol, ethanol), acetone, diethyl ether, and ethyl acetate. Other conventional extraction methods such as soxhlet extraction have shown low efficiency and potential environmental pollution due to large volumes of organic solvent used and long extraction time required in those methods. Also, they cannot be easily scaled-up.

In the last twenty years, HPLC has been the analytical technique that has dominated the separation and characterisation of phenolic compounds. HPLC techniques offer a unique chance to separate simultaneously all analysed components together with their possible derivatives products. In many cases, they allow the determination of low concentrations of analytes in the presence of many other interfering components.

However, phenolic acids are commonly detected using Ultraviolet/Visible (UV/Vis) spectroscopy, once the existence of conjugated double and aromatic bonds, every phenol exhibits a higher or

lower absorption in the UV/Vis region. Simple phenolics have absorption maximum peak between 220 and 320 nm but their absorption is affected by the nature of the solvent and the pH of the solution. On top of this, the possibility of interference by UV-absorbing substances such as proteins, nucleic acids, and amino acids should also be considered. Both UV and visible spectroscopic techniques are used for the identification of isolated phenolic compounds.

1.5 Objectives

In this work, the efficiency of aqueous biphasic systems in the extraction of three phenolic acids, caffeic, cinnamic and p-coumaric, from aqueous solutions was evaluated. For that purpose, the newly proposed ABS containing cholinium-based ILs were used.[8] The use of nontoxic ILs represents a further step towards the implementation of greener processes. One imidazolium-based Ils was also used in order to verify possible effects arising from the aromaticity of these IL family. Two different salting out agents were tested: K_3PO_4 and PEG-600. The choice of K_3PO_4 was due to its high salting out capacity. However, it should be kept in mind that this salt presents severe pH experimental conditions (pH around 12). PEG-600 was also used in the extraction was chosen since it provides milder extraction conditions.

For the quantification of the phenolic acids, the analytical method chosen here was the UV/vis spectrophotometry due to its simplicity and easy analysis. The quantification of the acids was always performed in both phases. A mass balance analysis was carried out in order to evaluate/detect any possible loss of compounds arising from the separation of the phases in equilibrium.

All the extractions were carried out at room temperature and atmospheric pressure. The effect of the concentration of the biomolecules in the extraction efficiency was also evaluated.

Last, selective extractions of each one of the acids were carried out using aqueous solutions with a mixture of two acids.

2. Methodologies

2. Methodologies

2.1 Chemicals and equipment

Two different types of ABS were used in this work for the extraction of the three phenolic acids: K_3PO_4 and PEG containing systems. The ionic liquids used were 1-butyl-3-methylimidazolium chloride ([C_4mim]Cl]; >98.0 wt. % pure), provided by Iolitec, cholinium chloride ([Ch]Cl; ≥ 98.0 wt. % pure), provided by Sigma-Aldrich, cholinium acetate ([Ch][Ac]), cholinium succinate, ([Ch][Suc]), cholinium glutarate, ([Ch][Glu]) and cholinium levulinate, ([Ch][Lev]). All the cholinium-based ILs, with the exception of cholinium chloride, were synthesized in the laboratory. In order to reduce the water content, the ILs were dried under constant stirring, at moderate temperature around (318.15 K) and high vacuum conditions (0.01 mbar) for a time minimum of 24h. Their purities were additionally determined by ^{1}H and ^{13}C NMR spectrums and are provided in Appendix E. The IL's chemical structures are shown in Figure 1.2. A brief explanation of the synthesis of the ionic liquids is presented in Appendix C.

Potassium phosphate tribasic salt (K_3PO_4) and poly(ethylene glycol), with an average molecular weight of 600 g·mol^{-1} (PEG 600) were purchased at Sigma-Aldrich and used as received.

The water content of all the ILs and the polyethylene glycol was measured with the Karl-Fisher Coulometer's equipment (831 KF Coulometer Metrohm) and was taken into account before the preparation of the ampoules. In general, the water content of IL samples after the drying procedure was found to be higher than 10.000 ppm, whereas the water content of PEG was lower than 3000 ppm (1 437.700 – 2 510.837 ppm). The typical water content data obtained for used ILs is depicted in Table 2.1.

Table 2.1 – Typical water content data obtained for all the ILs studied in this work.

Ionic Liquid	Water content / ppm	Water content / wt%
[C_4mim]Cl	2 001.42	0.200
[Ch]Cl	10 192.59	1.019
[Ch][Ac]	34 036.68	3.404
[Ch][Suc]	10 094.03	1.009
[Ch][Glu]	45 627.06	4.563
[Ch][Lev]	52 410.47	5.241

The phenolic acids used as partitioning solutes were cinnamic acid (CAS 140-10-3) ≥ 99.0% pure, p-coumaric acid (CAS 501-98-4) 98.0% pure and caffeic acid (CAS 331-39-5) with a mass percentage purity higher than 98.0%, supplied respectively by Fluka, Alfa Aesar and Sigma-Aldrich. These three acids are solid at room temperature.

Double distilled water, passed through a reverse osmosis system and further treated with a Milli-Q plus 185 water purification equipment, was used in all experiments.

In order to rank the hydration capacity of the ILs used, the water activity of aqueous solutions of ILs are here considered. The water activities (a_w) of the studied cholinium ionic liquids, namely

[Ch]Cl, [Ch][Suc] and [Ch][Glu], based on previous work,[33] are depicted on Figure 2.1. The water activity of the choline [Ch][Ac] was measured using a Rotronic HygroPalm AW1. Since cholinium levulinate was not available in the laboratory, it was impossible to measure the water activity for this ionic liquid. Aqueous solutions of each ionic liquid were prepared and their water contents were determined by Karl Fisher Titration (831 KF Coulometer, Metrohm). Then, the prepared solutions were placed in a sealed container connected to a probe. Each sample slowly exchanges moisture with the air inside the sealed container until the equilibrium was reached. The water activity values were considered constant when values were achieved in the thermo hygrometer. The measurements were performed under controlled temperature (25 ± 0.01 ºC) with an accuracy of ± 0.005 a_w. The experimental water activity are also presented in Figure 2.1.

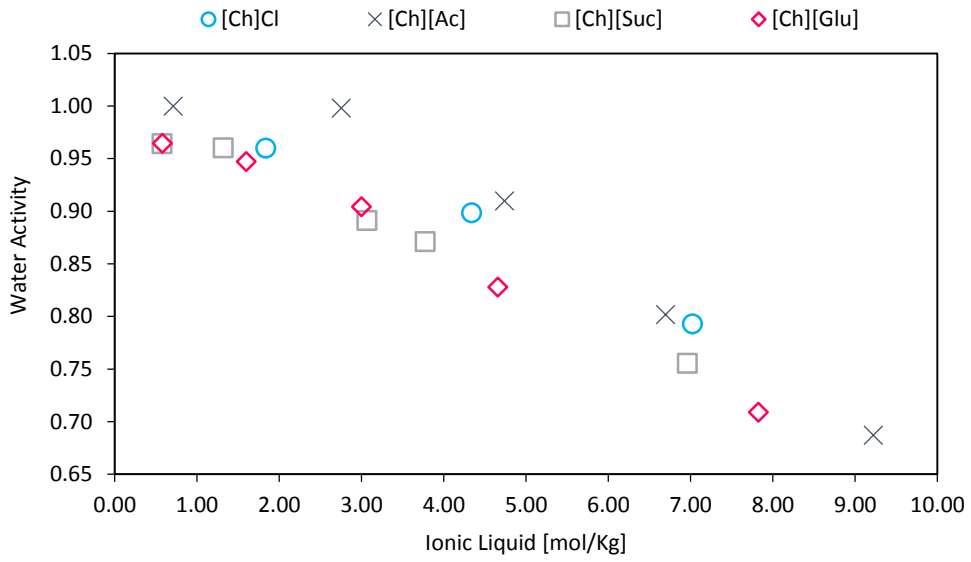

Figure 2.1 – Water activities at room temperature of cholinium-based ABSs: (○) [Ch]Cl; (×) [Ch][Ac]; (□) [Ch][Suc]; (◊) [Ch][Glu].

Since the water activity describes the energy of water in a given system, the higher the depression of the water activity, the more stable the hydration complexes are, and thus, the stronger the interactions between water and the solute. Hence, the hydrophilicity follow the order: [Ch][Ac] > [Ch]Cl > [Ch][Suc] ≈ [Ch][Glu].

2.2 Methods

2.2.1 Physicochemical properties of IL-based ABS

The physical properties of ABS, such as pH, viscosity and density are important properties to use these systems as extractive approaches in biotechnological applications, and particularly, when envisaging their design and scale-up. Viscosity is a property with a great importance since it provides information on mass transfers in ionic liquids. Therefore, pH, density and viscosity values were measured on both of the top and bottom phases for all initial mixtures prepared.

Density and viscosity data of the coexisting phases in ABS composed of used cholinium-based ILs + K_3PO_4 + H_2O previously measured in literature[8] were used in this work for comparison. However, for the [C_4mim]Cl-based ABS and the cholinium-based ILs + PEG 600 + H_2O, the density and viscosity of both the top and bottom phases were measured in this work. The mixtures at specific compositions were prepared, vigorously shaken to reach equilibrium and allowed to phase separate for at least 12h, at room temperature. After the separation of the immiscible phases, viscosity and density measurements were performed for both IL-rich and salting-agent-rich phases aqueous phases between 293.15 K and 303.15 K.

The pH values of both the ionic-liquid-rich and salt-rich phases were measured at room temperature using a FE20 – FiveEasy™ pH meter from METTLER TOLEDO. The pH meter was calibrated with two buffer (pH values of 4.00 and 7.00). After vigorous stirring and a subsequent period of settling (at least 12h), the separation was carried out, and the pH values of the two separate phases was measured. The pH values of the mixtures prepared with aqueous solutions of phenolic acids and the inorganic salt were also measured.

Measurements of the viscosity and the density were performed in the temperature range between 293.15 K and 303.15 K and at atmospheric pressure using an automated SVM 3000 Anton Paar rotational Stabinger viscometer-densimeter. The dynamic viscosity has a relative uncertainty of 0.35% while the absolute uncertainty on density is within 0.0005 $g \cdot cm^{-3}$.

2.2.2 Partitioning coefficients and extraction efficiencies

Mixtures of each IL, salting-agent and the aqueous solution of each one of the acids were prepared according to the compositions of the ternary mixtures used for the phenolic acids based on the phase diagrams determined in previous works.[3, 8]. These compositions were chosen based on tie-line data obtained from the literature. The longer the tie-line, the larger the difference in composition between the two co-existing phases and thus the more efficient the extraction should be. An effort was made to use mixtures with initial compositions that are very similar to each other so that a fair comparison could be carried out. Note, however, that due to the different shape of the phase diagrams, some differences especially in the salt concentration could not be avoided.

The concentration of each one of the acids in the aqueous solution used in the initial mixture was 0.147 $g \cdot dm^{-3}$ (9.95×10^{-4} $mol \cdot dm^{-3}$) for cinnamic acid; 0.800 $g \cdot dm^{-3}$ (4.87×10^{-3} $mol \cdot dm^{-3}$) for p-coumaric acid and 0.672 $g \cdot dm^{-3}$ (3.73×10^{-3} $mol \cdot dm^{-3}$) for caffeic acid. The ampoules were let to equilibrate for at least 12 h to achieve a complete separation of the two phases formed. After the phase separation, the presence of each phenolic acid in each one of the phases was measured by UV-vis absorbance spectroscopy using a UV-vis spectrophotometer, SHIMADZU UV-1700, at the corresponding maximum absorption wavelengths. To better account for possible interferences, ampoules with the same mass fraction composition were prepared for each individual system, using pure water (Milli-Q) instead of the phenolic acids aqueous solutions, to be used as blank samples. The calibration curves further established and listed in Table 3.3 were used to quantify the acid in both phases. The effects of the inorganic salt were also taken into account for p-coumaric and caffeic acids.

The mixtures were prepared and vigorously stirred in small ampoules of approximately 15 cm^{-3}. After stirring, the biphasic systems were allowed to equilibrate and to phase separate for at least 12h, at room temperature. After the separation of the phases, the concentration of phenolic acids was quantified through UV-vis, using the calibration curves previously established.

The experimental set up used for the phenolic acid extraction is depicted in Figure 2.2 *(a)*.

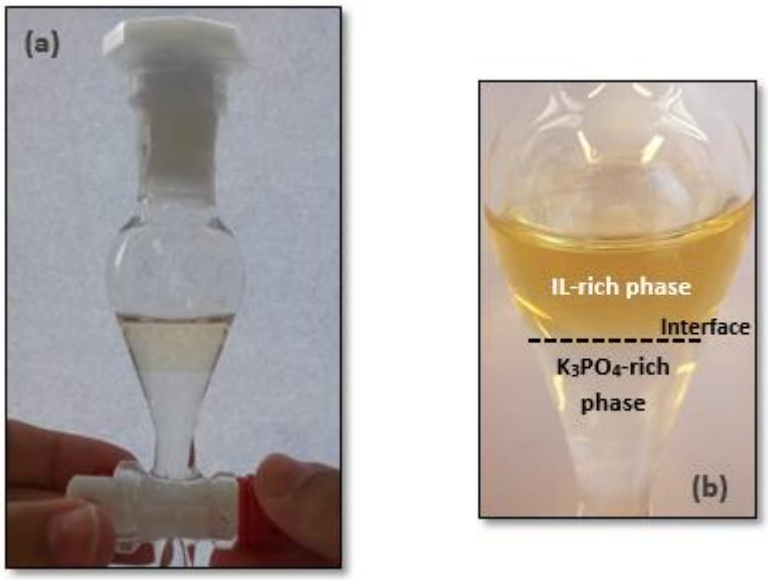

Figure 2.2 – (a) Experimental set up used for the determination of the partition coefficients and extraction efficiencies of phenolic acids and (b) macroscopic appearance of an ABS composed of an ionic liquid (used in this work) and an inorganic salt (K_3PO_4).

At the conditions used in this work, the top layer is the IL-rich phase while the bottom phase is the inorganic-salt-rich phase. As mentioned in the introduction, the addition of inorganic salt leads to the salting-out (exclusion) of the ionic liquid creating another aqueous phase. Figure 2.2 *(b)* shows the phase splitting process observed in the IL-based ABS used in this work. A flow sheet of the extraction procedure (valid for both K_3PO_4- and PEG-600-based system) is depicted in the next figure.

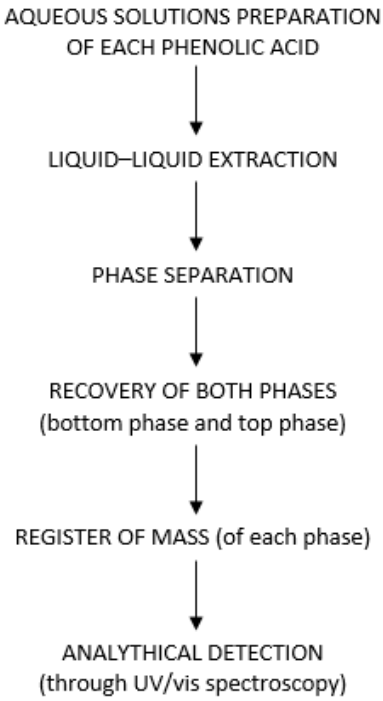

Figure 2.3 – Generalized flow sheet of the liquid–liquid extraction of phenolic acids.

The partition coefficients of the studied biomolecules, K_{CIN} for cinnamic acid, K_{COU} for p-coumaric acid and K_{CAF} for caffeic acid are defined as the ratio of the concentration of the biomolecules in the IL and in the salting-agent-aqueous-rich phases, as described by the following equation:

$$K_{acid} = \frac{[ACID]_{IL}}{[ACID]_{salting\ agent}} \qquad (1)$$

where $[ACID]_{IL}$ and $[ACID]_{salting\ agent}$, are respectively, the concentration of the acid in IL and in salting-agent-aqueous-rich phases. The salting agent may be either the inorganic salt (K_3PO_4) or the polyethylene glycol (PEG 600).

The extraction efficiencies of each biomolecule, EE_{CIN}% for cinnamic acid, EE_{COU}% for p-coumaric acid and EE_{CAF}% for caffeic acid, are defined as the percentage ratio between the amount of each phenolic acid in the IL-rich phase and in the initial mixture, according to Equation (2),

$$EE_{acid}\% = \frac{w_{acid}^{IL}}{w_{acid}^{IL} + w_{acid}^{salting\ agent}} \times 100 \qquad (2)$$

where w_{acid}^{IL} and $w_{acid}^{salting\ agent}$ are the weight of phenolic acid in the IL-rich and in the salting-agent-rich aqueous phases, respectively.

Note that after the phase separation and recovery of the two phases, both IL and salting-agent-rich phases were additionally weighted and density values of each IL and salting-agent were used to convert the mass values obtained to volume values, since it is aqueous solutions.

The validation of the quantification of phenolic acids was made for all the systems studied through a method denominated mass balance. The material balance is an application of conservation of mass to the analysis of physical systems. By accounting for compounds entering and leaving from the ampoule, the lost mass can be identified, which might have been unknown or difficult to measure during the extraction.

The data from this mass balance are presented in Appendix D for the three studied acids. Analysing the values obtained for each IL, it can be concluded that the material balance was almost achieved in all cases, since there are some cases where small deviations (in the fourth decimal place) were obtained. From these results it can also be concluded that the concentration of the acid in the inorganic-salt-rich phase is always lower than the concentration in the IL-rich phase.

3. Quantification of Phenolic Acids

3. Quantification of Phenolic Acids

3.1 Cinnamic, p-Coumaric and Caffeic Acids

As stated in the Introduction chapter, phenolic acids are widely present in plants and vegetable foods and also exert some biological activities, such as antioxidative and free-radical scavenging. There are many analytical methods for quantitative study of these acids, such as HPLC or thin-layer chromatography (TLC) among others. However, due to its simplicity, the most commonly used method is the UV-vis spectroscopy. Phenolic compounds display characteristic UV spectra which are useful for detection and quantification. Spectroscopic techniques offer a rapid and non-destructive approach to determine concentration changes in solution. This method is going to be adopted in this work, where the main objective is to study the extraction performance of ionic liquid-based aqueous biphasic systems of three phenolic acids: cinnamic acid (**CIN**), p-coumaric acid (**COU**) and caffeic acid (**CAF**) from aqueous solutions (see Figure 1.3 for the chemical structures).

In Table 3.1 the water solubility and the dissociation constants of cinnamic, p-coumaric and caffeic acid are presented. The dissociation constant together with the experimental pH conditions can provide useful information about the speciation of the acids, in other words, if they are in their neutral, cationic or anionic form. When in the anionic form (pH > pKa), phenolic acids can complex with other molecules by hydrogen bonds.[34] Chemical species and speciations of the phenolic acids are depicted in Figure 3.1, Figure 3.2 and Figure 3.3.[35]

Table 3.1 – Solubility in water (S_W) and dissociation constants of phenolic acids at 298.2 K [35-37].

Phenolic Acid	Solubility / g·dm^{-3}	pKa$_1$	pKa$_2$	pKa$_3$
Cinnamic Acid	0.23	4.51	-	-
p-Coumaric Acid	1.02	4.00	9.52	-
Caffeic Acid	0.98	3.64	9.52	12.45

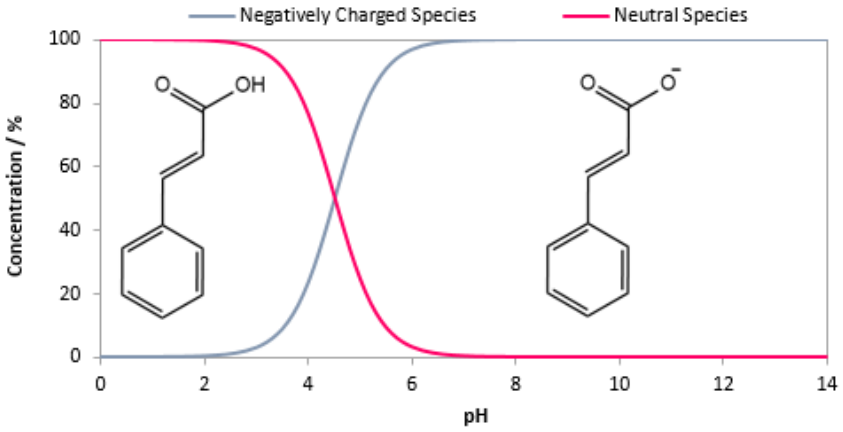

Figure 3.1 – Chemical species and speciation of cinnamic acid.

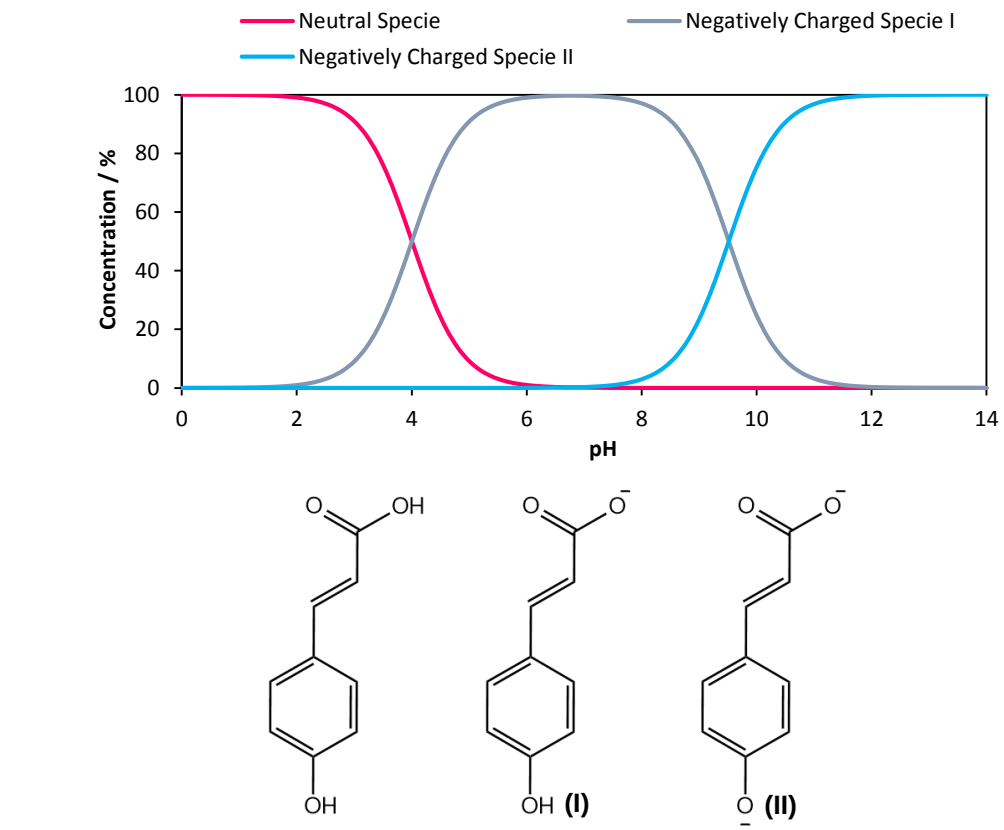

Figure 3.2 – Chemical species and speciation of p-coumaric acid.

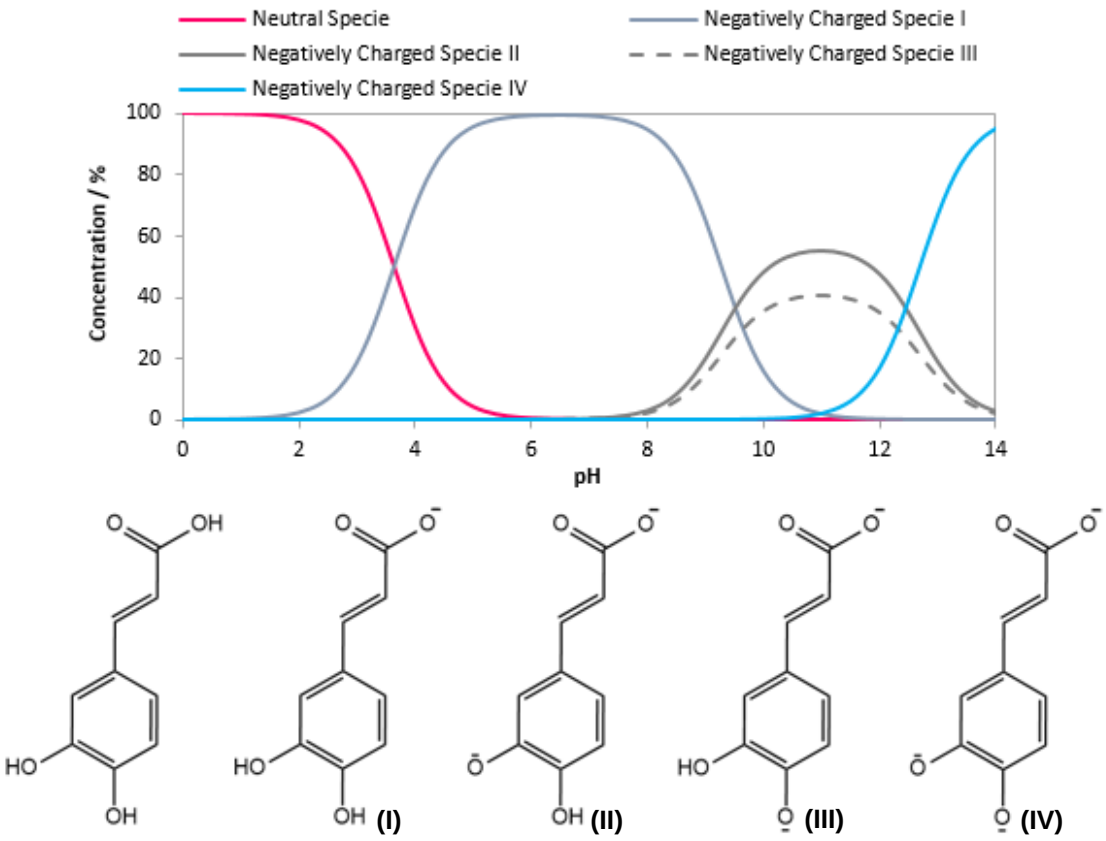

Figure 3.3 – Chemical species and speciation of caffeic acid.

The interest in investigating these three phenolic acids is that they have identical chemical structures, the only difference is the number of hydroxyl groups (-OH) attached to the benzene ring. p-Coumaric acid has one hydroxyl group in para-substitution, occupying the opposite ends (the carboxylic group) while caffeic acid possess two hydroxyl groups in meta- and para-substitution and thus forming a catechol group ($C_6H_4(OH)_2$). This is the reason why these two phenolic acids complex with other molecules, namely with ions [34]. The hetero-association of the phenolic acids is a very frequent and important phenomenon due to hydrogen bonding interactions of hydroxyl groups attached to the catechol group. These hydroxyl groups are more unprotected because of the high charge of the phenol group whereas the OH- group of the carboxylic group is protected by the resonance structure. Cinnamic acid does not have any hydroxyl group attached to the catechol group, and therefore, it should not present any formation of complexes between the acid and other ions.

The three acids were quantified analytically by UV-vis spectrophotometer and thus the electronic absorption spectra's were measured in the ranges of 190-400 nm. For that purpose, individual solutions with a proper concentration of the three acids were prepared. The spectra, shown in Figure 1.2, were obtained by subtracting the spectrum of pure solvent (water) from that of the solutions containing the each one of the acids.

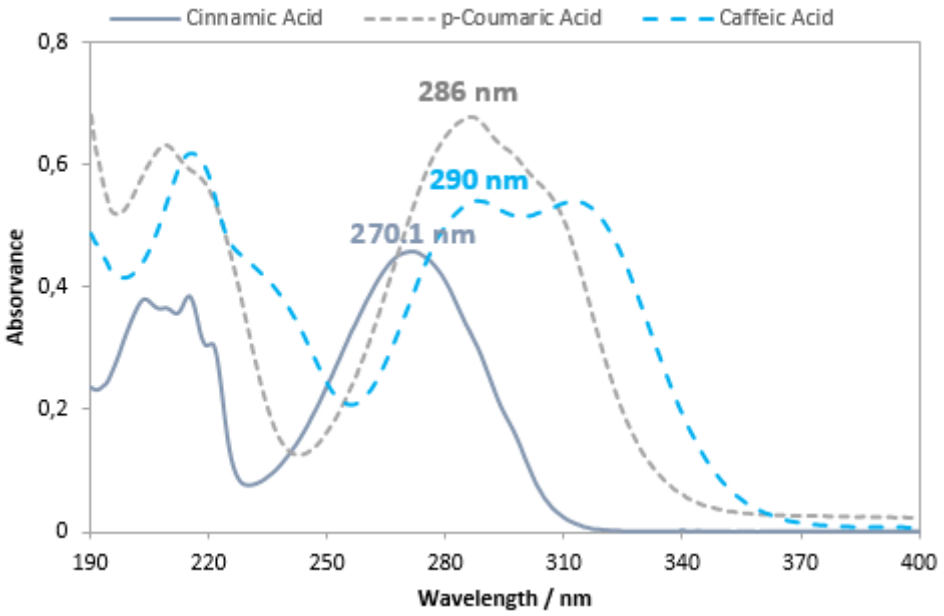

Figure 3.4 – Spectras of cinnamic, p-coumaric and caffeic acids in water at room temperature.

Analysing the overall bands of the spectra, it can be observed that bands are large and not very detailed. This can probably attributed to the effect of water, as a solvent. Water, and other polar compounds such as ethanol, can interact through hydrogen bonding with phenolic acids.

Comparing the spectra of the three phenolic acids, it is possible to verify that they are identical since the three phenolic acids possess identical chemical structures, as referred above. The electronic absorption spectrum of free cinnamic acid in water solution shows only one broad band

with a maximum wavelength of 270.1 nm, which is going to be used to quantify the concentration of the acid during the extraction procedure. The spectra of p-coumaric acid in water solution also shown in Figure 3.4, is mainly characterized by double absorption band with two maximum wavelengths at 286 nm and 209 nm. The quantification of this acid will be performed using the most intense band (286 nm). Similarly to what happens to p-coumaric acid, caffeic acid also exhibits a double band with maximum absorption intensities at 290 and 312 nm.

These bands at wavelengths of 270-290 nm correspond to the benzene ring since benzene absorbs at 255 nm. An hydroxyl group (-OH) affects the spectra of benzene forming peaks at longer wavelengths. This absorption shift to longer wavelength is called a bathochromic shift. Bands at lowers wavelength (210 nm) correspond to the carboxylic acid and are not very useful for analysis purposes, thus being disposed in the quantification of the phenolic acids.[38]

The functional groups influence the conjugated systems, causing the absorption peaks to appear at longer wavelengths than the band of benzene, although they do not go beyond 400 nm and enter the visible region.[39] The wavelengths of the functional group that constitute the phenolic acids are show in Table 3.2.

Table 3.2 – Wavelengths of functional group constituents of phenolic acids.

Functional Group	λ / nm
Benzene	255
Phenol	270
Carboxylic Acid	210

3.2 Calibration Curves

The method used to quantify the concentration of a compound in an aqueous solution is the UV-spectroscopy method based on the propriety that many compounds absorb in the ultraviolet (UV) and visible (vis) light. The Lambert-Beer law, establishes a linear relationship between the concentration and the absorbance according Equation (3):

$$A = \varepsilon \cdot b \cdot [C] \quad (3)$$

where A represent the absorbance, ε is the molar absorptivity (in units of $L \cdot mol^{-1} \cdot cm^{-1}$), b is the path length of the sample (cells with 1 cm of path length were used in this work) and finally, C is the concentration of the phenolic acid in solution.

In this way, a calibration curve needs to be established using solutions with varied concentrations of the phenolic acids and their respective absorbances. Aqueous solutions of each phenolic acid were prepared taking into account each one of the acids's solubility: individual solutions with a concentration of 0.147 $g \cdot dm^{-3}$ (9.95×10^{-4} $mol \cdot dm^{-3}$) for cinnamic acid (**CIN**); 0.800 $g \cdot dm^{-3}$ (4.87×10^{-3} $mol \cdot dm^{-3}$) for p-coumaric acid (**COU**) and 0.672 $g \cdot dm^{-3}$ (3.73×10^{-3} $mol \cdot dm^{-3}$) for caffeic acid (**CAF**) were prepared. The acid's initial concentration was carefully chosen after carrying out some preliminary tests aimed at achieving absorbance values in an adequate range ($0.3 < Abs < 1.3$) so that the Lambert- Beer law holds. The solutions were then quantified through UV-spectroscopy using a SHIMADZU UV-1800, Spectrophotometer (Figure 3.5).

Figure 3.5 – SHIMADZU UV-1800 Spectrophotometer (UV/vis) used in this work.

The extraction method used in this work requires the use of an ionic liquid together with an inorganic salt, K_3PO_4, or a polymer, polyethylene glycol. The presence of these compounds might cause significant interferences in the spectra of the phenolic acids under study and thus in the analytical method, at the dilutions carried out.

For K_3PO_4, it was concluded that all systems studied influenced the spectra of the phenolic acid, on the other hand, polyethylene glycol and cholinium containing ABSs did not cause interferences in the spectras, except for [Ch][Suc] and [Ch][Glu].

All the spectra were obtained by subtracting the spectrum of pure solvent from that of the aqueous solution containing phenolic acid. This procedure will be followed during all UV-vis measurements carried out during this work.

In particular, the use of K_3PO_4 might cause a significant interference since this salt changes the pH of the solutions. This fact is most relevant when using solutes that are sensible to the pH such as the case of acids. The UV-vis spectra of each one of the phenolic acids in water and in an aqueous solution of K_3PO_4 (with a salt concentration corresponding to 40% of the total solution) are shown in Figure 3.6, Figure 3.7 and Figure 3.8. The concentration used of the acids for both aqueous solutions was the same. For cinnamic acid a concentration of 0.1 $g \cdot dm^{-3}$ was used, for p-coumaric acid and caffeic acid it was used concentrations of 0.8 $g \cdot dm^{-3}$ and 0.5 $g \cdot dm^{-3}$ respectively.

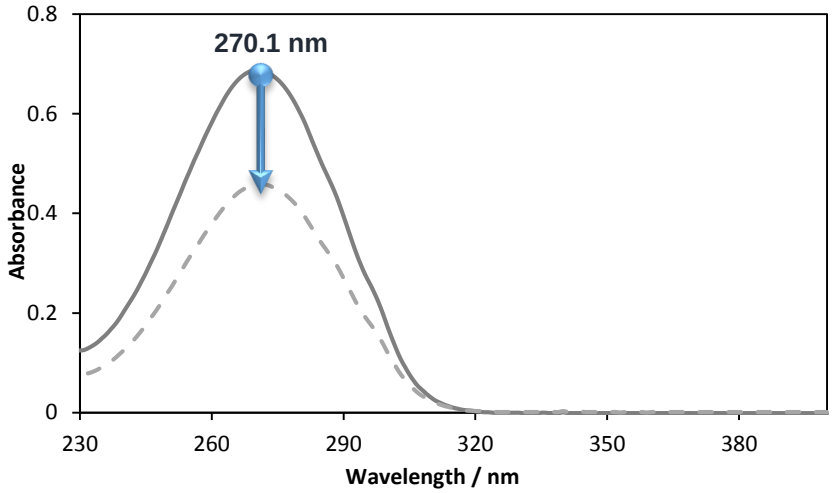

Figure 3.6 – UV-vis spectra of cinnamic acid in water (full line) and in aqueous solution of 40% of K_3PO_4 (dashed line).

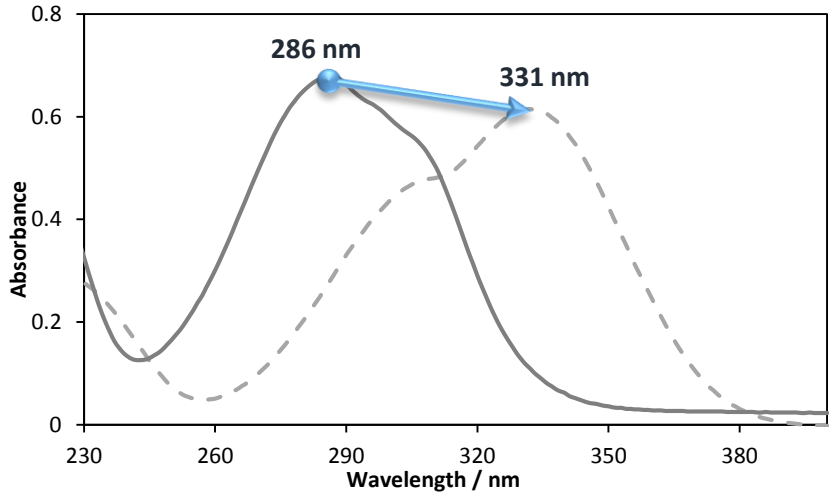

Figure 3.7 – UV-Vis spectra of p-coumaric acid in water (full line) and in an aqueous solution of 40% of K_3PO_4 (dashed line).

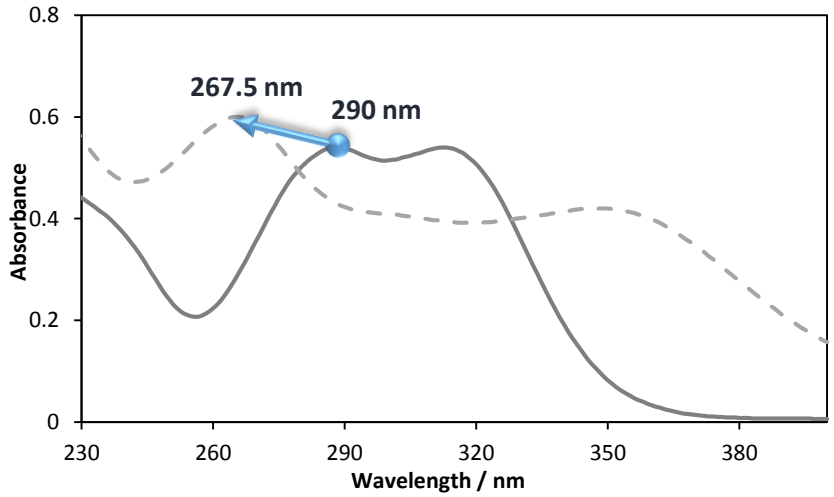

Figure 3.8 – UV-Vis spectra of caffeic acid in water (full line) and in an aqueous solution of 40% of K_3PO_4 (dashed line).

Information on the wavelength corresponding to the maximum absorbance of each phenolic acid in water and in an aqueous solution of K_3PO_4 as well as pH values of each solution gathered from these Figures is systematized in Table 3.3.

Table 3.3 – Wavelengths corresponding to the maximum absorption and respective pH in water and in an aqueous solutions of K_3PO_4.

Phenolic Acid	Water	pH	K_3PO_4 (aq.)	pH
Cinnamic Acid	270.1	3.98	270.1	13.29
p-Coumaric Acid	286	4.06	331	13.42
Caffeic Acid	290	3.73	267.5	13.44

Only cinnamic acid UV-vis absorbance spectra remains unchanged when K_3PO_4 is present in the solution. The other two acids, p-coumaric and caffeic acids, have their spectra greatly altered by the presence of this salt. For p-coumaric acid not only a deviation to higher wavelengths occurred (*bathochromic* shift to 331 nm), but also the relative intensity of the two bands changed. In other words, while in water the maximum wavelength corresponds to the first band in the group, in the K_3PO_4 solution the maximum absorbance was registered for the second band in the group. The caffeic acid spectra is the one that suffered larger changes, since there is a clear broadening of the band, with the two peaks moving in opposite directions: a deviation of the most intense band for lower wavelengths (*hipsochromic* shift to 267.5 nm) while the other band deviated to higher wavelengths.[(40)]

In order to further investigate the origin of the observed shifts, solutions with several pH were prepared and the spectra were registered. The study of the influence of the salt is presented forward.

According to Belay et. al. [(34)], solutions of caffeic acid and sodium hydroxide (NaOH) present a complexation of the Na^+ cation with the caffeic acid, which coordinates at the catechol sites by

replacing the H^+ in the hydroxyl group. A similar phenomenon probably happened in the present work, with the potassium cation establishing strong interactions with the oxygen in the hydroxyl group of p-coumaric acid and caffeic acid. This mechanism is presented in Figure 3.9 for p-coumaric acid and Figure 3.10 for caffeic acid.

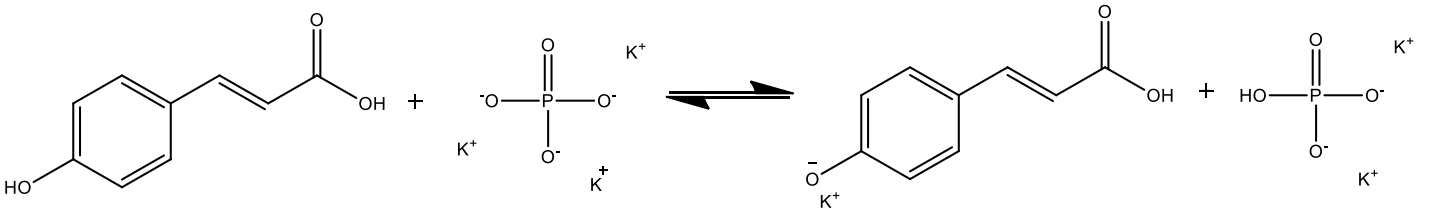

Figure 3.9 – Possible mechanism of p-coumaric complexation with K_3PO_4.

The hydroxyl group attached to the phenol releases the H^+ from the oxygen and binds to one of the deprotonated oxygens of the K_3PO_4, thus forming dipotassium phosphate ($K_2HPO_4^{2-}$). Meanwhile, K^+ connects to the deprotonated acid and form a salt termed as potassium-4-(2-carboxyvinyl) phenolate.

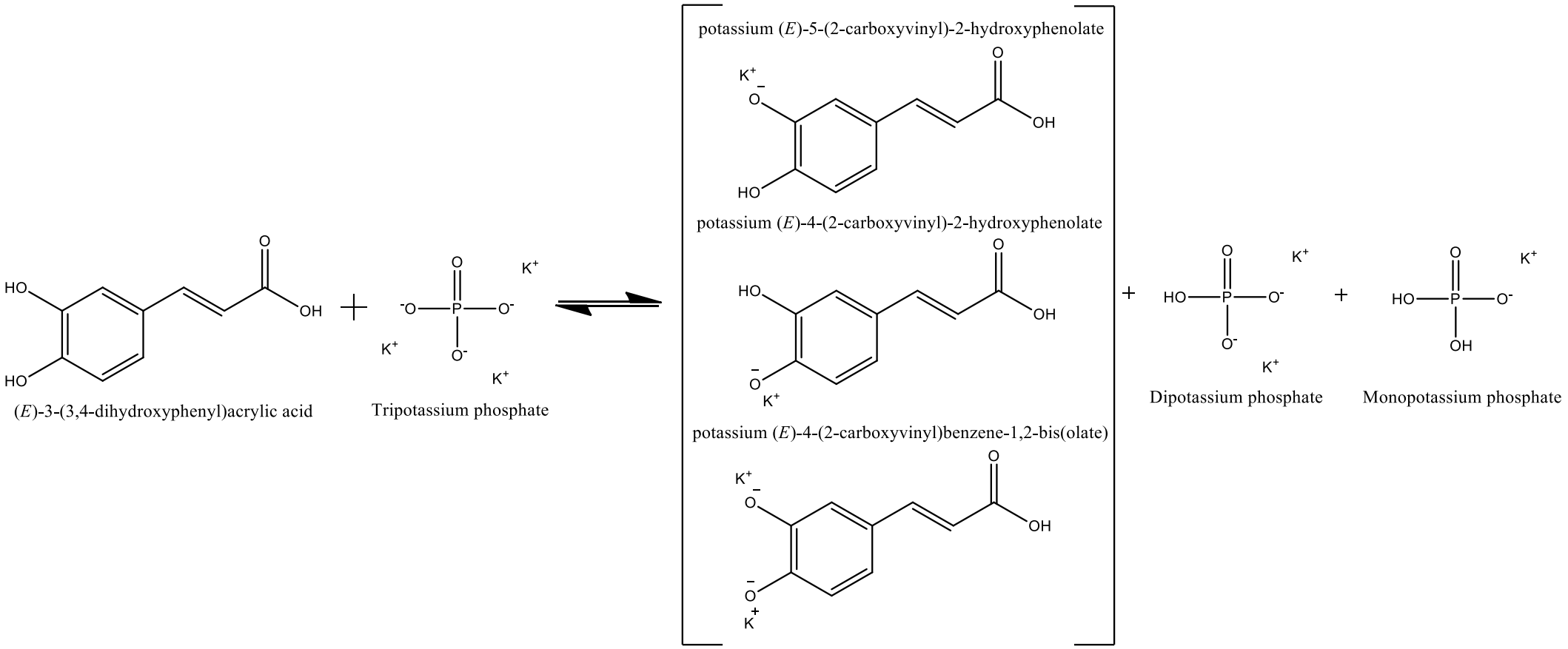

Figure 3.10 – Possible mechanism of caffeic acid complexation with K_3PO_4.

Figure 3.10 show the possible reaction that occurs between caffeic acid and K_3PO_4. Since the acid has several deprotonated species at a pH above its dissociation constants, there is a larger list of possible species that can be formed after complexation with phosphate anions, including dipotassium phosphate ($K_2HPO_4^{2-}$), monopotassium phosphate ($KH_2PO_4^{1-}$), and three inorganic salts: potassium-4-(2-carboxyvinyl)-2-hydroxyphenolate, potassium-5-(2-carboxyvinyl)-2-hydroxyphenolate and finally potassium-4-(2-carboxyvinyl)-benzene-1,2-bisolate.

The presence of all these compounds in the aqueous solution justifies the higher than the expected affinity of the caffeic acid to the inorganic salt. Consequently, the extraction of caffeic acid to the ionic liquid phase will be more difficult than that of the other two acids. The Figure 3.11 illustrates the possible partitioning of caffeic acid in IL + K_3PO_4 systems.

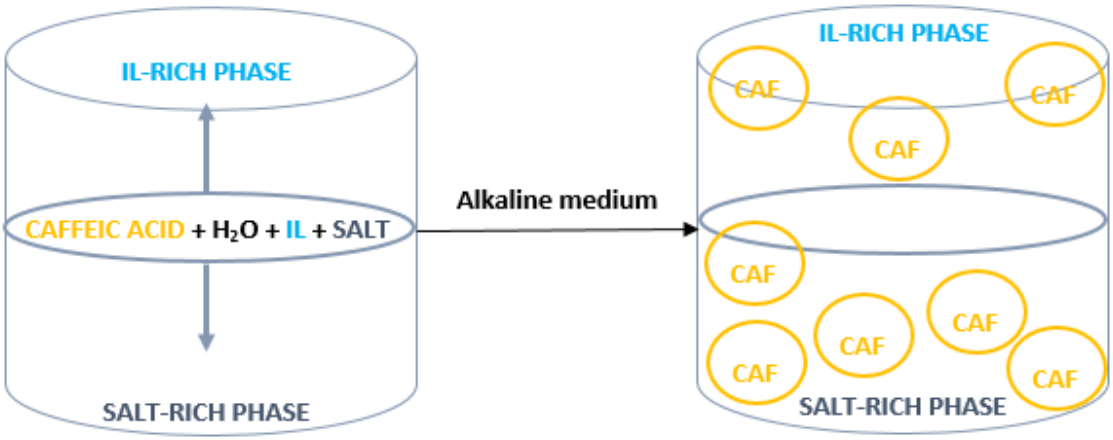

Figure 3.11 – Scheme of the partitioning of caffeic acid in alkaline medium.

Consequently, the changes observed in the p-coumaric and caffeic acids spectra can be attributed to the complexation between the ligand (p-coumaric and caffeic acids) and the phosphate anions. In order to further investigate the influence of the presence of K_3PO_4 in the p-coumaric and caffeic acids UV-vis spectra, solutions with a fixed acid concentration, but variable salt concentration were prepared. In Figure 3.12 and Figure 3.13 the effect of the concentration (in mass percentage) of the inorganic salt (K_3PO_4) in p-coumaric and caffeic acid aqueous solutions´s UV-vis spectra can be observed.

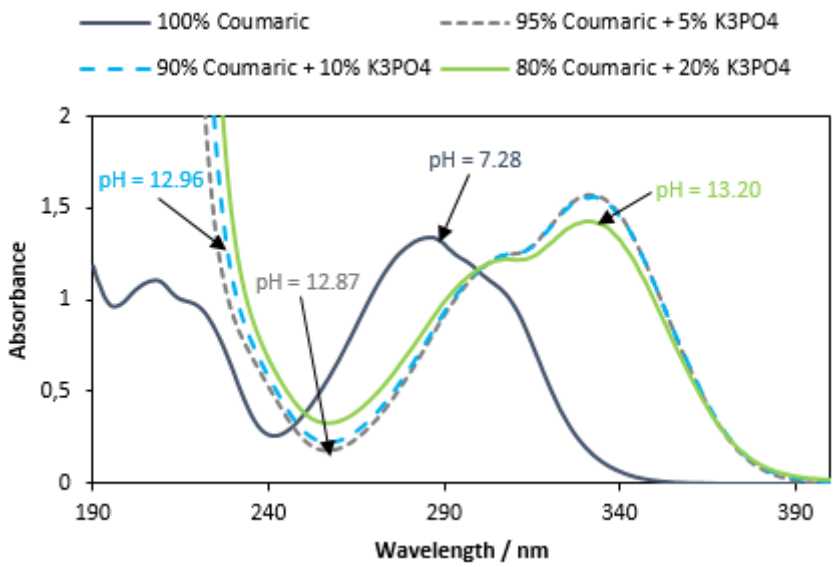

Figure 3.12 – Experimental UV spectra of p-coumaric acid at different compositions of K_3PO_4 (%wt.) and respective pH values with [COU] = 0.0133 g·L^{-1}, at room temperature.

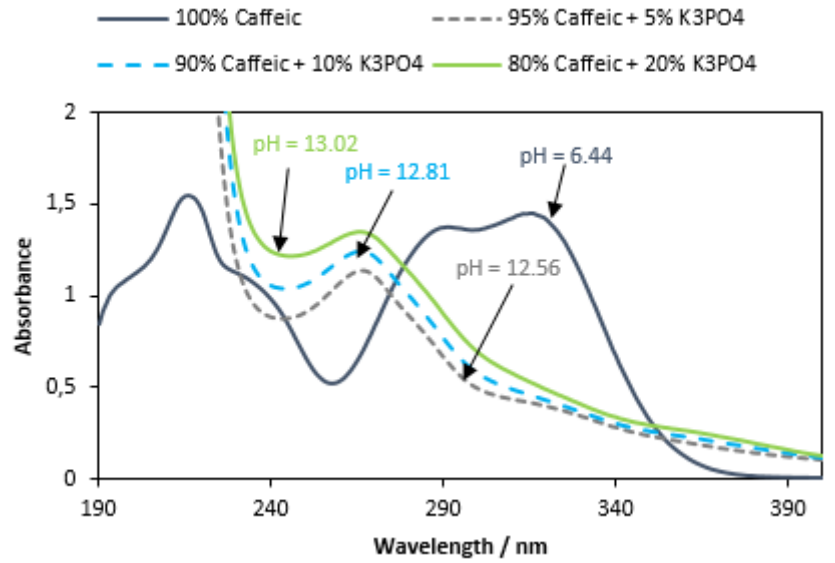

Figure 3.13 – Experimental UV spectra of caffeic acid at different compositions of K_3PO_4 (%wt.) and respective pH values with [CIN] = 0.0195 g·dm^{-1}, at room temperature.

Information on the wavelength corresponding to the maximum absorbance of each phenolic acid in water and in the aqueous solutions of K_3PO_4 as well as the pH values of each solution gathered from the these Figures is systematized in Table 3.3.

Table 3.4 – Effect of the compositions of K_3PO_4 in the absorbance *p-Coumaric acid and pH values, at room temperature.*

Composition	Absorbance	C_{COU} / g·dm^{-3}	Wavelength (nm)	pH
0% K_3PO_4	1.35	1.17×10^{-2}	286	7.28
5% K_3PO_4	1.56	3.09×10^{-2}	331	12.87
10% K_3PO_4	1.55	3.05×10^{-2}	331	12.96
20% K_3PO_4	1.41	2.77×10^{-2}	331	13.20

Table 3.5 – Effect of the compositions of K_3PO_4 in the absorbance *p-Coumaric acid and pH values, at room temperature.*

Composition	Absorbance	C_{CAF} / g·dm^{-3}	Wavelength (nm)	pH
0% K_3PO_4	1.36	1.86×10^{-2}	290.0	6.44
5% K_3PO_4	1.03	4.26×10^{-2}	267.5	12.56
10% K_3PO_4	1.03	4.28×10^{-2}	267.5	12.81
20% K_3PO_4	1.12	4.66×10^{-2}	267.5	13.02

For both acids the presence of K_3PO_4, even if in very small concentrations, greatly alters the spectra of both acids and the corresponding pH. When the composition of the inorganic salt is null, the pH value is lower than the dissociation constant pKa_2 of the acids, suggesting that they are in their neutral form and thus are not able to form a new species. Relatively to the other compositions, with just only 5% of K_3PO_4 added there is an immediate change in the spectrum of both phenolic acids due to the fact that pH value is higher than pKa_2.

The calibration curves for the three acids were carried out according to the information collected above:

i) For the cinnamic acid only one calibration curve was used throughout the work since the presence of K_3PO_4 and PEG did not affect the UV-vis spectra of this compound.

ii) For the other two acids, p-coumaric and caffeic acids, two calibrations curves were used: one when K_3PO_4 is not present in the solution (used in PEG containing systems) and the other when K_3PO_4 is present. Since no significant effect was observed between the absorbance of the acid and the concentration of K_3PO_4, only one calibration curve for each system was measured, at a fixed K_3PO_4 concentration (according to the compositions of the ternary systems based on the literature).

Table 3.6 presents a brief summary of the wavelengths used for each one of the phenolic acid with both K_3PO_4 and water (used for PEG 600 systems) and the respective extinction and correlation coefficients used to determine the calibration curve.

Table 3.6 - Calibration curves for each phenolic acid in aqueous solutions with or without K_3PO_4.

Solute		Cinnamic acid	p-Coumaric Acid	Caffeic Acid
Wavelength (nm)	**Water**	270.1	286	290
	K_3PO_4 (aq.)		331	267.5
Extinction Coefficient	**Water**	126.03	114.58	73.01
	K_3PO_4 (aq.)		50.89	24.11
Correlation Coefficient	**Water**	$R^2 = 0.9995$	$R^2 = 0.9982$	$R^2 = 0.9999$
	K_3PO_4 (aq.)		$R^2 = 0.9996$	$R^2 = 0.9979$

4. Ionic Liquid + Phenolic Acid (aq.) + K_3PO_4 systems

4. Ionic Liquid + Phenolic Acid (aq.) + K_3PO_4 systems

4.1 Implementation of K_3PO_4-based aqueous biphasic systems for the extraction of phenolic acids

As stated in the Methodologies chapter, the compositions of the ternary systems were chosen based on phase diagrams for the phenolic acids based on the phase diagrams determined in previous works.[3, 8] The experimental phase diagrams for IL + K_3PO_4 + H_2O systems used in this thesis are presented in Figure 4.1. The closer to the axis origin a bimodal curve is, the higher the ionic liquid hydrophobicity is, i.e., the weaker affinity for water and the higher their ability for phase split [4].

The composition of the mixtures (in mass percentage) used to carry out the extraction of the solutes and the respective tie line length are presented in Table 4.1.

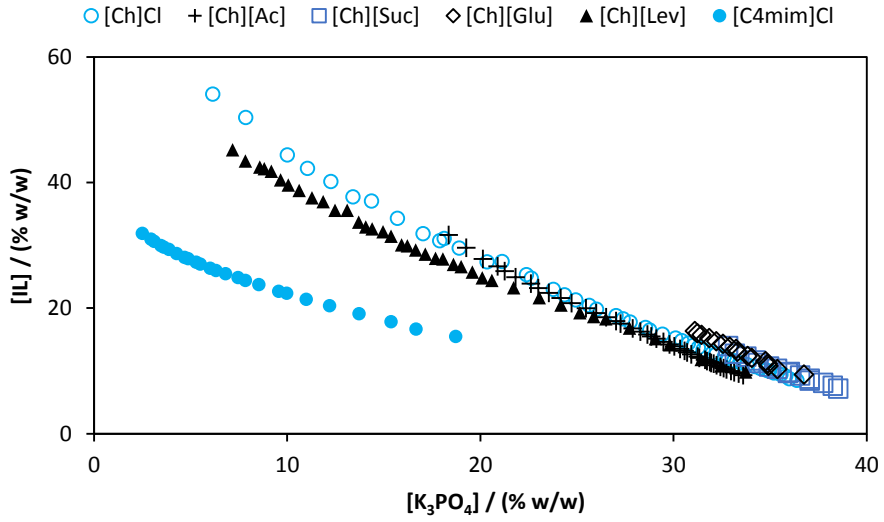

Figure 4.1 – Phase diagrams of the ternary systems composed of K_3PO_4 + ionic liquid + H_2O at 298 K (percentage weight fraction): (○)[Ch]Cl; (+) [Ch][Ac]; (□) [Ch][Suc]; (◊) [Ch][Glu]; (▲) [Ch][Lev]; (●) [C_4mim]Cl, literature data [3, 8, 41].

Table 4.1 – Composition of the initial mixtures used to prepare the ampoules.

Ionic Liquid	%wt. IL	%wt. K_3PO_4	%wt. ACID (aq.)	TLL
[C_4mim]Cl	25.02	15.02	59.96	47.01
[Ch]Cl	20.65	34.33	45.02	70.97
[Ch][Ac]	30.04	23.00	46.96	66.92
[Ch][Suc]	30.28	30.00	39.72	92.39
[Ch][Glu]	29.64	30.03	40.33	84.19
[Ch][Lev]	30.15	20.22	49.63	53.52

4.3 Physicochemical properties of IL-based ABS

For the sake of comparison, the pH, density and viscosity results of all systems studied at 298.15 K are reported in Table 4.2.

Table 4.2 – Comparison of the pH, density and viscosity at 298.15 K for the two phase in equilibrium in the K_3PO_4 - based ABS used in the present work.

Ionic Liquid	K_3PO_4-rich phase			Ionic Liquid-rich phase		
	pH	ρ (g·cm^{-3})	η (mPa s)	pH	ρ (g·cm^{-3})	η (mPa s)
[C_4mim]Cl	12.53	1.355	3.744	12.63	1.034	1.826
[Ch]Cl	13.80	1.493	8.616	14.00	1.126	5.859
[Ch][Ac]	13.22	1.487	9.271	13.43	1.142	6.012
[Ch][Suc]	10.15	1.538	20.874	10.30	1.289	14.308
[Ch][Glu]	11.54	1.620	28.342	11.41	1.223	14.929
[Ch][Lev]	13.15	1.522	10.233	13.29	1.123	8.219

Analysing the pH values, it is possible to conclude that all ABS used present alkaline phases due to the presence of the K_3PO_4 salt. The pH of the coexisting phases ranges between 10.15 and 14.00, depending on the ionic liquid present in the system. Succinate and Glutarate-based systems present somehow lower values than the other systems, which might be related to the hydration nature of the ILs.

Figure 4.2 presents a comparison between the density and the viscosity of both phases, IL-rich and K_3PO_4 - rich phases, in equilibrium for all the systems studied in this work.

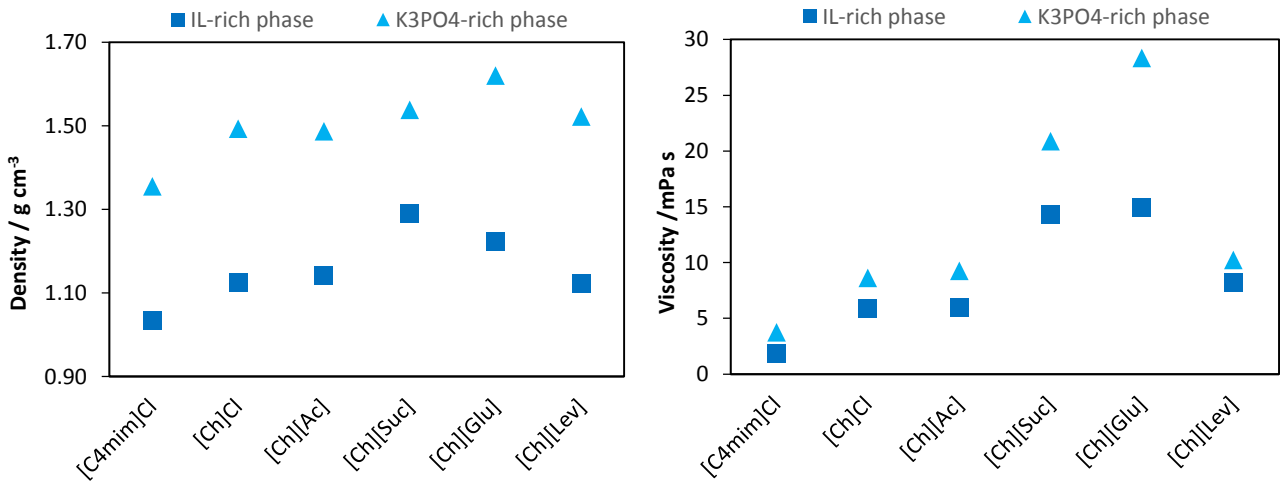

Figure 4.2 – Density (ρ) and viscosity (η) of the coexisting phases in ABS composed of IL + K_3PO_4 + H_2O at 298.15 K.

No significant differences in the density between the IL-rich and K_3PO_4-rich phases are observed. In all the systems, the density of the inorganic salt-rich phase is higher than that of the corresponding IL-rich phase. Moreover, these results also confirm that the bottom phase is the inorganic-salt-rich phase while the top phase is the IL-rich phase. A large difference in densities

values between the upper and the lower phase can be regarded as a main advantage when envisaging large-scale applications.

Concerning the viscosities, the inorganic-salt-rich phase is always more viscous than the corresponding IL-rich phase. The viscosity of the IL-rich phase ranges from 1.8 to 14.9 mPa·s, whereas the viscosity of the salt-rich phase lies between 3.7 and 28.3 mPa·s. Regarding the influence of the functional groups in the cholinium ILs on the viscosity order of respective phases, it can be seen that both phases decrease in the same order: [Ch][Glu] (η = 14.93 mPa·s) > [Ch][Suc] > [Ch][Lev] > [Ch][Ac] > [Ch]Cl (η = 1.83 mPa·s). The imidazolium-based ABS ([C_4mim]Cl) present the lowest values of viscosity due to its nature, in accordance to what has been found for the pure ILs.

To be mentioned that [Ch][Suc] and [Ch][Glu] are the systems that present the largest differences between the viscosities of the two phases, which indicates that the low affinity for water (hydrophobicity) of these two ILs complies with the hydration capacity referred in Chapter 2. The other ILs have higher affinity for water and thus, both phases have higher percentage of water decreasing the difference in viscosity between the two phases in equilibrium. Lowest differences in viscosities values, therefore, there is some IL migration for K_3PO_4-rich phase contributing for these deviations. Basically, systems that possess low differences in viscosities data have an easier phase separation and thus render aqueous biphasic systems that can be easily implemented.

4.4 Partitioning coefficients and extraction efficiencies

The partition coefficients and extraction efficiencies obtained for phenolic acids for the implemented ABS are depicted in Table 4.3 and Figure 4.3.

Table 4.3 –Partition coefficient and extraction efficiencies of phenolic acids obtained in this work at room temperature.

IL + K_3PO_4	K_{CIN}	$\%EE_{CIN}$	K_{COU}	$\%EE_{COU}$	K_{CAF}	$\%EE_{CAF}$
[C_4mim]Cl	49.97	99.13	77.82	99.41	11.09	96.31
[Ch]Cl	> 100	99.47	29.53	95.65	5.45	80.03
[Ch][Ac]	> 100	99.78	8.79	95.20	2.49	84.47
[Ch][Suc]	9.32	95.61	6.04	95.57	3.05	87.88
[Ch][Glu]	19.34	97.66	19.74	97.58	5.05	91.99
[Ch][Lev]	30.05	98.61	48.12	77.56	22.72	55.22

Overall, it can be concluded that much higher partition coefficients were obtained for cinnamic acid than for the other two acids. This is probably due to the establishment of preferential interactions between these acids and the inorganic salt, hindering the subsequent separation. Particularly high partition coefficients were obtained for systems composed of the most hydrophilic ionic liquids (which has more affinity for water), specifically [Ch]Cl and [Ch][Ac] as confirmed with the water activity (see Figure 2.1).

It is interesting to observe that both the anion and the cation play an important role in the extraction, since for each one of the acids there is a specific ionic liquid that performs better than the others. This indicates that these systems can be used to separate a mixture of these phenolic acids. Yet, high partition coefficients were observed and even complete extractions were verified for systems such as [Ch]Cl and [Ch][Ac] (K > 100) for cinnamic acid.

For **cinnamic acid**, the partition coefficients follow the order: *[Ch]Cl* ≈ *[Ch][Ac]* > *[C_4mim]Cl* > *[Ch][Lev]* > *[Ch][Glu]* > *[Ch][Suc]*. For **p-coumaric acid** and **caffeic acid**, the partition coefficients follow the exactly same rank: *[C_4mim]Cl* > *[Ch][Lev]* > *[Ch]Cl* > *[Ch][Glu]* > *[Ch][Ac]* > *[Ch][Suc],* but *[Ch][Lev]* switches positions with *[C_4mim]C* and *[Ch][Ac]* with *[Ch][Suc]l* for **caffeic acid**.

For **CIN** the results indicate that the partitioning behaviour increased with the IL hydrophilic nature, being [Ch]Cl the most efficient in its extraction, followed by [Ch][Ac]. Cinnamic acid preferentially migrates to the IL-rich phase (K_{CIN} > 1) and it can be concentrated over 200 times (K > 200) using these two ILs. Comparing results of cholinium-based ILs to those obtained when using [C_4mim]Cl, the partition of **CIN** is significantly lower when using this last IL. This can probably be attributed to the lower hydrophilic character of $[C_4mim]^+$ cation, when compared to cholinium cation.

The extraction efficiencies are very high for the three phenolic acids in all ABS studied, in particular for cinnamic acid: a single-step extraction efficiencies of this acid to the IL-rich phase were always higher than 99%, confirming the great potential of ILs to be applied in this extraction.

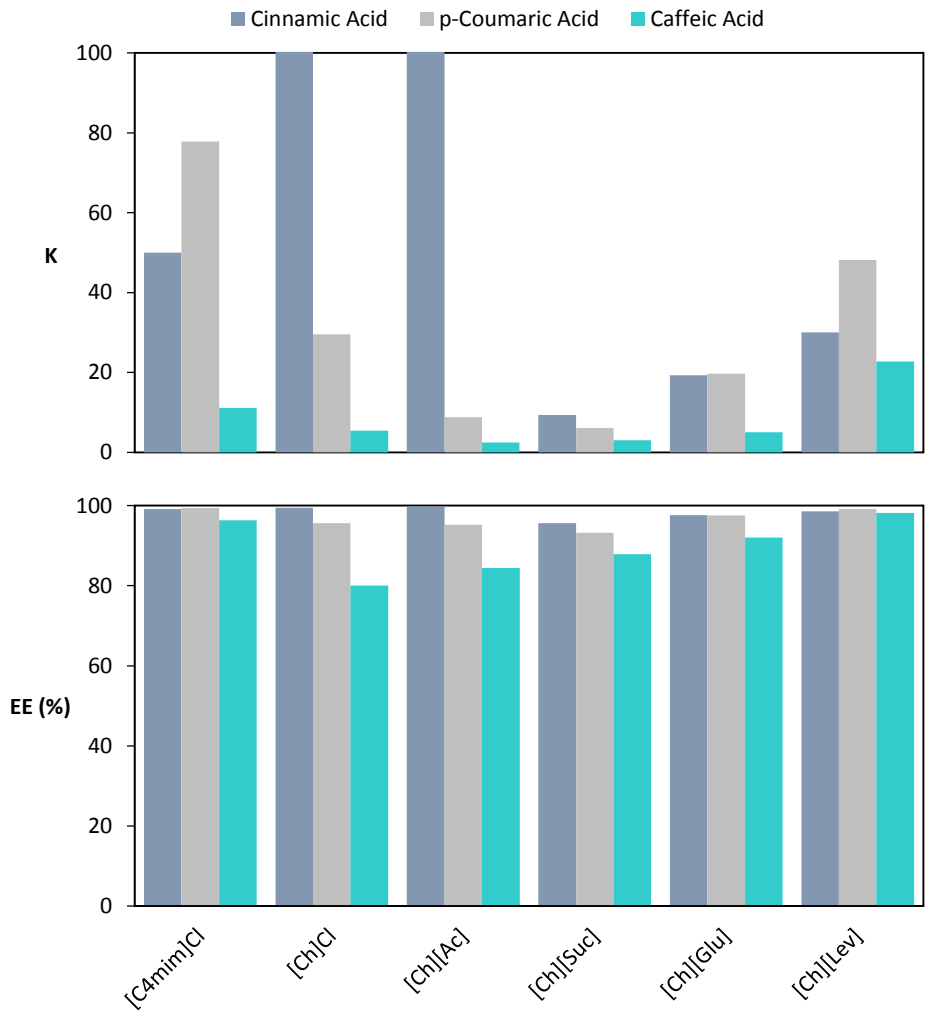

Figure 4.3 – Partition coefficients (K_{ACID}) and extraction efficiencies percentages ($\%EE_{ACID}$) of cinnamic acid (■), p-coumaric acid (■) and caffeic acid (■) for the systems composed of IL + K_3PO_4 at room temperature.

For cinnamic acid the highest partition were obtained for [Ch]Cl and [Ch][Ac]. p-Coumaric acid and caffeic acid were better extract with [C_4mim]Cl and [Ch][Lev] respectively.

An explanation can be extrapolated to the lower partition coefficients observed with caffeic acid: the fact of owning a chemical structure propitious to interferences with the inorganic salt, and thus K_3PO_4 tend to attract the acid to its phase.

In summary, it can be established that high partition coefficients can be reached for cinnamic acid using hydrophilic cholinium-based ionic liquids, and that these systems could be a successful approach for the extraction of biomolecules and purification in industrial processes. Furthermore, the large range obtained in the K values for the other acids by changing the IL indicates that the individual biomolecules extraction efficiency from a mixture can be manipulated by the correct choice of the IL.

4.5 Influence of Ionic liquid ions in phenolic acids partitioning

The influence of the ionic liquid on the partition coefficient for cinnamic acid is shown in Figure 4.4: particularly high partition coefficients were attained for systems composed of the most hydrophilic ionic liquids, [Ch]Cl and [Ch][Ac]. On the other hand, the lowest partition coefficients are observed for the systems constituted by [Ch][Glu] and [Ch][Suc], even though these systems have greater amounts of K_3PO_4 which should promote the preferential migration of the acid to the IL-rich phase.

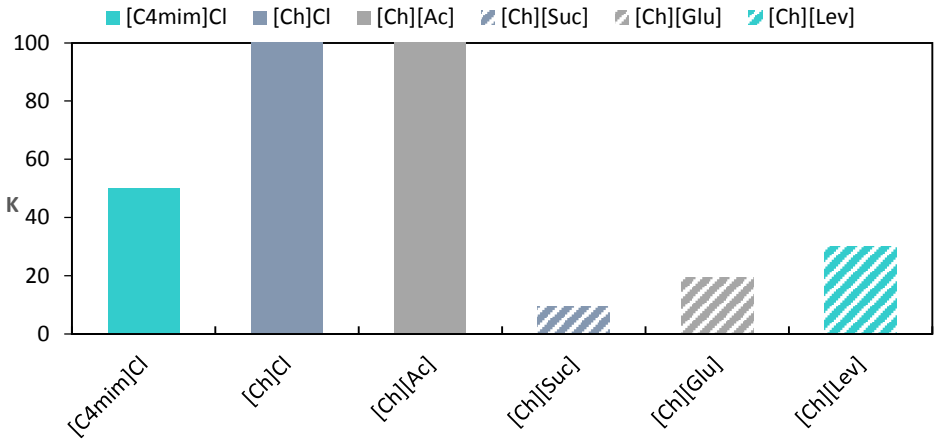

Figure 4.4 – Influence of the IL on the partition coefficient of the cinnamic acid (0.147 g·dm^{-3}) using IL-based ABS and K_3PO_4, at room temperature.

Figure 4.5 and Figure 4.6 are refer to the influence of the ILs studied on the partitioning of p-coumaric acid and caffeic acid. Both these acids display very similar behaviours, probably due to their similar chemical structure. The rank of the partition coefficients of p-coumaric acid is: [C_4mim]Cl > [Ch][Lev] > [Ch]Cl > [Ch][Glu] > [Ch][Ac] > [Ch][Suc], while for caffeic acid is: [Ch][Lev] > [C*4*mim]Cl > [Ch]Cl > [Ch][Glu] > [Ch][Suc] > [Ch][Ac]. However, coumaric acid presents higher partition coefficients than caffeic acid for all the systems. This can probably be explained by the fact that caffeic acid has one extra hydroxyl group than p-coumaric acid, thus enhancing the probability of being engaged in hydrogen–bonding interactions with phosphate anions, forming new species.

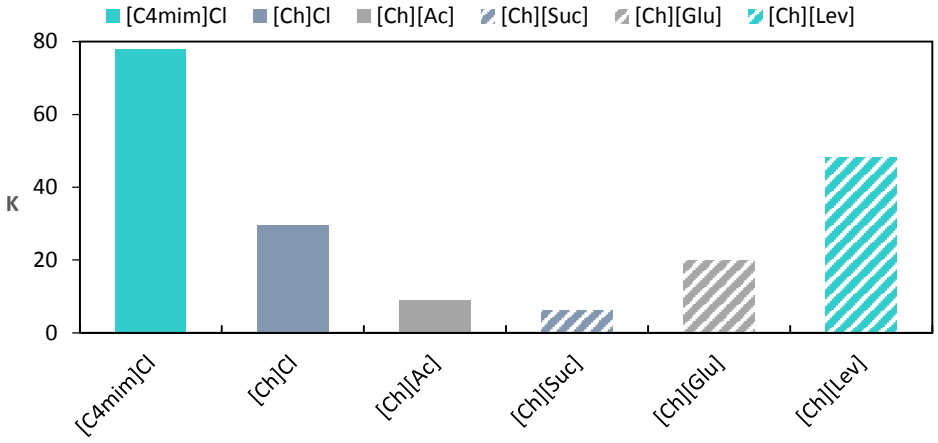

Figure 4.5 – Influence of the IL on the partition coefficient for p-coumaric acid (0.800 g·dm^{-3}) using IL-based ABS and K_3PO_4, at room temperature.

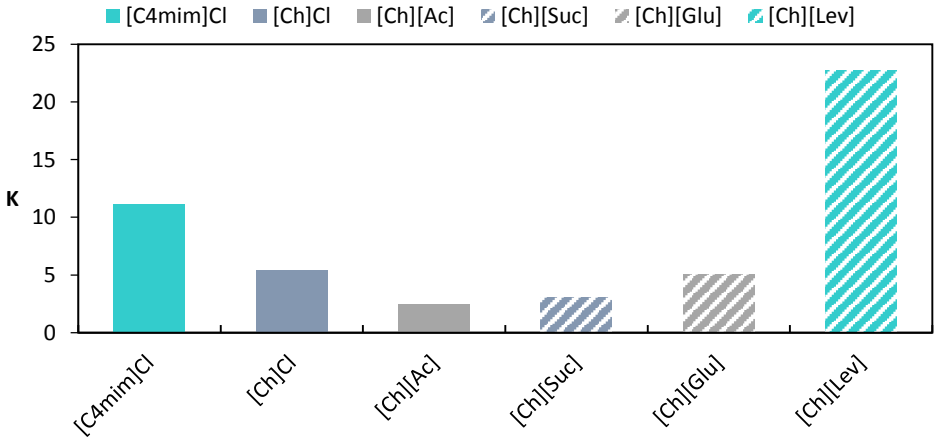

Figure 4.6 – Influence of the IL on the partition coefficient for caffeic acid (0.672 g·dm^{-3}) using IL-based ABS and K_3PO_4, at room temperature.

The partition coefficients of caffeic acid are relatively higher than unity ($K_{CAF} > 1$), that is, **CAF** migrates to the IL-rich phase. The low values obtained for caffeic acid are due to the fact that it complex with $PO4^{3-}$ and is more concentrated in the K_3PO_4-rich phase, decreasing greatly the partition coefficient. These suggest that the chemical structure of the acid and the properties of the aqueous medium, namely the pH of the phases, has a main impact in the partitioning of **CAF.**

As it was referred in the Methodology chapter, both aqueous-rich phases were weighted and it was possible to determine the concentrations (through the density of the acid) in each phase. This process is usually called as mass balance (or mass transfer and it was found that the disclosure of the balance was found to be positive. These balance are show in Appendix D.

4.6 Effect of concentration of the phenolic acids in their partitioning

To test the influence of the concentration of phenolic acid, three ionic liquids were selected. For this purpose, the cholinium ($[Ch]^+$) anion was fixed and was combined with two anions, Cl^- and $[Ac]^-$. On the other hand, and regarding the structural variations at the cation, the chloride (Cl^-) anion was fixed and was combined with the following cations: $[Ch]^+$ and $[C_4mim]^+$.

The range of concentrations used to study the influence of the concentration of each one of the phenolic acids in their extraction can be seen in Table 4.4.

Table 4.4 – Concentration of the phenolic acids in two new aqueous solutions, at room temperature.

	Cinnamic Acid	**p-Coumaric Acid**	**Caffeic Acid**
M_w / g·mol^{-1}	148.16	164.16	180.16
Concentration *1* / g·dm^{-3}	0.071	0.657	0.521
Concentration *1* / mol·dm^{-3}	4.79×10^{-4}	4.00×10^{-3}	2.89×10^{-3}
Concentration 2 / g·dm^{-3}	0.147	0.800	0.672
Concentration 2 / mol·dm^{-3}	9.95×10^{-4}	4.87×10^{-3}	3.73×10^{-3}
Concentration *3* / g·dm^{-3}	0.228	0.994	0.888
Concentration *3* / mol·dm^{-3}	1.54×10^{-3}	6.06×10^{-3}	4.93×10^{-3}

The extraction methodology for the phenolic acids described above in the Methodologies chapter was adopted and the determination of the partition coefficients carried out. The partition coefficients obtained are listed in Table 4.5, while the extraction efficiencies are shown in Table 4.6. The influence of the concentration of cinnamic, p-coumaric and caffeic acid in their partition coefficients is shown in Figure 4.7, Figure 4.8 and Figure 4.9, respectively.

Table 4.5 – Initial concentration and partition coefficient of phenolic acids obtained in this work at room temperature.

Ionic Liquid	Cinnamic Acid		p-Coumaric Acid		Caffeic Acid	
	C_{CIN} / mol·dm^{-3}	K_{CIN}	C_{COU} / mol·dm^{-3}	K_{COU}	C_{CAF} / mol·dm^{-3}	K_{CAF}
[Ch]Cl	4.79×10^{-4}	78.82	4.00×10^{-3}	2.04	2.89×10^{-3}	2.53
	9.95×10^{-4}	247.40	4.87×10^{-3}	29.53	3.73×10^{-3}	5.45
	1.54×10^{-3}	280.00	6.05×10^{-3}	2.02	4.93×10^{-3}	9.92
[Ch][Ac]	4.79×10^{-4}	56.12	4.00×10^{-3}	0.86	2.89×10^{-3}	3.65
	9.95×10^{-4}	227.50	4.87×10^{-3}	8.79	3.73×10^{-3}	2.49
	1.54×10^{-3}	51.36	6.05×10^{-3}	0.79	4.93×10^{-3}	88.88
[C_4mim]Cl	4.79×10^{-4}	12.74	4.00×10^{-3}	38.89	2.89×10^{-3}	21.55
	9.95×10^{-4}	49.97	4.87×10^{-3}	77.82	3.73×10^{-3}	11.09
	1.54×10^{-3}	13.97	6.05×10^{-3}	39.92	4.93×10^{-3}	58.85

Table 4.6 – Initial concentration and extraction efficiencies of phenolic acids (%EE_{ACID}) obtained in this work at room temperature.

Ionic Liquid	Cinnamic Acid		p-Coumaric Acid		Caffeic Acid	
	C_{CIN} / mol·dm^{-3}	%EE_{CIN}	C_{COU} / mol·dm^{-3}	%EE_{COU}	C_{CAF} / mol·dm^{-3}	%EE_{CAF}
[Ch]Cl	4.79×10^{-4}	98.20	4.00×10^{-3}	59.54	2.89×10^{-3}	63.45
	9.95×10^{-4}	99.47	4.87×10^{-3}	95.65	3.73×10^{-3}	80.03
	1.54×10^{-3}	99.49	6.06×10^{-3}	59.30	4.93×10^{-3}	87.20
[Ch][Ac]	4.79×10^{-4}	99.18	4.00×10^{-3}	36.21	2.89×10^{-3}	85.85
	9.95×10^{-4}	99.78	4.87×10^{-3}	95.20	3.73×10^{-3}	84.47
	1.54×10^{-3}	99.82	6.06×10^{-3}	38.38	4.93×10^{-3}	99.33
[C_4mim]Cl	4.79×10^{-4}	96.47	4.00×10^{-3}	98.89	2.89×10^{-3}	98.02
	9.95×10^{-4}	99.13	4.87×10^{-3}	99.41	3.73×10^{-3}	96.31
	1.54×10^{-3}	96.77	6.06×10^{-3}	98.92	4.93×10^{-3}	99.26

Experimental data obtained for the partition coefficients of cinnamic acid are represented in Figure 4.7. For a given concentration, the partition coefficients, as well as the extraction efficiencies, follow the order: [Ch]Cl > [Ch][Ac] > [C_4mim]Cl. The choice of the cation is crucial for the extraction of cinnamic acid, since the ILs based on cholinum-cation always display much higher partition coefficients than those obtained for the [C_4mim]Cl. Cinnamic acid presents the same tendency for both cholinium-based ILs: the partition coefficient increases as the concentration of the solute increases. In the case of [C_4mim]Cl, the partition coefficient reaches the maximum value at an intermediate concentration (9.95×10^{-3} mol·dm^{-3}). Comparing both cholinium and imidazolium-based IL, the first class are more efficient in the extraction of cinnamic acid, probably due to the

more hydrophobic nature of the imidazolium-cation. Between [Ch]Cl and [Ch][Ac], [Ch]Cl displays the best results.

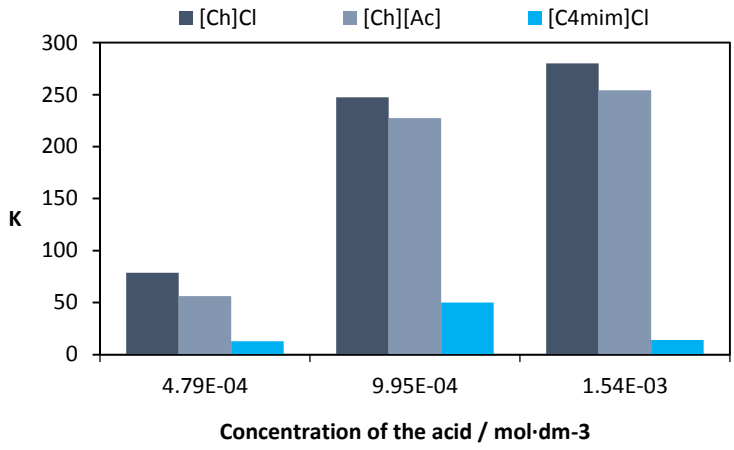

Figure 4.7 – Influence of the concentration of cinnamic acid on the partition coefficient, K_{CIN}, using ABS based on IL: ■ – [Ch]Cl; ■ – [Ch][Ac]; ■ – [C_4mim]Cl. Th results were obtained with a concentration between 4.79×10^{-4} and 1.54×10^{-3} mol·dm^{-3} at room temperature.

In Figure 4.8, the influence of the p-coumaric concentration in the partition coefficient is presented. For the three studied ILs, the partition coefficient for the p-coumaric acid shows a maximum for at an intermediate concentration of 4.87 × 10^{-3} mol·dm^{-3} (0.800 g·dm^{-3}). [Ch]Cl and [C_4mim]Cl are more efficient in extracting p-coumaric acid than [Ch][Ac], indicating that in this particular case de anion display a major role in the extraction. To a fixed concentration of 4.87 × 10^{-3} mol·dm^{-3} of **COU**, it is possible to compare the effect of IL on the extraction efficiency. On the other hand, it can also be concluded that the cation is also important since very different K values were obtained for [Ch]Cl and [C_4mim]Cl, being this last IL the most efficient in the p-coumaric acid extraction.

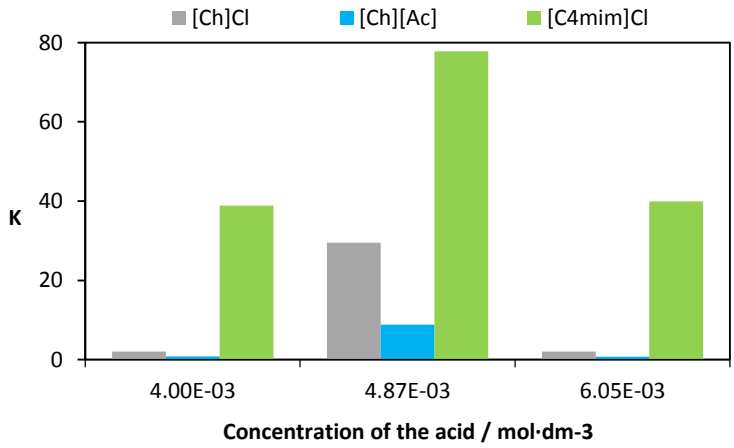

Figure 4.8 – Influence of the concentration of p-coumaric acid on the partition coefficient, K_{COU}, using ABS based on IL: ■ – [Ch]Cl; ■ – [Ch][Ac]; ■ – [C_4mim]Cl. This results were obtained with a concentration between 4.00×10^{-3} and 6.05×10^{-3} mol·dm^{-3} at room temperature.

Figure 4.9 presents the influence of the concentration of caffeic acid on the partition coefficient. Different behaviours were obtained for the different ILs: while for the [Ch]Cl the partition coefficient

always increases with concentration, in the studied concentration range, for the other two ILs the K value reaches a minimum value at an intermediate concentration of 4.93×10^{-3} mol·dm^{-3} (0.888 g·dm^{-3}) for the system based on [Ch][Ac]. Nevertheless, for all the studied ILs the highest K values were obtained for the highest concentration.

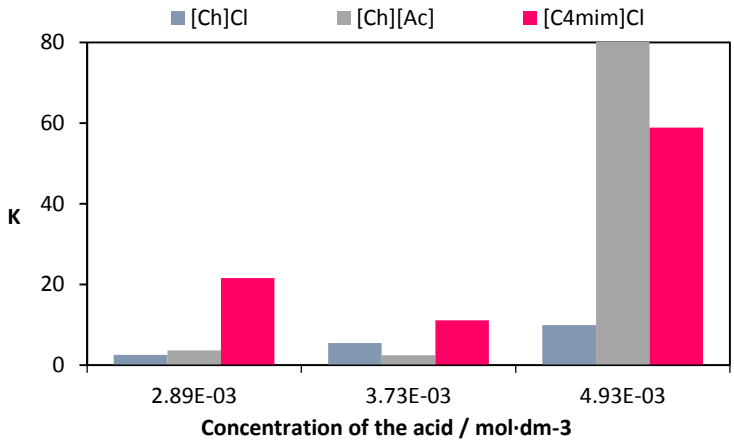

Figure 4.9 – Influence of the concentration of caffeic acid on the partition coefficient, K_{CAF}, using ABS based on IL: ■ – [Ch]Cl; ■ – [Ch][Ac]; ■ – [C$_4$mim]Cl. This results were obtained with a concentration between 2.89×10^{-3} and 4.93×10^{-3} mol·dm^{-3} at room temperature.

5. Ionic Liquid + Phenolic Acid (aq.) + Polyethylene Glycol systems

5. Ionic Liquid + Phenolic Acid (aq.) + Polyethylene Glycol systems

5.1 Implementation of PEG-based ABS

The addition of polyethylene glycol (PEG) to hydrophilic ionic liquids solutions can also induce phase separation. These systems confer very mild extraction conditions, compared to those provided by inorganic salts, especially in what concerns pH. However, one of the main disadvantages of PEG containing systems is their higher viscosity, hindering the mass transfer between phases and taking a long time to reach equilibrium. In order to circumvent this problem, low molecular weight PEGs are usually used. In this work, polyethylene glycol with a molecular weight of 600 $g \cdot mol^{-1}$ was employed.

Four ionic liquids were used to implement these ABS, namely cholinium chloride, cholinium acetate, cholinium succinate and cholinium glutarate. PEG-600 was used as the phase splitting agent. Phase diagrams of the systems composed of PEG 600 and ILs have been determined in the literature and are presented in Figure 5.1. [13, 33]

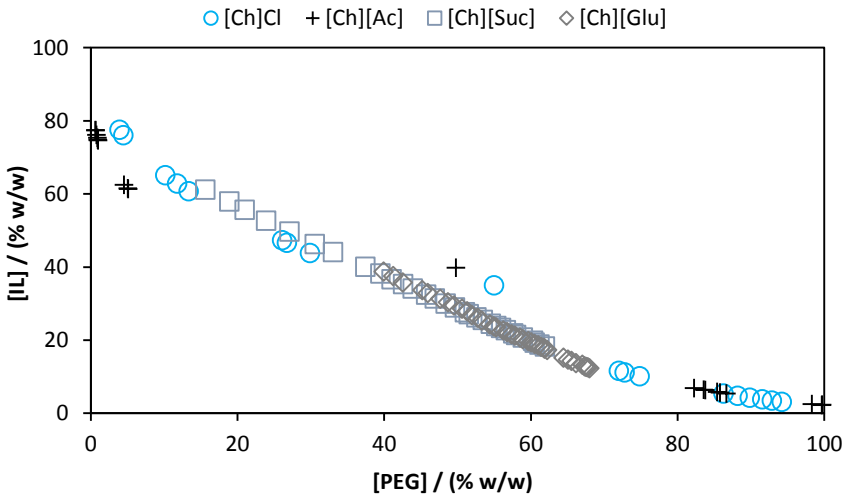

Figure 5.1 – Phase diagrams of the ternary systems composed of PEG 600 + ionic liquid + H_2O at 298 K (percentage weight fraction): (○)[Ch]Cl; (+) [Ch][Ac]; (□) [Ch][Suc]; (◊) [Ch][Glu]. [13, 33]

The compositions of the ternary mixtures used for the phenolic acids partitioning were also chosen based on the phase diagrams determined in previous works. These compositions are presented in Table 5.1 as well as their respective tie line lengths.

Table 5.1 - Compositions of ionic liquid and PEG at the initial mixture used to prepare the ampoules.

Ionic Liquid	$[IL]_M$	$[PEG]_M$	$[ACID]_M$ (aq.)	TLL
[Ch]Cl	34.93	54.94	10.13	115.65
[Ch][Ac]	39.82	49.79	10.39	123.64
[Ch][Suc]	43.87	41.26	14.87	105.38
[Ch][Glu]	42.14	42.62	15.24	100.86

5.2 Physicochemical properties of IL-based ABS

The pH values of the coexisting phases of the systems shown in Table 5.2 range between 6.8 and 10.3, depending in the ionic liquid present in the system.

Table 5.2 – Experimental pH, density and viscosity for the cholinium-rich phase and PEG-600-rich phase for systems composed by IL + PEG + H_2O at 298.15 K.

Ionic Liquid	PEG-600-rich phase			Cholinium-rich phase		
	pH	ρ (g·cm^{-3})	η (mPa s)	pH	ρ (g·cm^{-3})	η (mPa s)
[Ch]Cl	7.40	1.123	138.020	7.410	1.107	45.269
[Ch][Ac]	10.20	1.120	199.497	10.31	1.096	70.004
[Ch][Suc]	6.81	1.165	175.333	6.97	1.137	159.833
[Ch][Glu]	7.12	1.147	169.263	7.33	1.133	254.167

pH values are slightly higher in IL-rich phase comparing with the PEG 600-rich phase. The highest value of pH (> 10) is obtained for the system composed by [Ch][Ac], either in IL-rich phase or PEG 600-rich phase. Thus, it can be anticipated that phenolic acids in this ABS are mainly in its deprotonated form (pH > pKa_2 = 10.20), while in the other systems they are in their neutral form (pKa_1 = 6.81 < pH < 7.41 = pKa_2). Consequently, the acids can complex with other molecules, namely with the cholinium succinate and form new species. However, after extracting both phases, quantifying analytically the acids and analysing the spectrums, no interactions between the biomolecules and the cholinium succinate were found.

Data for densities and viscosities of the PEG 600-based ABS are presented in Figure 5.2 and Figure 5.3, in the temperature range between 293.15 K and 303.15 K, for all the systems studied. Both density and viscosity for both phases of the prepared ABS are found to decrease with temperature.

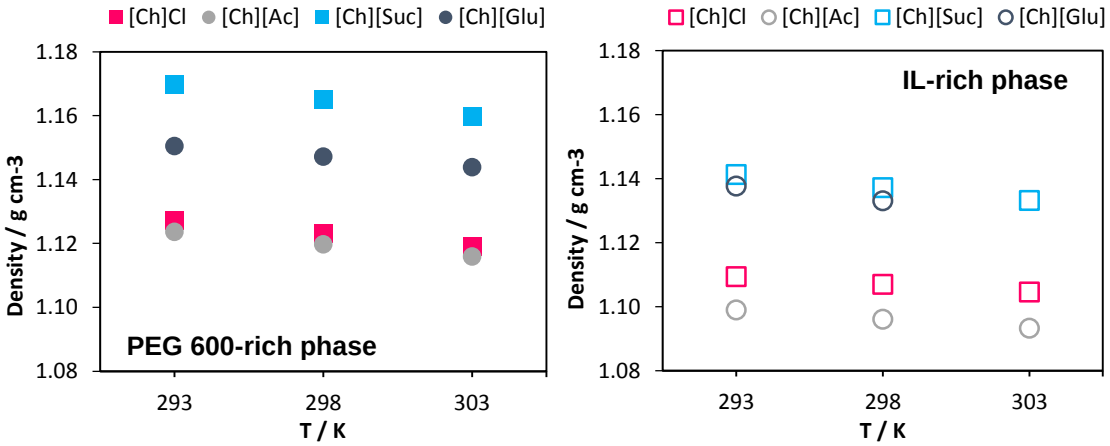

Figure 5.2 – Experimental density (ρ) as a function of temperature for the PEG-rich phase (full symbols) and IL-rich phase (open symbols) for systems composed by ILs: (■) [Ch]Cl; (●) [Ch][Ac]; (■) [Ch][Suc]; (●) [Ch][Glu].

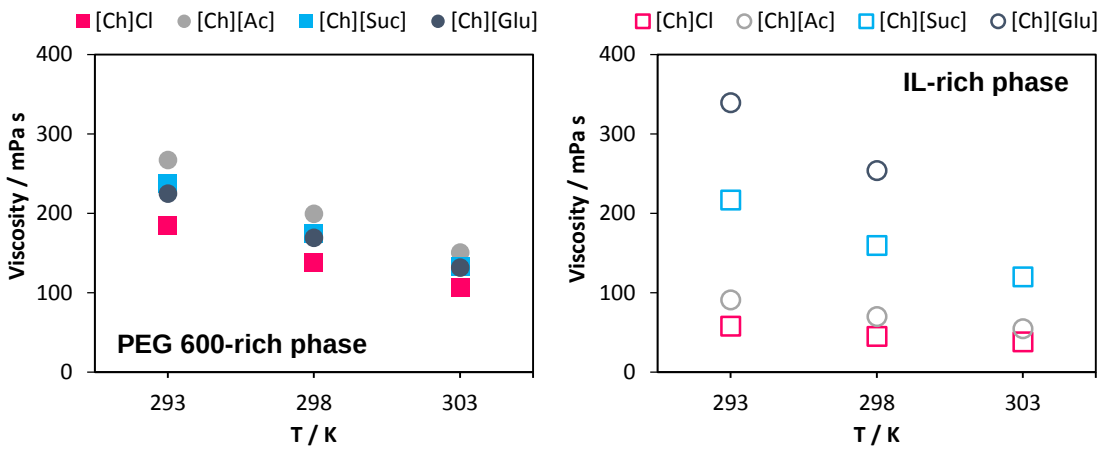

Figure 5.3 – Experimental viscosity (η) as a function of temperature for the PEG-rich phase (full symbols) and IL-rich phase (open symbols) for systems composed by ILs: (■) [Ch]Cl; (●) [Ch][Ac]; (■) [Ch][Suc]; (●) [Ch][Glu].

In all the studied systems, the density of the PEG 600-rich phase is always higher than the corresponding IL-rich phase, indicating that the bottom phase is composed of PEG 600 while the top layer is the IL-rich phase. The densities of both PEG 600-rich phase and cholinium-rich phase follow the same trend, *[Ch][Ac] > [Ch][Glu].> [Ch][Suc] >[Ch]Cl*. Of all the systems studied, none of them present large differences in the values of density between both phases.

As for the viscosity of IL-rich phase, it can observed from Figure 5.3 that there is a large difference in the values among the different ILs. For IL-rich phase, the viscosities increase with the increase from [Ch]Cl (η = 45.269 mPa·s at 298.15 K) to [Ch][Glu] (η = 254.167 mPa·s at 298.15 K). Regarding the PEG 600-rich phase the values of viscosities at 298.15 K range between 139.020 mPa·s for [Ch]Cl and 199.497 mPa·s for [Ch][Ac].

Viscosities of cholinium-based-rich phases are substantially lower than those observed for the PEG 600-rich phase, except for the most viscous system based on [Ch][Glu], where there is an inversion on the relative viscosities with the temperature.

Figure 5.4 shows the viscosity data of both aqueous-rich phases for cholinium containing ABSs.

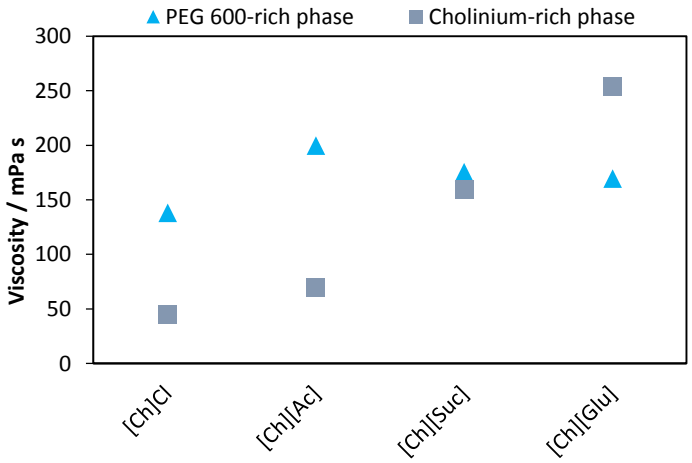

Figure 5.4 – Viscosity (η) of the coexisting phases in ABS composed of IL + PEG 600 + H_2O at 298.15 K.

Of all systems considered, differences between the viscosities of both phases for the system composed by [Ch][Suc] are the smallest due to the low affinity for water as it is possible to see in Figure 5.4. This could lead to a less favourable mass transfer and a tougher separation.

The viscosity of PEG/IL-based systems are significantly higher than those obtained for the corresponding IL/Inorganic Salt-based ABS. Consequently, the mass transfer is more difficult and the extraction of the phenolic acids is weaker.

5.3 Partitioning coefficients and extraction efficiencies

It was impossible to determine the partition coefficients for p-coumaric acid in [Ch][Suc] and [Ch][Glu], since the the UV-vis spectra of the aqueous solution of pure p-coumaric and the p-coumaric in both the IL-rich phase and the PEG 600-rich phase were different. In order to solve this problem, the ideal partition coefficients were calculated by means of the solubilities of the p-coumaric acid in each phase. In order to validate this procedure, ideal partition coefficients using the solubility of p-coumaric acid in both phases of [Ch]Cl and [Ch][Ac] containing system were calculated and compared to the real partition coefficients obtained using the usual procedure described in the Methodologies chapter.

In order to measure the solubilities of the p-coumaric acid in both ABS phases, an ampoule with [Ch][Suc] + PEG 600 + H_2O (pure) was prepared, stirred and then the phases separated. Afterwards, a known quantity of p-coumaric acid was added in both separated phases until the solid-liquid equilibrium was achieved. Both phases were centrifuged to guarantee the separation of the precipitate from the supernatant. Samples of the supernatant of each phases were diluted and quantified through the UV-Vis. Calibration curves, shown in Figure 10.7 in Appendix B, were established for these particular situations.

The concentration of p-coumaric acid was quantified in both phases at wavelength of 286 nm using the calibration curves. The ideal partition coefficients were determined according to the equation (4).

$$K_{IDEAL} = \frac{S_{IL}}{S_{PEG\ 600}} \qquad (4)$$

where S_{IL} represent the solubility of p-coumaric acid in the IL-rich phase and $S_{PEG\ 600}$ is the concentration of **COU** in the PEG-600-rich phase.

The measured p-coumaric acid solubilities are presented in Table 5.3. Solubility in the IL-rich phase is lower PEG 600-rich phase for the [Ch]Cl containing system, while for that containing [Ch][Ac] the solubilities are almost equal.

In order to establish the feasibility of this method, the ideal and the real K values were compared in Table 5.3. It can be observed that the values are in good agreement with each other, providing the correct trend of the p-coumaric acid phase affinity. Thus, it can be concluded that it is possible to use the ideal partition coefficients for p-coumaric for comparison with the partition coefficients for the other two acids. For consistency, and despite the fact that real K values were measured [Ch]Cl and [Ch][Ac] containing systems, always ideal K values were used for p-coumaric acid.

Table 5.3 – Solubility of p-coumaric acid in both aqueous phases.

IL + PEG 600	S_{IL} / g·dm^{-3}	$S_{PEG\ 600}$ / g·dm^{-3}	$K_{IDEAL-COU}$	$K_{REAL-COU}$
[Ch]Cl	51.66	113.94	0.45	0.52
[Ch][Ac]	97.67	101.66	0.96	1.39
[Ch][Suc]	47.14	316.80	0.15	-
[Ch][Glu]	155.15	154.69	1.00	-

The values of the partition coefficients and extraction efficiencies obtained for the three acids with the proposed PEG-ABS systems is presented in Table 5.4. The calculated associate errors to these measurements are listed in Table 5.5.

Table 5.4 – Weight fraction composition of the initial mixture, TLL and partition coefficient of phenolic acids obtained at room temperature.

IL + PEG 600	K_{CIN}	$\%EE_{CIN}$	K_{COU}	$\%EE_{COU}$	K_{CAF}	$\%EE_{CAF}$
[Ch]Cl	0.32	22.46	0.45	31.56	1.15	53.43
[Ch][Ac]	0.43	26.11	0.96	54.71	4.97	80.65
[Ch][Suc]	5.06	86.81	0.14	-	0.49	44.02
[Ch][Glu]	2.73	71.48	1.00	-	0.45	33.40

Table 5.5 – Standard deviations and errors obtained for the partition coefficients values at room temperature.

IL + PEG 600	Cinnamic acid		p-Coumaric acic		Caffeic acid	
	Standard Deviation σ	Standard Error (%)	Standard Deviation σ	Standard Error (%)	Standard Deviation σ	Standard Error (%)
[Ch]Cl	0.012	3.81	0.008	1.57	0.010	0.84
[Ch][Ac]	0.034	7.97	0.175	12.63	0.283	5.69
[Ch][Suc]	0.900	17.79	-	-	0.107	21.75
[Ch][Glu]	0.270	9.88	-	-	0.024	5.47

Figure 5.5 illustrates the partition data obtained for phenolic acids in the PEG 600-based ABS studied in this work. The extraction efficiencies of the acids are also shown to allow comprehensive comparisons between different ILs.

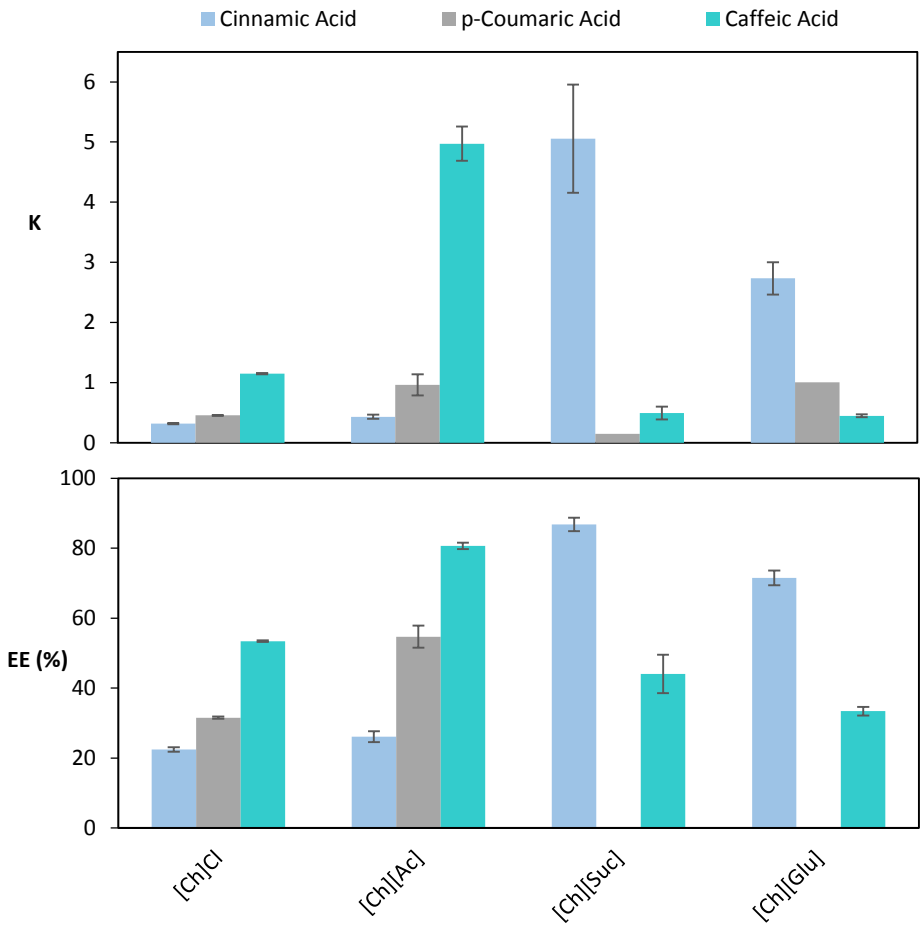

Figure 5.5 - Partition coefficients (K_{ACID}) and extraction efficiencies percentages ($\%EE_{BIO}$) of cinnamic acid (■), p-coumaric acid (■) and caffeic acid (■) for PEG 600-based ABS at room temperature.

The first observation to be made is that the partition coefficient and the extraction efficiencies values obtained here are very different from those previously observed for K_3PO_4-based systems. Much lower partition coefficient values are obtained for the PEG-based systems indicating a less efficient extraction. Also to be noted that, in some cases, K values bellow 1 were obtained indicating that the acids are better extracted to the PEG 600-rich phase than to the IL-rich phase. In order to better discuss these results, a log-scale representation of K values obtained is presented in Figure 5.6.

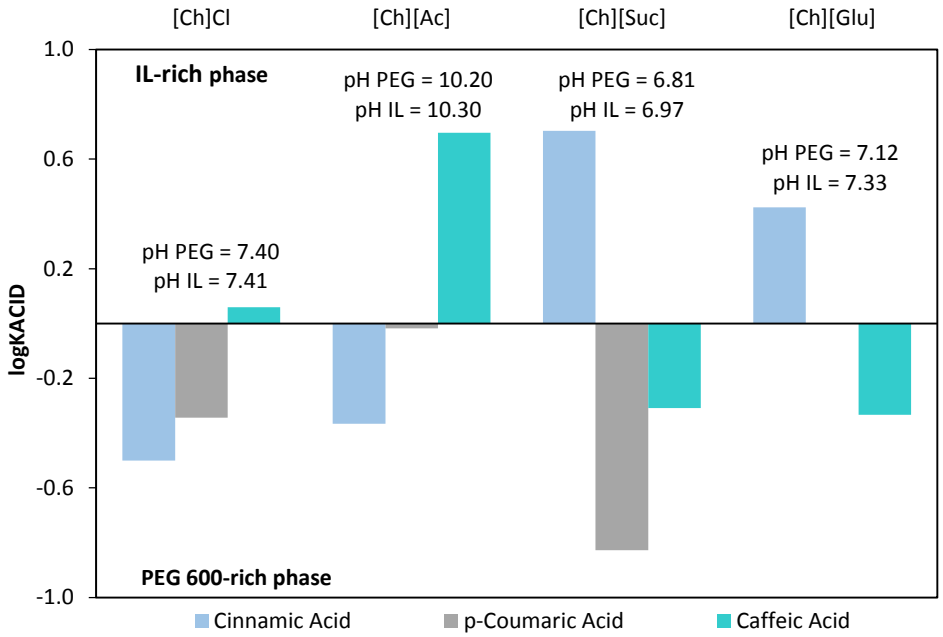

Figure 5.6 – Logarithm representation of the phenolic acids partition coefficients ($logK_{ACID}$) for PEG 600-based ABS at room temperature. The pH values of the top (IL) and bottom (PEG 600) phases are also presented.

In Figure 5.6 it is very clear that, overall, there is a high affinity of the phenolic acids to the PEG 600-rich phase. p-Coumaric acid is better extract by the system containing [Ch][Suc] but it partite more favourably towards the PEG 600 phase. Cinnamic acid prefers the cholinium-rich phase for the systems composed of [Ch][Glu] and [Ch][Suc], and caffeic acid also shows a higher affinity for the IL-rich phases when [Ch][Ac] is used. This variety of behaviours is very attractive for the implementation of selective separation methodologies of these acids, as it will be discussed in the next chapter.

Regarding the pH conditions offered by these systems, milder conditions can be attained in comparison to the K3PO4-based systems, as expected. The pH of both phases in equilibrium is very similar to each other and displays values around 7, with the exception of the system based on [Ch][Ac].

5.4 Influence of Ionic liquid ions in phenolic acids partitioning

The set of results showed before allows the analysis of the impact of the IL on the partition coefficients of the phenolic acids, as well as the nature of the solute and its partitioning pattern. The partition coefficients ($logK_{ACID}$) in log-scale representation for each one of the three phenolic acids alone are depicted in Figure 5.7, Figure 5.8 and Figure 5.9.

Cinnamic acid presents very different affinities for the PEG 600-rich or the IL-rich phase depending on the IL used in the extraction. For the systems composed of [Ch]Cl and [Ch][Ac], this acid preferentially migrates for the PEG-rich phase while for the other two ILs, [Ch][Suc] and [Ch][Glu], the opposite behaviour is observed. Nevertheless, the highest K value was obtained for the systems containing [Ch][Suc].

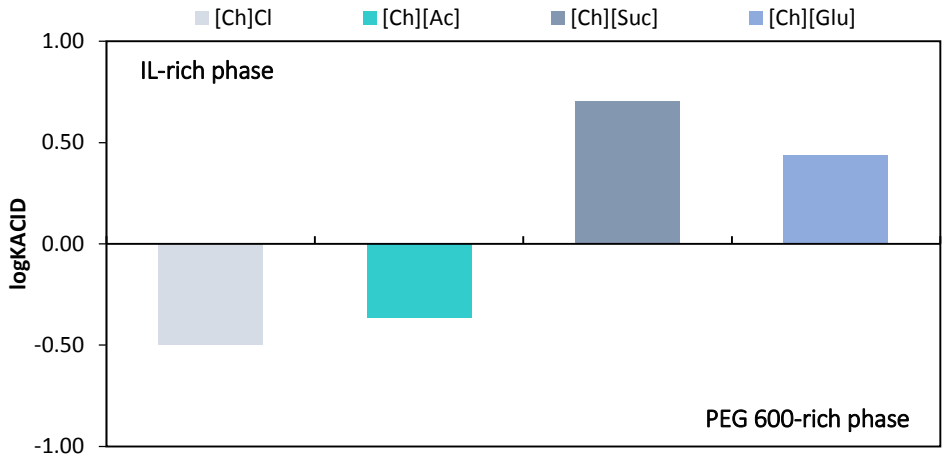

Figure 5.7 – Influence of the IL on the partition coefficient for cinnamic acid (0.147 g·dm^{-3}) using IL-based ABS and PEG 600 at room temperature.

Figure 5.8 show the partition for both IL- and PEG 600-rich phases of p-coumaric acid. The affinity trend for the different phases observed for cinnamic acid is also valid for the p-coumaric acid, with the exception of the systems containing [Ch][Suc], which in this case show higher affinity for the PEG 600-rich phase. Also to be mentioned, the results obtained for the systems containing [Ch][Ac] and [Ch][Glu, where partition coefficients similar to the unit were obtained, indicating that there is no preference for any phase.

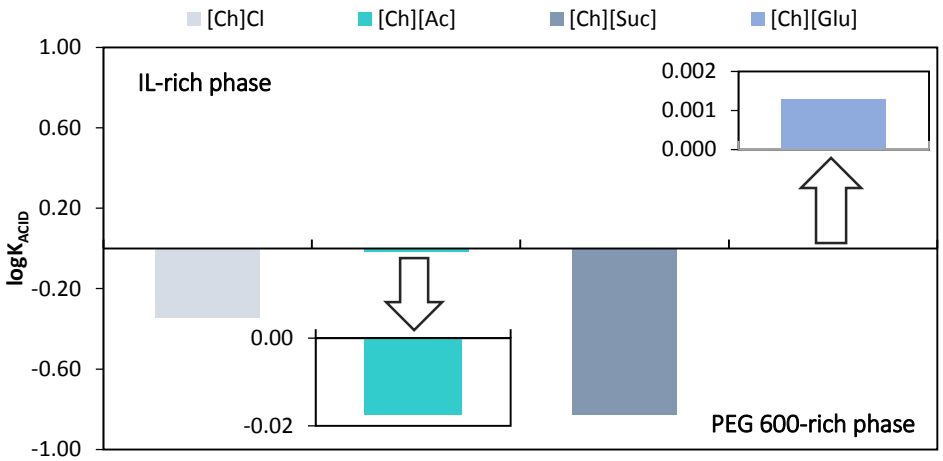

Figure 5.8 – Influence of the IL on the partition coefficient for p-coumaric acid (0.800 g·dm^{-3}) using IL-based ABS and PEG 600 at room temperature.

Caffeic acid preferentially migrate to the cholinium-based-rich phase for the most hydrophilic ILs: [Ch]Cl and [Ch][Ac], being the partition coefficients obtained for this last IL the highest. For the two other systems, **CAF** is transferred to the bottom phase constituted by PEG-600.

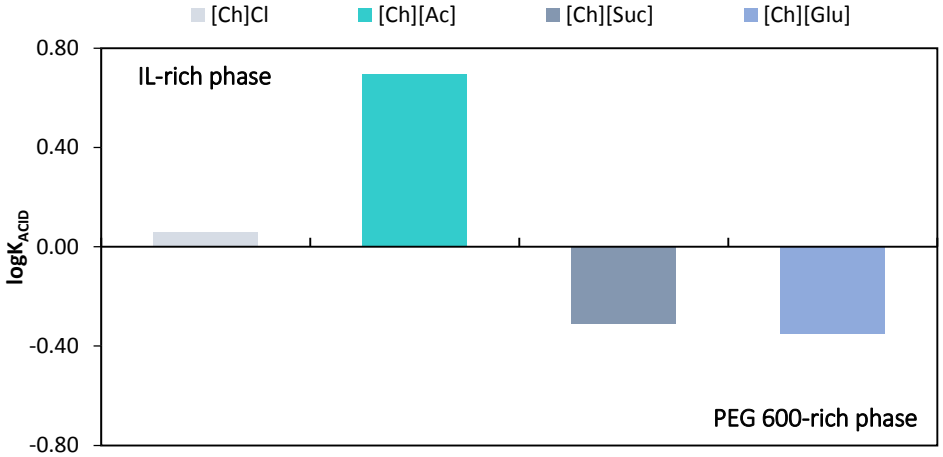

Figure 5.9 – Influence of the IL on the partition coefficient for caffeic acid (0.672 g·dm^{-3}) using IL-based ABS and PEG 600 at room temperature.

The validation of the quantification of phenolic acids methodology was achieved through the use of a mass balance. The material balance for the PEG 600-based systems is described in Table 12.4,

Table 12.5 and Table 12.6 in Appendix D.

6. Selective Extraction

6. Selective Extraction

Selective extraction

Several extraction techniques have been developed in the literature in an attempt to obtain more efficient extraction of the analytes from the matrix by improving the selectivity for target compounds, reducing of both extraction time and organic solvent consumption. Selective extraction by means of partitioning of the biomolecules in ABS has been shown to be a feasible alternative as suggested by *J.F.B. Pereira et al*.[42]

The migration of a target solute in an ABS depends on the physicochemical properties of the two aqueous phases in equilibrium, so that specific interactions can be manipulated. Several conditions, such as the chemical composition of the system, temperature, pH, and the inclusion of adjuvants, affinity ligands or amphiphilic structures [7, 43, 44], can be used to control the biomolecules partitioning. In the previous chapters, several aqueous biphasic systems comprising ILs and K_3PO_4 or PEG were tested for the separation of each one of the studied phenolic acids. As it can be seen in Figure 5.6, some of the PEG-based systems might allow for the selective extraction of one phenolic acid to one phase and the other acids to the other phase. This chapter focuses on the use of Ionic Liquid + Phenolic Acid (aq.) + Polyethylene Glycol systems to establish a selective extraction of the phenolic acids studied in this work.

The selectivity was calculated using the partition coefficients obtained according to Equations (5) and (6).

$$S_{CAF/CIN} = \frac{K_{CAF}}{K_{CIN}} \quad (5)$$

$$S_{CIN/COU} = \frac{K_{CAF}}{K_{COU}} \quad (6)$$

Where ($S_{CAF/CIN}$) and ($S_{CAF/COU}$) are the selectivities of caffeic acid regarding cinnamic acid and coumaric acid, respectively.

The calculated selectivity data is shown in Table 6.1 and allow the evaluation of the IL structural influence in the selectivity, at room temperature. The selectivity data indicate that the IL chemical structure has a huge influence on the selective separation of caffeic acid from the remaining phenolic acids.

Table 6.1 – Selectivities of caffeic/cinnamic ($S_{CAF/CIN}$) and caffeic/coumaric ($S_{CAF/COU}$) considering all PEG 600-ILs-based ABS, tested at room temperature.

Ionic Liquid	Selectivity	
	$S_{CAF/CIN}$	$S_{CAF/COU}$
[Ch]Cl	3.625	2.528
[Ch][Ac]	11.540	5.176
[Ch][Suc]	0.175	3.303
[Ch][Glu]	0.097	0.463

It can concluded that [Ch][Ac] provides the best results regarding the implementation of a system that would be selective towards caffeic acid, in particular for the separation of caffeic and cinnamic acids. For this specific separation, caffeic acid would be concentrated in the IL-rich phase while cinnamic acid would be concentrated in the PEG-600 rich phase. Similar results in terms separation efficiency can also be obtained for the ABS composed of [Ch][Glu] although the use of this IL would reverse the relative affinity of the acids for the two phases in equilibrium.

Based on these ideal selectivity results, a system composed of IL + PEG 600 + an aqueous solution containing both caffeic (4.44×10^{-3} mol·L^{-1}) and cinnamic acid (5.40×10^{-4} mol·L^{-1}) was used – one of the systems leading to higher selectivity values. Initially, a 1:1 proportion was used but the peaks of both acid overlapped when quantified through UV-Vis. Thus, a proportion of 1:10 (CIN:CAF) was used. A proportion of 10:1 (CIN:CAF) was also studied but only the peak of cinnamic acid at a wavelength of 270.1 nm was visible in the spectra obtained.

Only the most performant systems were chosen to implement the selective extraction. Consequently, the systems containing [Ch]Cl and [Ch][Ac] were used for the selective extraction of *caffeic/cinnamic* and [Ch][Ac] for *caffeic/coumaric*. Using a deconvolution technique to separate the peaks of the spectra of the two compounds, the respective K values were calculated and the experimental selectivity parameter were determined and their values are depicted in Table 6.2.

Table 6.2 – Partition coefficients of caffeic (K_{CAF}) and cinnamic (K_{CIN}), and selectivity parameters for the caffeic + cinnamic ($S_{CAF/CIN}$) pair in the ABS composed of PEG 600 + [Ch][Ac] at 298.15 K.

Ionic Liquid	Phenolic aqueous solution	K_{CAF}	K_{CIN}	$S_{CAF/CIN}$
[Ch][Ac]	**Caffeic**	4.97	-	11.54
	Cinnamic	-	0.43	
	Caffeic + Cinnamic	**0.96**	**2.10**	**0.46**
[Ch]Cl	**Caffeic**	1.15	-	3.62
	Cinnamic	-	0.32	
	Caffeic + Cinnamic	**0.99**	**1.11**	**0.89**

Figure 6.1 depicts the logarithmic function of cinnamic acid and caffeic acid partition coefficients and consequently the migration of both acids.

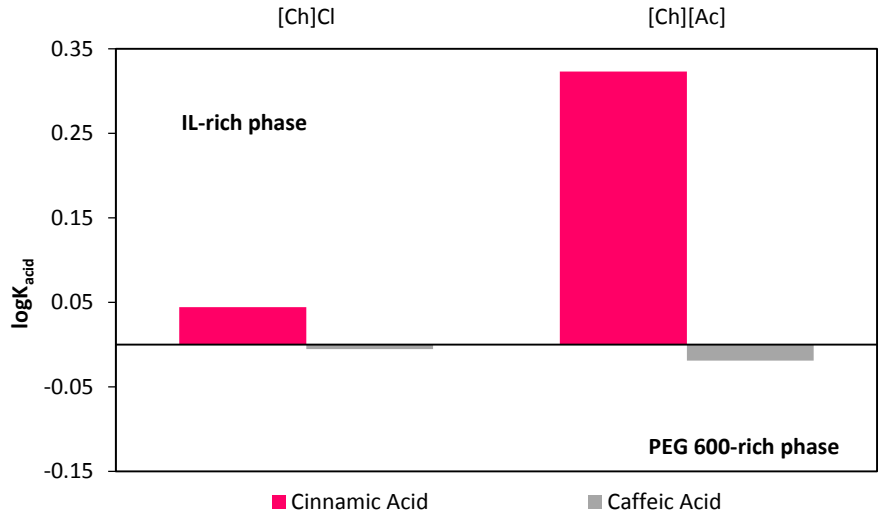

Figure 6.1 – Logarithmic function of cinnamic and caffeic acids partition coefficients ($logK_{acid}$) in the ABS composed of PEG 600 + [Ch]Cl and [Ch][Ac] at room temperature.

Comparing the results in Table 6.2 for the separation of caffeic and cinnamic acids it can be seen that the cinnamic acid is preferentially extracted to the cholinium-rich phase whereas caffeic acid is mainly concentrated in the PEG-600-rich phase. This was the opposite of what was expected from the partition coefficients obtained from the individual solutions of the acids. A possible explanation is the occurrence of interactions between the two acids, due to the similarity of the chemical structures, in other words, there is a hetero-association between cinnamic acid and caffeic acid leading to the formation of complexes. The formation of hetero-complexes could explain the change in the UV-vis spectra that was observed when the two acids are present in the mixture. This indicates that a separation of these organic acids is in fact quite complex, and that not only a more sophisticated analytical technique is in need, but also a speciation study needs to be carried out before new separations experiments can be planned.

The results obtained for the mixture of phenolic acids ($S_{CAF/CIN\text{-}[Ch][Ac]}$ = 0.46 and $S_{CAF/CIN\text{-}[Ch][Ac]}$ = 0.89) show low selectivity values, lower than those obtained using the ideal partition coefficients. This is due to the similar partition coefficients obtained when the acid mixture is used. The partition coefficients of caffeic acid regarding p-coumaric acid and the respective selectivity values are shown in Table 6.3.

Table 6.3 – Partition coefficients of caffeic (K_{CAF}) and p-coumaric (K_{COU}), and selectivity parameters for the caffeic + p-coumaric ($S_{CAF/COU}$) pair in the ABS composed of PEG 600 + [Ch][Ac] at room temperature.

Phenolic aqueous solution	K_{CAF}	K_{COU}	$S_{CAF/COU}$
Caffeic	4.97	-	5.18
p-Coumaric	-	0.96	
Caffeic + p-Coumaric	**0.18**	**1.29**	**7.18**

Again, a change in the preferential migration of the acids towards each one of the phases is observed, i.e., when mixtures of each one of the acids were prepared using PEG 600 and [Ch][Ac] ABS, the caffeic acid preferred the IL-rich phase, while p-coumaric acid the PEG 600-rich phase. In the case where a mixture of the acids was used, caffeic acid is mainly transferred to the PEG 600-rich phase and p-coumaric acid to the IL-rich phase. Nevertheless, it should be pointed out that despite the lower K values obtained when the mixture of the acids is used, a higher selectivity was also obtained. Contrary to what happened when solutions of a single acid were studied, the K values obtained in this case are further apart leading to a large selectivity value. A log-scale representation of the K values obtained is presented in Figure 6.2.

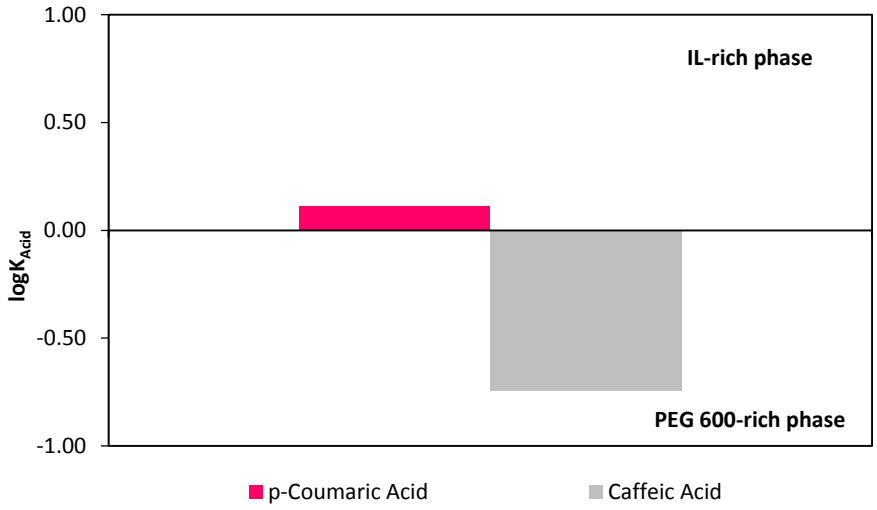

Figure 6.2 – Logarithmic function of p-coumaric and caffeic acids partition coefficients ($logK_{acid}$) in the ABS composed of PEG 600 + [Ch][Ac] at room temperature.

Again, the switch of both phenolic acids phase affinity can be attributed to a possible hetero-association between the p-coumaric acid and the caffeic acid, in a similar manner to what happens to cinnamic and caffeic. Belay [34], suggested the existence of self-association of caffeic acid due to hydrogen bonding of carboxylic or catechol groups due to a shift of maximum absorbance relevant to the concentration of caffeic acid.

7. General Conclusions

7. General Conclusions

General Conclusions

The overall objective of this work was to study the extraction efficiency in the liquid–liquid separation of some cholinium-based ILs and an imadazolium of three phenolic acids, cinnamic acid, p-coumaric acid and caffeic acid, due to their importance in their beneficial effects in the human health.

The advantages of using ABS as extractions processes include the rapid mass transfer due to low-interfacial tension, the facility in operation under continuous mode, the rapid and selective separation, the biocompatibility, separation at room temperature and high yield of biomolecules. Due to the nature of the ILs, these compounds can be tuned via different cation/anion combinations to allow more efficient separations. In this work, imidazolium and choline-based ILs were used, allowing the study of the influence of the cation and the anion chemical in the ABS extraction capability.

Two different types of ABS were used: i) containing K_3PO_4 and ii) containing PEG-600. The first system tested was the IL-K_3PO_4-H_2O-Phenolic Acid (aq.) system. The order of the partition coefficients of phenolic acids obtained was: *[Ch]Cl ≈ [Ch][Ac] > [C_4mim]Cl > [Ch][Lev] > [Ch][Glu] > [Ch][Suc]* for **cinnamic acid**; *[C_4mim]Cl > [Ch][Lev] > [Ch]Cl > [Ch][Glu] > [Ch][Ac] > [Ch][Suc]* for **p-coumaric acid**; and *[Ch][Lev] > [C_4mim]Cl > [Ch]Cl > [Ch][Glu] > [Ch][Ac] > [Ch][Suc]* for **caffeic acid**. Complete extractions were obtained for the cinnamic acid when systems composed of [Ch]Cl and [Ch][Ac] were used. The data obtained for the extraction of the phenolic acids showed that cholinium-based ABS provide real and improved alternatives to extraction with imidazolium- and phosphoniums-based ABSs. Compared to the low partition coefficients observed in typical polymer-based ABSs, cholinium-salt based systems led to the complete extraction of phenolic acids to the ionic liquid-rich phase in a single-step, by way of the targeted manipulation of the phase-forming components and their concentration.

The evaluation of the extraction results lead to the conclusion that cholinium chloride is a good choice of a solvent for the extraction of cinnamic acid, since beside its good efficient extraction it is nontoxic and environmentally acceptable.

The second part of this work addressed the use of ABS containing polyethylene glycol 600/IL systems, where phenolic acids may be recovered in both the bottom phase (PEG-rich phase) and upper phase (IL-rich phase) depending on the ionic liquid nature, with K_{ACID} values in the range of 7 – 10.

Both examples suggest that, independently of the pH, the salting-out agent employed has a major influence on the partitioning of phenolic acids. High extraction efficiencies of biologically active phenolic acids are attained using a high charge inorganic salt (K_3PO_4). Systems composed with cholinium chloride and cholinium acetate, the most hydrophilic ionic liquids used in this work, display high partition coefficients. Aqueous biphasic systems formed by PEG 600 show lower partition coefficients and consequently lower extraction efficiencies.

This work shows that the extraction of phenolic acids from aqueous solutions is not a trivial task. Despite the existence of different species in solution, according to the different pKas, the possibility of dimerization or other forms of self-association including polymerization, and particularly hetero-association with other charged species present in solution, such as salts or other acids, makes the extraction, purification and quantification a rather difficult task. ABS showed that they are complex systems that can severely affect the phenolic acids extraction due to their intrinsic characteristics. It is thus desirable to carefully choose not only a suitable IL to carry out the extraction, but the nature of the salting out agent is also very important in success of operation.

8. References

8. References

References

1. Marques, C. F. C.; Mourão, T.; Neves, C. M. S. S.; Lima, Á. S.; Boal-Palheiros, I.; Coutinho, J. A. P.; Freire, M. G., Aqueous biphasic systems composed of ionic liquids and sodium carbonate as enhanced routes for the extraction of tetracycline. *Biotechnol. Progr.* **2013,** *29*, 645-654.
2. Hatti-Kaul, R., Aqueous two-phase systems. *Mol Biotechnol* **2001,** *19*, 269-277.
3. Cláudio, A. F. M.; Freire, M. G.; Freire, C. S. R.; Silvestre, A. J. D.; Coutinho, J. A. P., Extraction of vanillin using ionic-liquid-based aqueous two-phase systems. *Sep. Purif. Technol.* **2010,** *75*, 39-47.
4. Freire, M. G.; Claudio, A. F. M.; Araujo, J. M. M.; Coutinho, J. A. P.; Marrucho, I. M.; Lopes, J. N. C.; Rebelo, L. P. N., Aqueous biphasic systems: a boost brought about by using ionic liquids. *Chem. Soc. Rev.* **2012,** *41*, 4966-4995.
5. Friberg, S. E., A review of: "AQUEOUS TWO-PHASE PARTITIONING: Physical Chemistry and Bioanalytical Applications," Boris Y. Zaslavsky, ed., Marcel Dekker, NY, 1995. *J. Dispersion Sci. Technol.* **1995,** *16*, 393-394.
6. Gutowski, K. E.; Broker, G. A.; Willauer, H. D.; Huddleston, J. G.; Swatloski, R. P.; Holbrey, J. D.; Rogers, R. D., Controlling the Aqueous Miscibility of Ionic Liquids: Aqueous Biphasic Systems of Water-Miscible Ionic Liquids and Water-Structuring Salts for Recycle, Metathesis, and Separations. *J. Am. Chem. Soc.* **2003,** *125*, 6632-6633.
7. Pereira, J. F. B.; Lima, A. S.; Freire, M. G.; Coutinho, J. A. P., Ionic liquids as adjuvants for the tailored extraction of biomolecules in aqueous biphasic systems. *Green Chemistry* **2010,** *12*, 1661-1669.
8. Shahriari, S.; Tome, L. C.; Araujo, J. M. M.; Rebelo, L. P. N.; Coutinho, J. A. P.; Marrucho, I. M.; Freire, M. G., Aqueous biphasic systems: a benign route using cholinium-based ionic liquids. *RSC Advances* **2013,** *3*, 1835-1843.
9. Almeida, M. R.; Passos, H.; Pereira, M. M.; Lima, Á. S.; Coutinho, J. A. P.; Freire, M. G., Ionic liquids as additives to enhance the extraction of antioxidants in aqueous two-phase systems. *Sep. Purif. Technol.* **2014,** *128*, 1-10.
10. Pereira, J. F. B.; Kurnia, K. A.; Cojocaru, O. A.; Gurau, G.; Rebelo, L. P. N.; Rogers, R. D.; Freire, M. G.; Coutinho, J. A. P., Molecular interactions in aqueous biphasic systems composed of polyethylene glycol and crystalline vs. liquid cholinium-based salts. *PCCP* **2014,** *16*, 5723-5731.
11. Massonne, D. K. In *Ionic Liquids at BASF SE*, Leuven Ionic Liquid Summer School, 23. - 27. August 2010, 2010; 2010.
12. Claudio, A. F. M.; Marques, C. F. C.; Boal-Palheiros, I.; Freire, M. G.; Coutinho, J. A. P., Development of back-extraction and recyclability routes for ionic-liquid-based aqueous two-phase systems. *Green Chemistry* **2014,** *16*, 259-268.
13. Pereira, J. F. B.; Vicente, F.; Santos-Ebinuma, V. C.; Araújo, J. M.; Pessoa, A.; Freire, M. G.; Coutinho, J. A. P., Extraction of tetracycline from fermentation broth using aqueous two-phase systems composed of polyethylene glycol and cholinium-based salts. *Process Biochem.* **2013,** *48*, 716-722.
14. Freire, M. G.; Pereira, J. F. B.; Francisco, M.; Rodríguez, H.; Rebelo, L. P. N.; Rogers, R. D.; Coutinho, J. A. P., Insight into the Interactions That Control the Phase Behaviour of New Aqueous Biphasic Systems Composed of Polyethylene Glycol Polymers and Ionic Liquids. *Chemistry – A European Journal* **2012,** *18*, 1831-1839.
15. Shahla Sharhriari, L. C. T., João M. M. Araújo, Luís Paulo N. Rebelo, João A. P. Coutinho, Isabel M. Marrucho, Mara G. Freire, Aqueous biphasic systems: a benign route using cholinium-based ionic liquids. *RSC Advances* 2013.
16. de Souza, R. L.; Campos, V. C.; Ventura, S. P. M.; Soares, C. M. F.; Coutinho, J. A. P.; Lima, Á. S., Effect of ionic liquids as adjuvants on PEG-based ABS formation and the extraction of two probe dyes. *Fluid Phase Equilib.* **2014,** *375*, 30-36.
17. Plechkova, N. V.; Seddon, K. R., Applications of ionic liquids in the chemical industry. *Chem. Soc. Rev.* **2008,** *37*, 123-150.

18. Han, D.; Row, K. H., Recent Applications of Ionic Liquids in Separation Technology. *Molecules* **2010,** *15*, 2405-2426.
19. Neves, C. M. S. S.; Ventura, S. P. M.; Freire, M. G.; Marrucho, I. M.; Coutinho, J. A. P., Evaluation of Cation Influence on the Formation and Extraction Capability of Ionic-Liquid-Based Aqueous Biphasic Systems. *The Journal of Physical Chemistry B* **2009,** *113*, 5194-5199.
20. Andrews, B. A.; Schmidt, A. S.; Asenjo, J. A., Correlation for the partition behavior of proteins in aqueous two-phase systems: Effect of surface hydrophobicity and charge. *Biotechnol. Bioeng.* **2005,** *90*, 380-390.
21. Freire, M. G.; Neves, C. M. S. S.; Marrucho, I. M.; Canongia Lopes, J. N.; Rebelo, L. P. N.; Coutinho, J. A. P., High-performance extraction of alkaloids using aqueous two-phase systems with ionic liquids. *Green Chemistry* **2010,** *12*, 1715-1718.
22. Huaxi, L.; Zhuo, L.; Jingmei, Y.; Changping, L.; Yansheng, C.; Qingshan, L.; Xiuling, Z.; Urs, W.-B., Liquid-liquid extraction process of amino acids by a new amide-based functionalized ionic liquid. *Green Chemistry* **2012,** *14*, 1721-1727.
23. Robbins, R. J., Phenolic Acids in Foods: An Overview of Analytical

Methodology. *J. Agric. Food. Chem.* **2003,** *51*, 2866-2887.
24. Dai, J.; Mumper, R. J., Plant Phenolics: Extraction, Analysis and Their Antioxidant and Anticancer Properties. *Molecules* **2010,** *15*, 7313-7352.
25. Apelblat, A.; Manzurola, E.; Abo Balal, N., The solubilities of benzene polycarboxylic acids in water. *The Journal of Chemical Thermodynamics* **2006,** *38*, 565-571.
26. Stalikas, C. D., Extraction, separation, and detection methods for phenolic acids and flavonoids. *J. Sep. Sci.* **2007,** *30*, 3268-3295.
27. Hoskins, J. A., The occurrence, metabolism and toxicity of cinnamic acid and related compounds. *J. Appl. Toxicol.* **1984,** *4*, 283-292.
28. De, P.; Baltas, M.; Bedos-Belval, F., Cinnamic Acid Derivatives as Anticancer Agents-A Review. *Current Medicinal Chemistry* **2011,** *18*, 1672-1703.
29. Luceri, C.; Giannini, L.; Lodovici, M.; Antonucci, E.; Abbate, R.; Masini, E.; Dolara, P., p-Coumaric acid, a common dietary phenol, inhibits platelet activity in vitro and in vivo. *British Journal of Nutrition* **2007,** *97*, 458-463.
30. Jiang, R.-W.; Lau, K.-M.; Hon, P.-M.; Mak, T. C. W.; Woo, K.-S.; Fung, K.-P., Chemistry and biological activities of caffeic acid derivatives from Salvia miltiorrhiza. *Current Medicinal Chemistry* **2015,** *12*, 237-246.
31. Gulçin, I., Antioxidant activity of caffeic acid (3,4-dihydroxycinnamic acid). *Toxicology* **2006,** *217*, 213-220.
32. Boerjan, W.; Ralph, J.; Baucher, M., LIGNIN BIOSYNTHESIS. *Annual Review of Plant Biology* **2003,** *54*, 519-546.
33. Mourão, T.; Tomé, L. C.; Florindo, C.; Rebelo, L. P. N.; Marrucho, I. M., Understanding the Role of Cholinium Carboxylate Ionic Liquids in PEG-based Aqueous Biphasic Systems. *ACS Sustainable Chemistry & Engineering* **2014**.
34. Belay, A., Spectrophotometric Method for the Determination of Caffeic Acid Complexation and Thermodynamic Properties. *International Journal of Biophysics* **2012,** *2*, 12-17.
35. ChemSpider The free chemical database. www.chemspider.com
36. Sabriye, P. O.; José, L. B. n.; Gemma, F.; Dolores, B.; Güleren, A.; José, B., Determination of Dissociation Constants of Some Hydroxylated Benzoic and Cinnamic Acids in Water from Mobility and Spectroscopic Data Obtained by CE-DAD. *J Chem Eng Data* **2009,** *54*, 807-811.
37. Dippy, J. F. J.; Page, J. E., 72. Chemical constitution and the dissociation constants of monocarboxylic acids. Part IX. Monosubstituted [small beta]-phenylpropionic and cinnamic acids. *Journal of the Chemical Society (Resumed)* **1938**, 357-363.
38. SHIMADZU The Relationship Between UV-VIS Absorption and Structure of Organic Compounds. http://www.shimadzu.com/an/uv/support/uv/ap/apl.html

39. Lawrence, S. A., *Amines: Synthesis, Properties and Applications*. Cambridge University Press: 2004.
40. Meier, H.; Petermann, R.; Gerold, J., Bathochromic or hypsochromic effects via the extension of conjugation: a study of stilbenoid squaraines. *Chem. Commun.* **1999**, 977-978.
41. Passos, H.; Sousa, A. C. A.; Pastorinho, M. R.; Nogueira, A. J. A.; Rebelo, L. P. N.; Coutinho, J. A. P.; Freire, M. G., Ionic-liquid-based aqueous biphasic systems for improved detection of bisphenol A in human fluids. *Analytical Methods* **2012,** *4*, 2664-2667.
42. Pereira, J. F. B.; Ventura, S. P. M.; e Silva, F. A.; Shahriari, S.; Freire, M. G.; Coutinho, J. A. P., Aqueous biphasic systems composed of ionic liquids and polymers: A platform for the purification of biomolecules. *Sep. Purif. Technol.* **2013,** *113*, 83-89.
43. Cláudio, A. F. M.; Ferreira, A. M.; Freire, C. S. R.; Silvestre, A. J. D.; Freire, M. G.; Coutinho, J. A. P., Optimization of the gallic acid extraction using ionic-liquid-based aqueous two-phase systems. *Sep. Purif. Technol.* **2012,** *97*, 142-149.
44. Ni, X.; Xing, H.; Yang, Q.; Wang, J.; Su, B.; Bao, Z.; Yang, Y.; Ren, Q., Selective Liquid–Liquid Extraction of Natural Phenolic Compounds Using Amino Acid Ionic Liquids: A Case of α-Tocopherol and Methyl Linoleate Separation. *Industrial & Engineering Chemistry Research* **2012,** *51*, 6480-6488.
45. Petkovic, M.; Ferguson, J. L.; Gunaratne, H. Q. N.; Ferreira, R.; Leitao, M. C.; Seddon, K. R.; Rebelo, L. P. N.; Pereira, C. S., Novel biocompatible cholinium-based ionic liquids-toxicity and biodegradability. *Green Chemistry* **2010,** *12*, 643-649.
46. Tomé, L. C.; Patinha, D. J. S.; Ferreira, R.; Garcia, H.; Silva Pereira, C.; Freire, C. S. R.; Rebelo, L. P. N.; Marrucho, I. M., Cholinium-based Supported Ionic Liquid Membranes: A Sustainable Route for Carbon Dioxide Separation. *ChemSusChem* **2014,** *7*, 110-113.

Appendix A

Spectra of Phenolic Acids

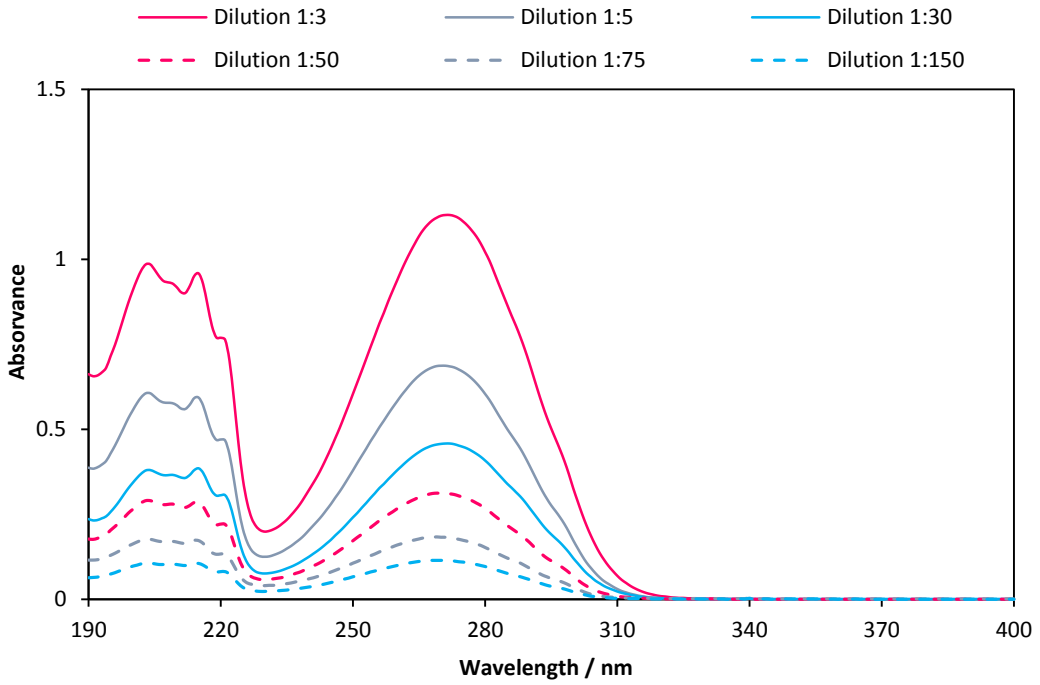

Figure 9.1 – Spectra of cinnamic acid absorbance at a wavelength of 270.1 nm in different diluted aqueous solutions.

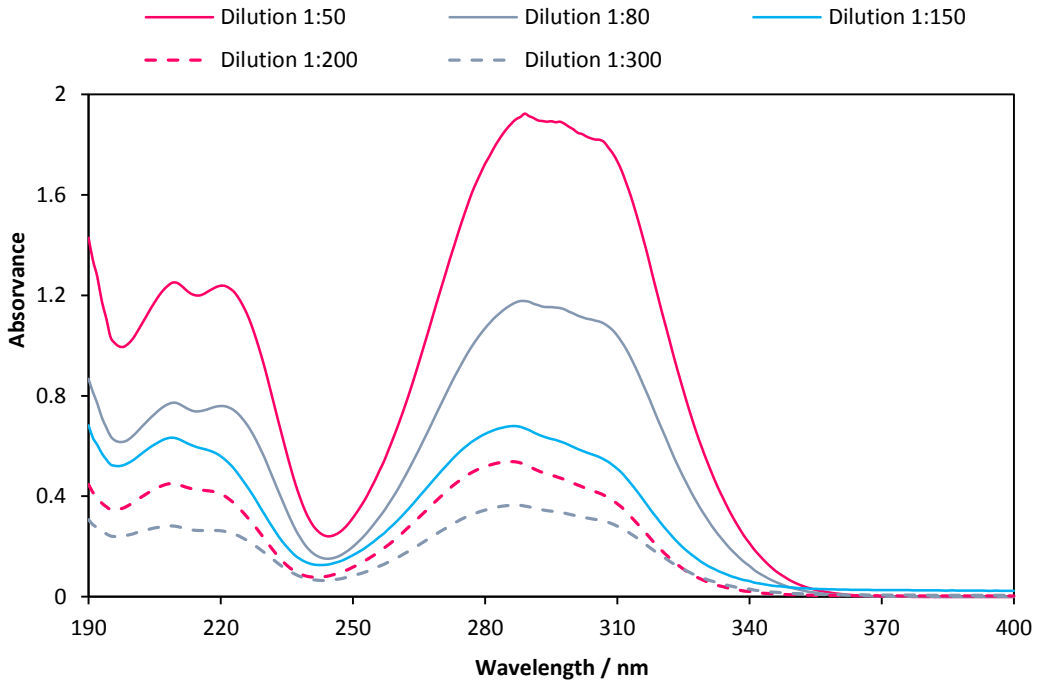

Figure 9.2 – Spectra of p-coumaric acid absorbance at a wavelength of 286 nm in different aqueous solutions.

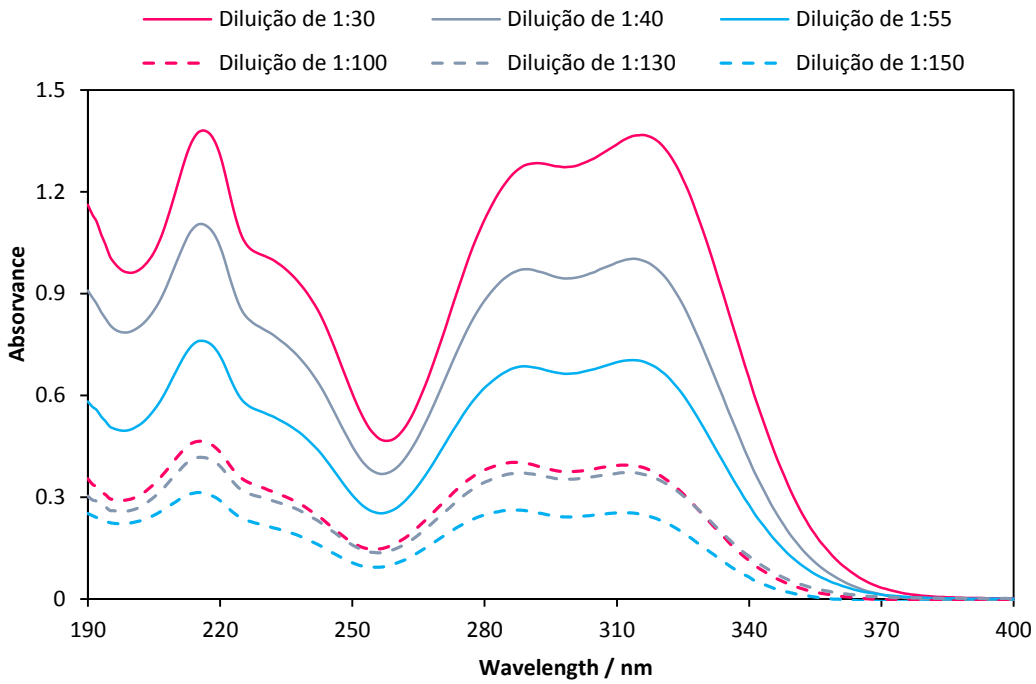

Figure 9.3 – Spectra of caffeic acid absorbance at a wavelength of 290 nm in different diluted aqueous solutions.

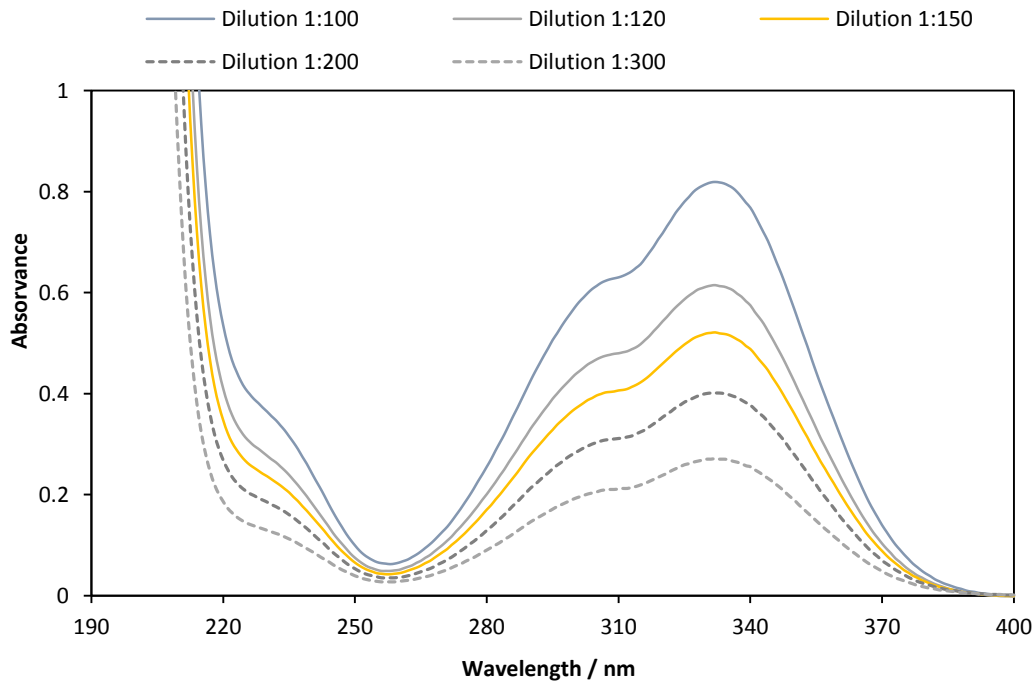

Figure 9.4 – Spectra of p-coumaric acid absorbance at a wavelength of 331 nm in different diluted aqueous solutions of K_3PO_4.

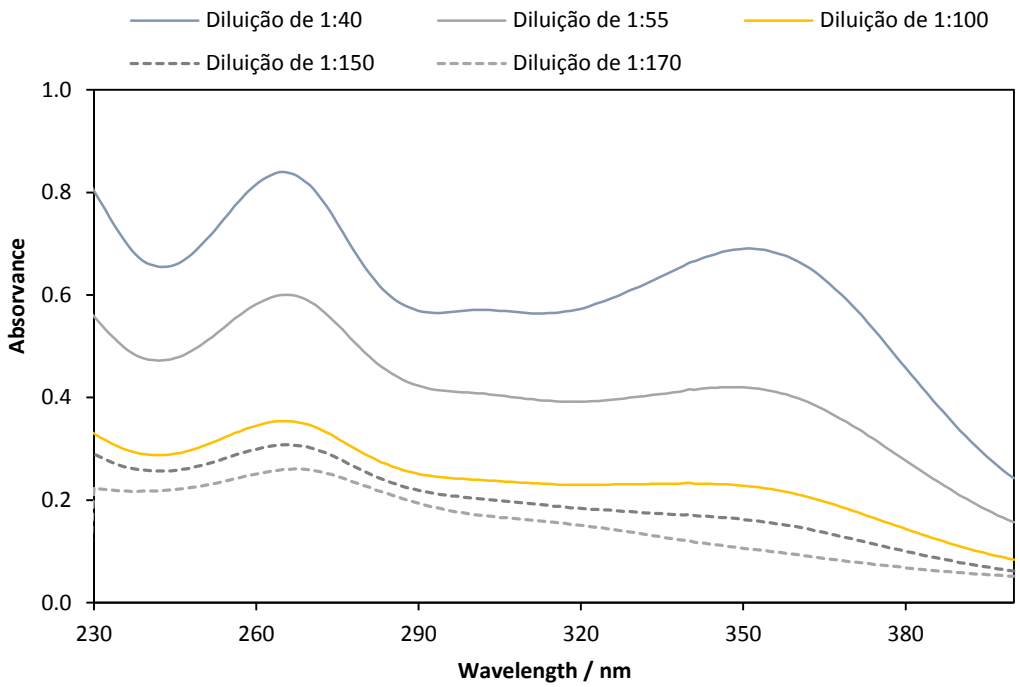

Figure 9.5 – Spectra of caffeic acid absorbance at a wavelength of 267.5 nm in different diluted aqueous solutions of K_3PO_4.

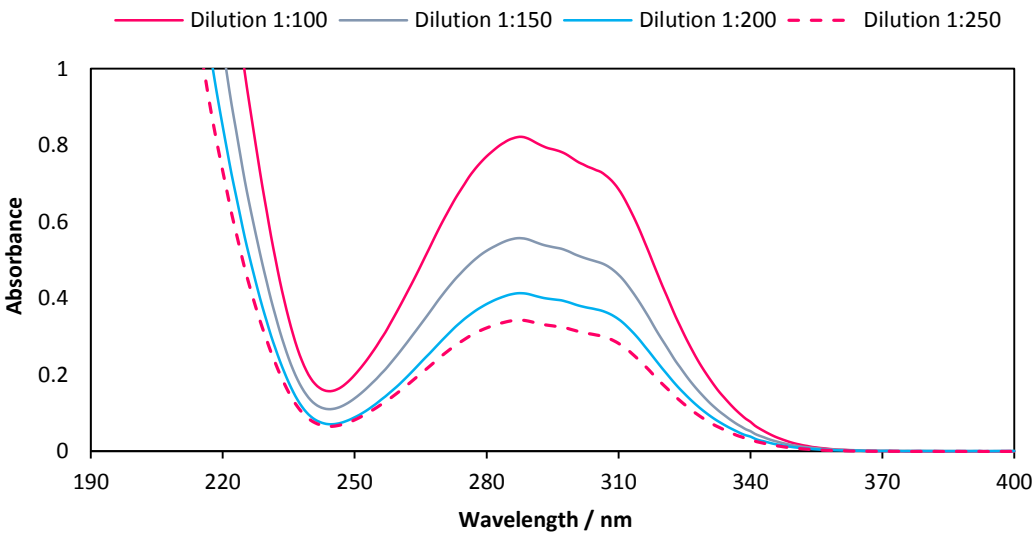

Figure 9.6 – Spectra of p-coumaric acid (286 nm) in IL-rich phase of system composed of PEG 600 + Cholinium-based IL.

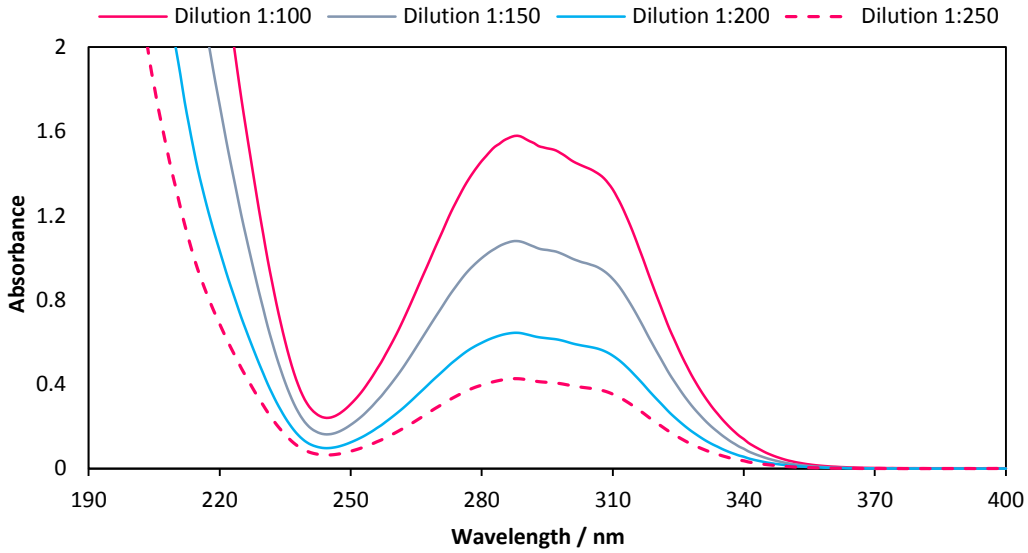

Figure 9.7 – Spectra of p-coumaric acid (286 nm) in PEG 600-rich phase of system composed of PEG 600 + Cholinium-based IL.

Appendix B

Calibration Curves

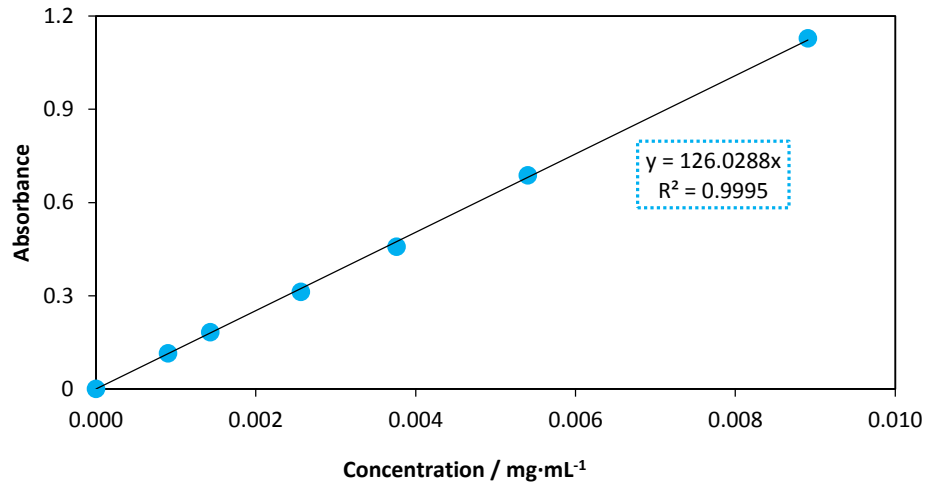

Figure 10.1 – Calibration curve for cinnamic acid (270.1 nm) in aqueous solution at room temperature.

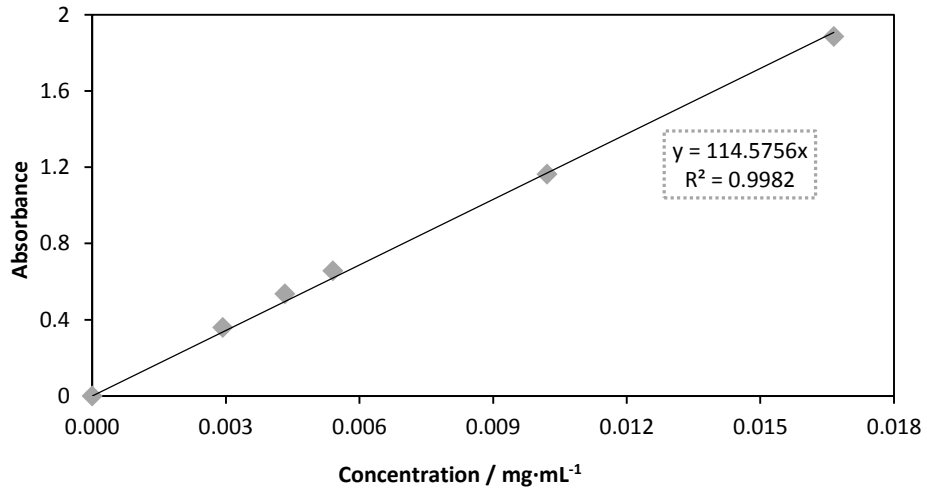

Figure 10.2 – Calibration curve for p-coumaric acid (286 nm) in aqueous solution *at room temperature*.

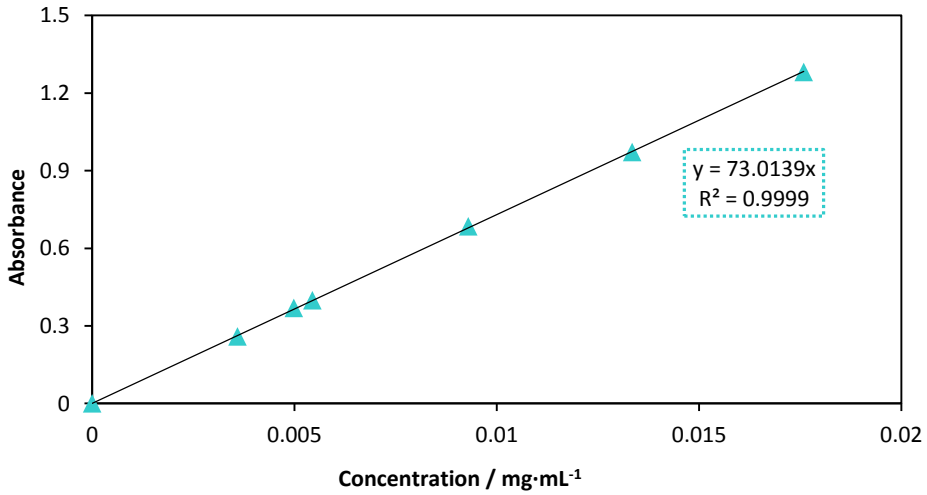

Figure 10.3 – Calibration curve for caffeic acid (290 nm) in aqueous solution at *room temperature*.

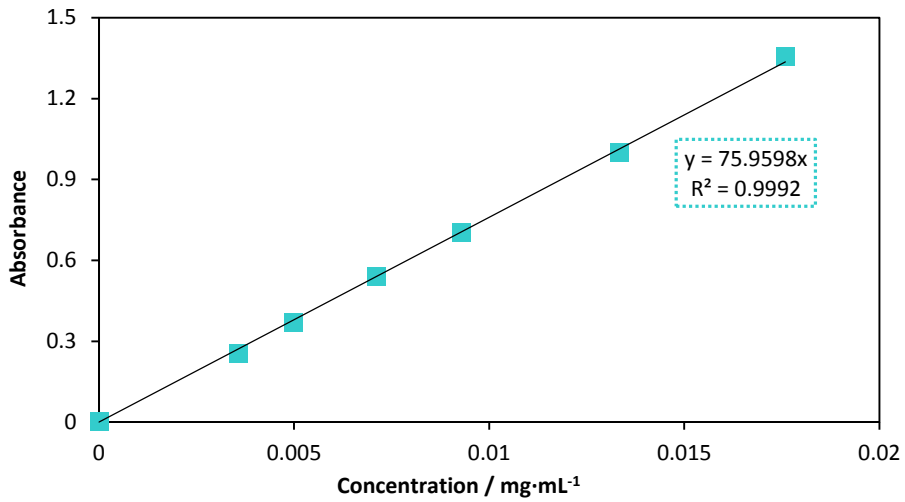

Figure 10.4 – Calibration curve for caffeic acid (312 nm) in aqueous solution at room temperature.

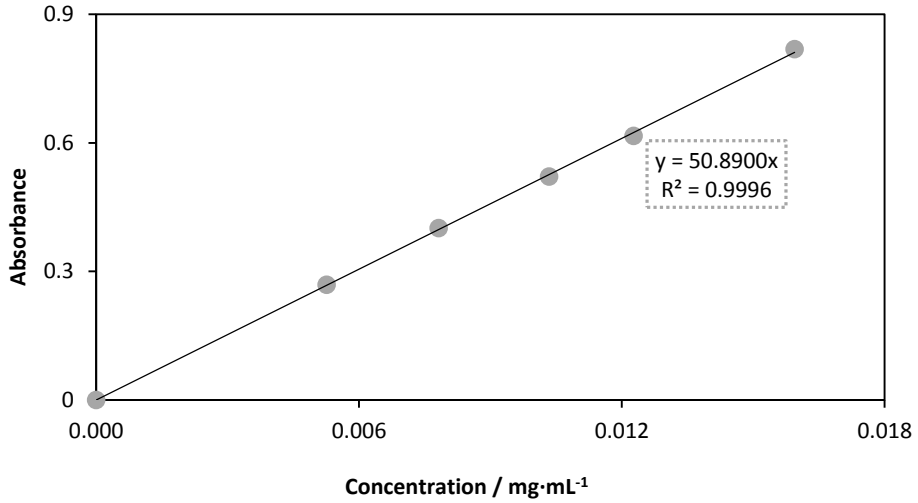

Figure 10.5 – Calibration curve for p-coumaric acid (331 nm) in aqueous solution of K_3PO_4 at room temperature.

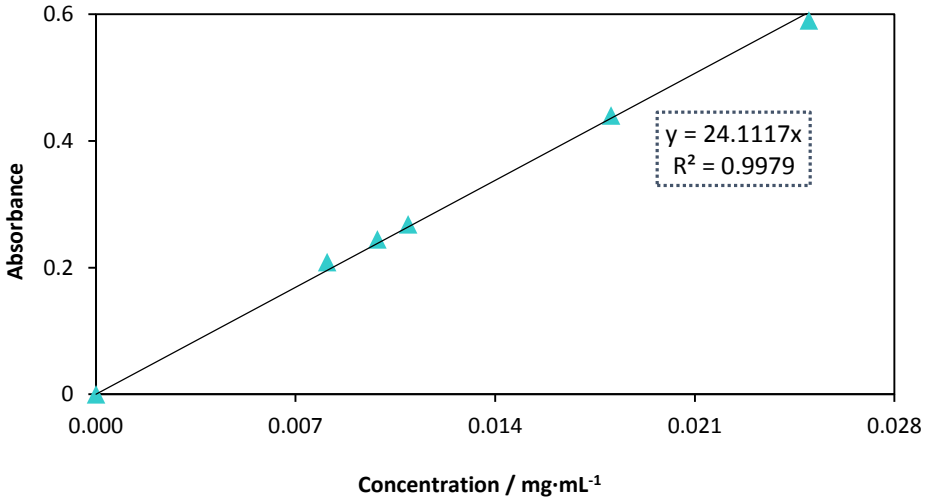

Figure 10.6 – Calibration curve for caffeic acid (267.5 nm) in aqueous solution of K_3PO_4 at room temperature.

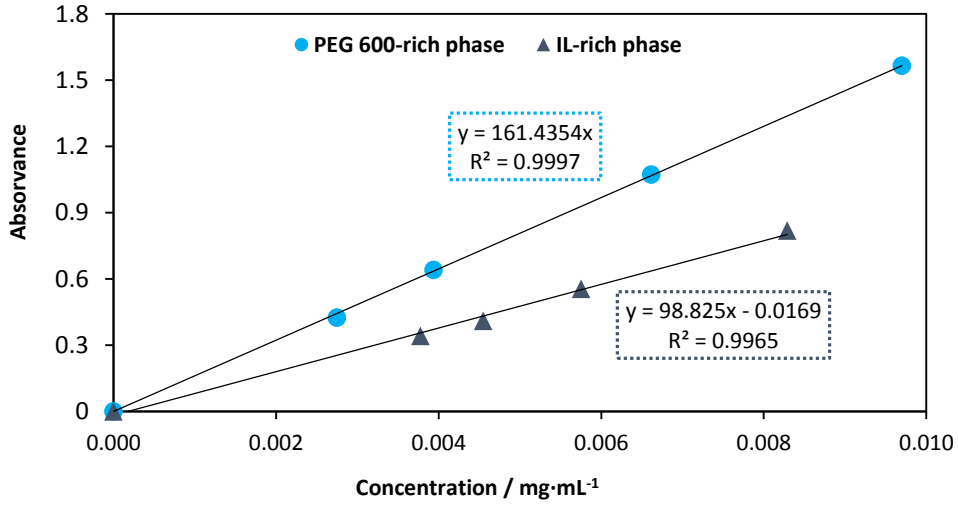

Figure 10.7 – Calibration curve for p-coumaric acid in PEG 600 (●) and IL-rich (▲) phases at room temperature.

Appendix C

Physicochemical Properties of Ionic Liquids

Table 11.1 – Viscosity (η) and density (ρ) of the coexisting phases in ABS composed of cholinium-based ionic liquid + PEG 600 + H_2O at various temperatures.

Ionic Liquid	T / K	PEG 600-rich phase (bottom phase)		Cholinium-rich phase (top phase)	
		η / mPa·s	ρ / g·cm^{-3}	η / mPa·s	ρ / g·cm^{-3}
[Ch]Cl	293.15	184.267	1.127	57.898	1.109
	298.15	138.020	1.123	45.269	1.107
	303.15	106.735	1.119	38.287	1.105
[Ch][Ac]	293.15	267.593	1.124	90.987	1.099
	298.15	199.497	1.120	70.004	1.096
	303.15	150.953	1.116	55.024	1.093
[Ch][Suc]	293.15	237.993	1.170	216.913	1.141
	298.15	175.333	1.165	159.833	1.137
	303.15	132.827	1.160	120.130	1.133
[Ch][Glu]	293.15	225.183	1.150	339.780	1.138
	298.15	169.263	1.147	254.167	1.133
	303.15	131.993	1.144	-	-

Experimental Data of the Partition Coefficients

Table 11.2 – Partition coefficients (K), respective standard deviations (σ) and mixture compositions at room temperature.

IL + K_3PO_4	Weight fraction percentage / wt%			TLL	K_{acid}
	$[IL]_M$	$[K_3PO_4]_M$	$[ACID]_M$ (aq.)		
Cinnamic Acid					
[Ch]Cl	20.65	34.33	45.02	70.97	247.40
[Ch][Ac]	30.04	23.00	46.96	66.92	227.50
[Ch][Suc]	30.28	30.00	39.72	92.39	9.32
[Ch][Glu]	29.64	30.03	40.33	84.19	19.34
[Ch][Lev]	30.15	20.22	49.63	53.52	30.05
[C_4mim]Cl	25.02	15.02	59.96	47.01	49.97
p-Coumaric Acid					
[Ch]Cl	20.65	34.33	45.02	70.97	383.90
[Ch][Ac]	30.04	23.00	46.96	66.92	26.06
[Ch][Suc]	30.28	30.00	39.72	92.39	9.48
[Ch][Glu]	29.64	30.03	40.33	84.19	19.74
[Ch][Lev]	30.15	20.22	49.63	53.52	1.39
[C_4mim]Cl	25.02	15.02	59.96		37.32
Caffeic Acid					
[Ch]Cl	20.65	34.33	45.02	70.97	5.45
[Ch][Ac]	30.04	23.00	46.96	66.92	2.49
[Ch][Suc]	30.28	30.00	39.72	92.39	3.05
[Ch][Glu]	29.64	30.03	40.33	84.19	5.05
[Ch][Lev]	30.15	20.22	49.63	53.52	0.34
[C_4mim]Cl	25.02	15.02	59.96		11.09

Table 11.3 – Partition coefficients (K), respective standard deviations (σ) and mixture compositions at room temperature.

IL + PEG 600	Weight fraction percentage / wt%			TLL	$K_{acid} \pm \sigma$
	$[IL]_M$	$[PEG\ 600]_M$	$[ACID]_M$ (aq.)		
Cinnamic Acid					
[Ch]Cl	34.93	54.94	10.13	115.65	0.31 ± 0.01
[Ch][Ac]	39.82	49.79	10.39	123.64	0.43 ± 0.03
[Ch][Suc]	43.87	41.26	14.87	105.38	5.06 ± 0.90
[Ch][Glu]	42.14	42.62	15.24	100.86	2.73 ± 0.27
p-Coumaric Acid					
[Ch]Cl	34.93	54.94	10.13	115.65	1.15 ± 0.008
[Ch][Ac]	39.82	49.79	10.39	123.64	4.97 ± 3.15
[Ch][Suc]	43.87	41.26	14.87	105.38	0.49
[Ch][Glu]	42.14	42.62	15.24	100.86	0.45
Caffeic Acid					
[Ch]Cl	34.93	54.94	10.13	115.65	0.45 ± 0.01
[Ch][Ac]	39.82	49.79	10.39	123.64	0.96 ± 0.28
[Ch][Suc]	43.87	41.26	14.87	105.38	0.15 ± 0.11
[Ch][Glu]	42.14	42.62	15.24	100.86	1.00 ± 0.02

Synthesis of Ionic Liquids

The ionic liquids/salts used in this work, namely the cholinium acetate ([Ch][Ac]), cholinium succinate ([Ch][Suc]), cholinium glutarate ([Ch][Glu]) and cholinium levulinate ([Ch][lev]), were prepared by dropwise addition of the corresponding acid (1:1) to aqueous cholinium bicarbonate, following an established procedure.[45, 46] The mixtures were stirred at ambient temperature and pressure for 12 h. The resulting products were washed with diethyl ether to remove unreacted acid. Excess of water and traces of other volatile substances were removed first by rotary evaporation, and then by stirring and heating under vacuum. The chemical structures and the purities of the synthesized cholinium-based ILs were confirmed by ^{1}H and ^{13}C NMR. All the ionic liquid samples were dried prior to their use by stir-heating under vacuum at moderate temperature (40–50 ºC, > 48 h, ca. 0.01 mbar). Their water contents were determined by Karl Fischer titration (831 KF Coulometer, Metrohm) and considered in all experiments.

Appendix D

Mass Transfer

Mass Transfer in IL + Phenolic Acids (aq.) + K_3PO_4 systems

Table 12.1 – Validation of cinnamic acid quantification through mass balance.

Ionic Liquid	**[C_4mim]Cl**	**[Ch]Cl**	**[Ch][Ac]**	**[Ch][Suc]**	**[Ch][Glu]**	**[Ch][Lev]**
[Total CIN] / g·dm^{-3}	0.167	0.167	0.167	0.167	0.163	0.163
TOTAL m_{CIN} / g	1.50×10^{-3}	7.53×10^{-4}	6.26×10^{-4}	6.62×10^{-4}	6.41×10^{-4}	7.87×10^{-4}
Dilution Factor	-	-	-	-	-	1:50
$[CIN]_{IL}$ at 270.1 nm / g·dm^{-3}	0.081	0.243	0.149	0.093	0.127	0.012
$[CIN]_{K3PO4}$ at 270.1 nm / g·dm^{-3}	1.61×10^{-3}	9.82×10^{-4}	6.54×10^{-4}	9.96×10^{-3}	6.59×10^{-3}	1.93×10^{-2}
m_{CIN-IL} at 270.1 nm / g	7.14×10^{-4}	7.58×10^{-4}	6.04×10^{-4}	4.64×10^{-4}	6.20×10^{-4}	3.20×10^{-3}
$m_{CIN-K3PO4}$ at 270.1 nm / g	6.06×10^{-6}	4.05×10^{-6}	6.54×10^{-7}	9.96×10^{-6}	6.59×10^{-6}	1.93×10^{-5}
Closure of balance	7.78×10^{-4}	-8.78×10^{-6}	2.15×10^{-5}	1.88×10^{-4}	1.44×10^{-5}	-2.43×10^{-3}

Table 12.2 – Validation of p-coumaric acid quantification through mass balance.

Ionic Liquid	[C_4mim]Cl	[Ch]Cl	[Ch][Ac]	[Ch][Suc]	[Ch][Glu]	[Ch][Lev]
[Total COU] / g·dm^{-3}	0.013	0.013	0.013	0.013	0.013	0.013
TOTAL m_{COU} / g	7.93×10^{-5}	5.98×10^{-5}	6.53×10^{-5}	5.07×10^{-5}	5.23×10^{-5}	5.07×10^{-5}
Dilution Factor	-	-	-	-	-	1:50
$[COU]_{IL}$ at 331 nm / g·dm^{-3}	0.010	0.032	0.020	0.012	0.009	0.001
$[COU]_{K3PO4}$ at 331 nm / g·dm^{-3}	2.65×10^{-4}	1.07×10^{-3}	2.32×10^{-3}	2.04×10^{-3}	4.85×10^{-4}	1.00×10^{-3}
m_{COU-IL} at 331 nm / g	1.22×10^{-4}	9.80×10^{-5}	1.14×10^{-4}	5.97×10^{-5}	4.61×10^{-5}	2.72×10^{-4}
$m_{COU-K3PO4}$ at 331 nm / g	6.98×10^{-7}	4.45×10^{-6}	2.32×10^{-6}	2.04×10^{-6}	4.85×10^{-7}	1.00×10^{-6}
Closure of mass balance	-4.37×10^{-5}	-4.27×10^{-5}	-5.06×10^{-5}	-1.11×10^{-5}	5.75×10^{-6}	-2.22×10^{-4}

Table 12.3 – Validation of caffeic acid quantification through mass balance.

Ionic Liquid	[C_4mim]Cl	[Ch]Cl	[Ch][Ac]	[Ch][Suc]	[Ch][Glu]	[Ch][Lev]
[Total CAF] / g·dm^{-3}	0.022	0.017	0.017	0.022	0.022	0.022
TOTAL m_{CAF} / g	1.29×10^{-4}	6.29×10^{-5}	7.98×10^{-5}	4.22×10^{-5}	8.47×10^{-5}	1.04×10^{-4}
Dilution Factor	1:2	-	-	-	-	1:50
$[CAF]_{IL}$ at 267.5 nm / g·dm^{-3}	0.006	0.045	0.022	0.023	0.026	0.005
$[CAF]_{K3PO4}$ at 267.5 nm / g·dm^{-3}	0.001	0.008	0.009	0.008	0.005	0.010
m_{CAF-IL} at 267.5 nm / g	8.31×10^{-5}	1.11×10^{-4}	1.18×10^{-4}	5.78×10^{-5}	1.30×10^{-4}	1.32×10^{-3}
$m_{CAF-K3PO4}$ at 267.5 nm / g	3.08×10^{-6}	2.76×10^{-5}	8.83×10^{-6}	7.59×10^{-6}	5.15×10^{-6}	1.05×10^{-5}
Closure of mass balance	4.30×10^{-5}	-7.52×10^{-5}	-4.69×10^{-5}	-2.32×10^{-5}	-5.08×10^{-5}	-1.23×10^{-3}

Mass Transfer in IL + Phenolic Acids (aq.) + Polyethylene Glycol systems

Table 12.4 – Validation of the quantification of cinnamic acid through mass transfer.

Ionic Liquid	[Ch]Cl	[Ch][Ac]	[Ch][Suc]	[Ch][Glu]
[Total CIN] / g·dm^{-3}	0.147	0.147	0.147	0.147
TOTAL m_{CIN} / g	1.14×10^{-4}	1.10×10^{-4}	1.06×10^{-4}	1.56×10^{-4}
Dilution Factor	1:4	1:3	1:3	1:3
$[CIN]_{IL}$ at 270.1 nm / g·dm^{-3}	0.006	0.008	0.027	0.023
$[CIN]_{PEG}$ at 270.1 nm / g·dm^{-3}	0.019	0.016	0.006	0.009
m_{CIN-IL} at 270.1 / g	2.01×10^{-5}	2.46×10^{-5}	6.30×10^{-5}	7.59×10^{-5}
$m_{CIN-PEG}$ at 270.1 nm / g	6.86×10^{-5}	6.43×10^{-5}	1.09×10^{-5}	3.40×10^{-5}
Closure of balance	2.51×10^{-5}	2.16×10^{-5}	3.16×10^{-5}	4.65×10^{-5}

Table 12.5 – Validation of the quantification of caffeic acid through mass transfer.

Ionic Liquid	[Ch]Cl	[Ch][Ac]	[Ch][Suc]	[Ch][Glu]
[Total CAF] / g·dm^{-3}	0.672	0.672	0.672	0.672
TOTAL m_{CAF} / g	5.49×10^{-4}	5.03×10^{-4}	4.86×10^{-4}	7.13×10^{-4}
Dilution Factor	1:5	1:3	1:10	1:10
$[CAF]_{IL}$ at 290 nm / g·dm^{-3}	0.053	0.093	0.058	0.045
$[CAF]_{PEG}$ at 290 nm / g·dm^{-3}	0.047	0.018	0.098	0.099
m_{CAF-IL} at 290 nm / g	1.88×10^{-4}	2.97×10^{-4}	1.49×10^{-4}	1.61×10^{-4}
$m_{CAF-PEG}$ at 290 nm / g	1.65×10^{-4}	6.78×10^{-5}	1.55×10^{-4}	3.18×10^{-4}
Closure of balance	1.96×10^{-4}	1.38×10^{-4}	1.82×10^{-4}	2.33×10^{-4}

Table 12.6 – Validation of the quantification of p-coumaric acid through mass transfer.

Ionic Liquid	[Ch]Cl	[Ch][Ac]
[Total COU] / g·dm^{-3}	0.800	0.800
TOTAL m_{COU} / g	5.90×10^{-4}	6.02×10^{-4}
Dilution Factor	1:5	1:3
$[COU]_{IL}$ at 286 nm / g·dm^{-3}	0.015	0.030
$[COU]_{PEG}$ at 286 nm / g·dm^{-3}	0.030	0.019
m_{COU-IL} at 286 nm / g	4.98×10^{-5}	9.88×10^{-5}
$m_{COU-PEG}$ at 286 nm / g	1.09×10^{-4}	7.22×10^{-5}
Closure of balance	4.31×10^{-4}	4.31×10^{-4}

Appendix E

NMRs spectrums of Ionic Liquids

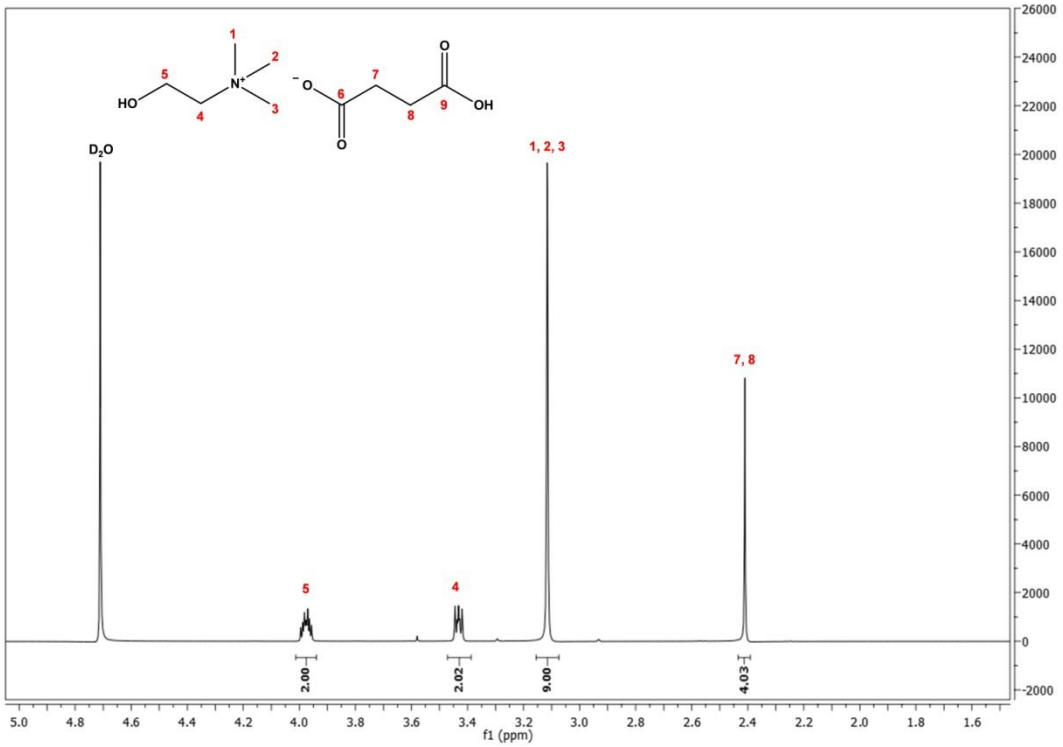

Figure 13.1 – ^{1}H-NMR spectrum of [Ch][Suc] in D_2O.

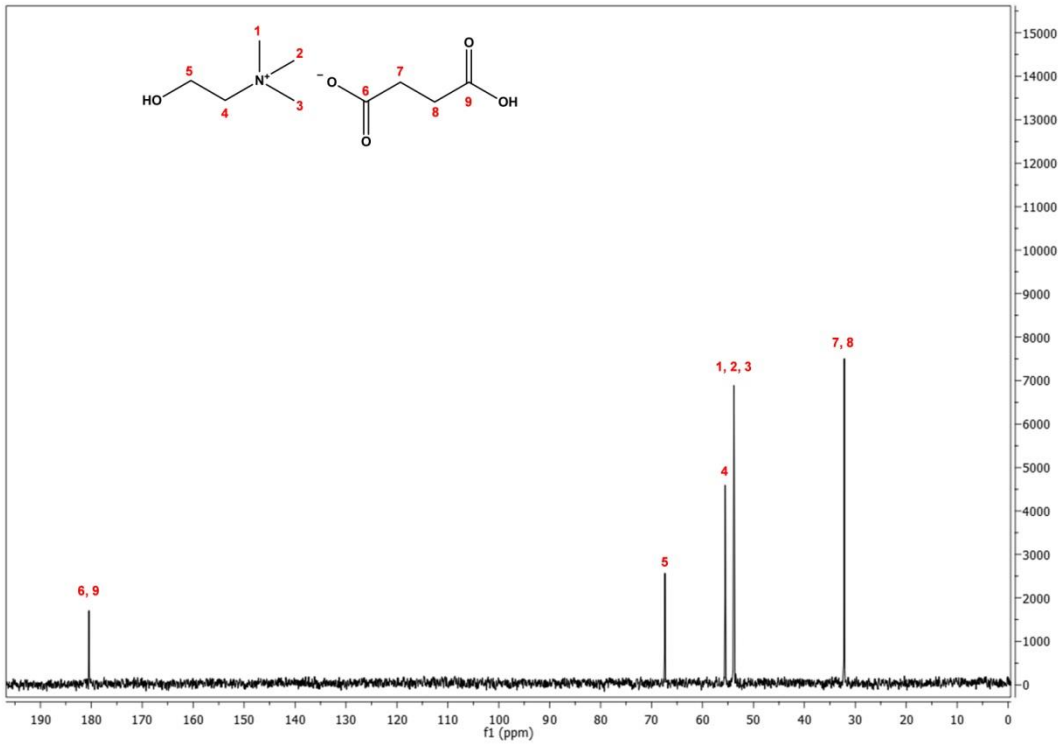

Figure 13.2 – ^{1}C-NMR spectrum of [Ch][Suc] in D_2O.

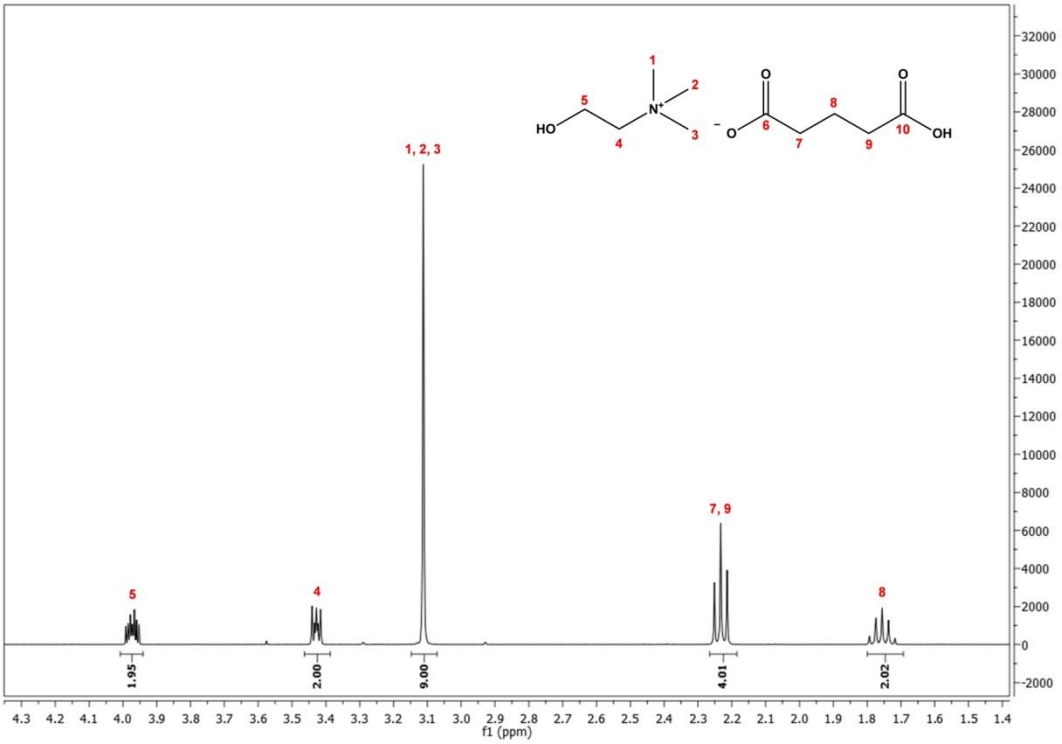

Figure 13.3 – ^{1}H-NMR spectrum of [Ch][Glu] in D_2O.

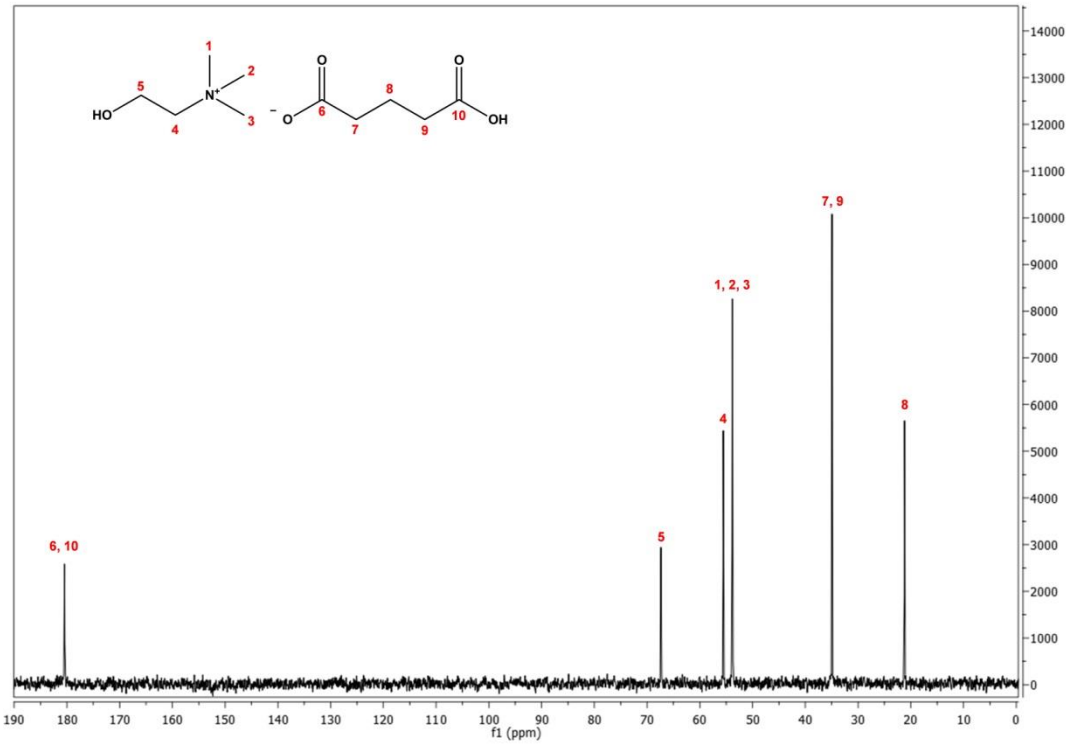

Figure 13.4 – ^{1}C-NMR spectrum of [Ch][Glu] in D_2O.